NASA/CR—2017–219474

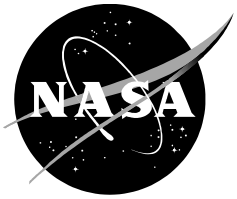

Tiltrotor Conceptual Design

Franklin D. Harris
F. D. Harris & Associates
Ames Research Center, Moffett Field, California

Prepared for Monterey Technologies, Inc.
Subcontract No. REMS.201303
Task Order No. NNA15BB93T

March 2017

NASA STI Program ... in Profile

Since its founding, NASA has been dedicated to the advancement of aeronautics and space science. The NASA scientific and technical information (STI) program plays a key part in helping NASA maintain this important role.

The NASA STI program operates under the auspices of the Agency Chief Information Officer. It collects, organizes, provides for archiving, and disseminates NASA's STI. The NASA STI program provides access to the NTRS Registered and its public interface, the NASA Technical Reports Server, thus providing one of the largest collections of aeronautical and space science STI in the world. Results are published in both non-NASA channels and by NASA in the NASA STI Report Series, which includes the following report types:

- TECHNICAL PUBLICATION. Reports of completed research or a major significant phase of research that present the results of NASA Programs and include extensive data or theoretical analysis. Includes compilations of significant scientific and technical data and information deemed to be of continuing reference value. NASA counterpart of peer-reviewed formal professional papers but has less stringent limitations on manuscript length and extent of graphic presentations.

- TECHNICAL MEMORANDUM. Scientific and technical findings that are preliminary or of specialized interest, e.g., quick release reports, working papers, and bibliographies that contain minimal annotation. Does not contain extensive analysis.

- CONTRACTOR REPORT. Scientific and technical findings by NASA-sponsored contractors and grantees.

- CONFERENCE PUBLICATION. Collected papers from scientific and technical conferences, symposia, seminars, or other meetings sponsored or co-sponsored by NASA.

- SPECIAL PUBLICATION. Scientific, technical, or historical information from NASA programs, projects, and missions, often concerned with subjects having substantial public interest.

- TECHNICAL TRANSLATION. English-language translations of foreign scientific and technical material pertinent to NASA's mission.

Specialized services also include organizing and publishing research results, distributing specialized research announcements and feeds, providing information desk and personal search support, and enabling data exchange services.

For more information about the NASA STI program, see the following:

- Access the NASA STI program home page at http://www.sti.nasa.gov

- E-mail your question to help@sti.nasa.gov

- Phone the NASA STI Information Desk at 757-864-9658

- Write to:
  NASA STI Information Desk
  Mail Stop 148
  NASA Langley Research Center
  Hampton, VA 23681-2199

NASA/CR—2017–219474

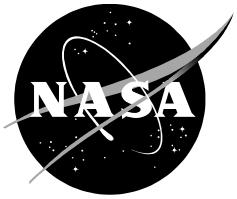

Tiltrotor Conceptual Design

Franklin D. Harris
F. D. Harris & Associates
Ames Research Center, Moffett Field, California

Prepared for Monterey Technologies, Inc.
Subcontract No. REMS.201303
Task Order No. NNA15BB93T

National Aeronautics and
Space Administration

Ames Research Center
Moffett Field, CA 94035-1000

March 2017

Available from:

NASA STI Support Services
Mail Stop 148
NASA Langley Research Center
Hampton, VA 23681-2199
757-864-9658

National Technical Information Service
5301 Shawnee Road
Alexandria, VA 22312
webmail@ntis.gov
703-605-6000

This report is also available in electronic form at

http://ntrs.nasa.gov

TABLE OF CONTENTS

LIST OF FIGURES

LIST OF FIGURES (cont.)

LIST OF TABLES

INTRODUCTION

This year-end progress report summarizes an engineering study, which began in August 2015, of a large VTOL civil transport. The task was to follow up on work reported in reference 1, which described a NASA 2005 design study showing that a 120-passenger tiltrotor aircraft, capable of cruising at 350 knots at 30,000 feet, was quite feasible. The objective of the task this year was to investigate the feasibility of a 120-passenger tiltrotor aircraft capable of cruising at 425 to 450 knots at altitude and having V/STOL capability at Denver (i.e., 5,000 feet) with an outside air temperature (OAT) of 95°F. A corollary to this work was to examine the suitability of the engineering tools available to conduct the concept design study begun herein.

Two key pieces of corollary work were relegated to an appendix, and the body of this report was used to transmit progress in the preliminary performance trend studies.

By way of background, in January of 2016, Mr. Harris presented a paper titled *The V/STOL Performance Gap* at the American Helicopter Society (AHS) Technical Meeting on Aeromechanics Design for Vertical Lift. That presentation is included herein as Appendix A. A key concluding chart in that presentation is repeated here as figure 1. The Rotorcraft Branch at NASA Ames was already studying a tiltrotor suited for regional carrier routes, but no effort beyond the 2005 results reported in reference 1 was going on. Therefore, the task of extending the 350-knot, 120-passenger tiltrotor studies up to speeds associated with major airline routes began.

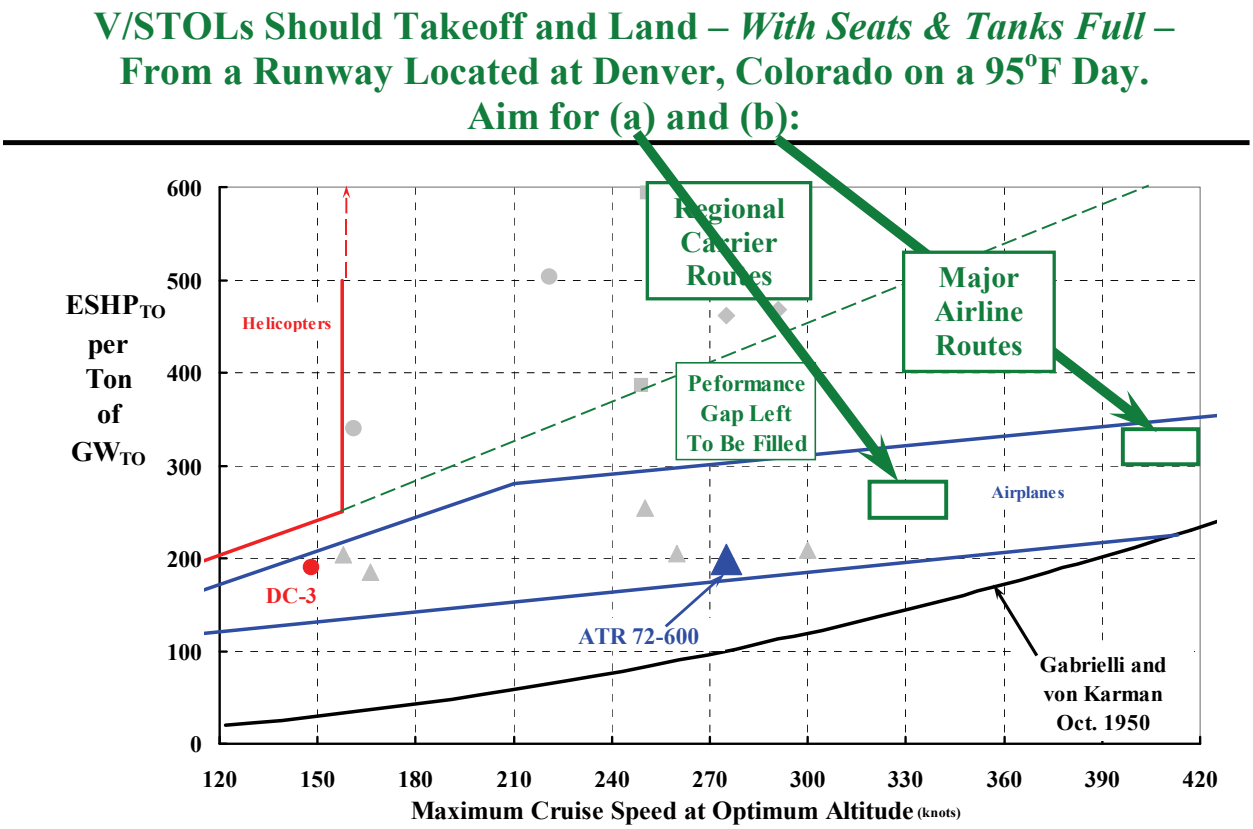

Figure 1. V/STOL performance goals.

PRELIMINARY PERFORMANCE TREND STUDIES

The performance trend studies reported herein have been made assuming two design points. The first design point is cruising at speeds between 400 and 450 knots at pressure altitudes between 20,000 and 35,000 feet in standard atmosphere. The second design point is hovering at 5,000 feet pressure altitude with an outside air temperature (OAT) of 95°F. The objective has been to meet the design points with the lowest, uninstalled, engine manufacturer's maximum rated power ($MRP_{SL,\ V\ =\ 0}$) assuming a gross weight on the order of 124,000 pounds (62 tons).

Performance Fundamentals

Performance at the two design points has been calculated with the very fundamental equations shown in figure 2. The first equation is the cruise equation, which is just a statement that proprotor power required is simply aircraft drag times velocity. Here the aircraft's drag is calculated as gross weight divided by the aircraft's lift-to-drag (L/D) ratio in cruise. This drag is the proprotor thrust (T_P) required to ensure equilibrium. The actual proprotor power (i.e., T_P times V_{cruise}) represents the ideal power required. This ideal power is increased by the proprotor propulsive efficiency (η_{prop}), which is generally denoted as proprotor horsepower (RHP). Of course, the engine provides RHP, but with additional losses due to a transmission (η_{xmsn}) and the usual penalty (not quoted by the manufacturer) for the installation of their engine in the aircraft ($C_{install}$). Finally the engine also provides horsepower for accessories (SHP_{acc}). Thus,

$$(1)\quad SHP_{Cruise} = [RHP]\left[\frac{1}{\eta_{xmsn}\left(1-C_{Install}\right)}\right] + SHP_{acc}\,.$$

Of course, to obtain this engine shaft horsepower in cruise at speed and altitude (SHP_{cruise}) generally requires installation of a much larger engine having a manufacturer's sea level rating

CRUISE EQUATIONS

1. Assume that in cruise, all the engines (N_{eng}) are operating at Maximum Continous Power (MCP) and that cruise power required is approximated as:

$$\text{Total Cruise } MCP_{req.} \text{ at altitude} = SHP_{Cruise} = \left[\frac{GW}{(L/D)\eta_{prop}} \times \frac{1.69V_{kts}}{550}\right]\left[\frac{1}{\eta_{xmsn}\left(1-C_{Install}\right)}\right] + SHP_{acc}$$

Therefore, the engine manufacturer's maximum rated shaft horsepower at sea level standard and zero speed $\left(MRP_{S.L,V=0}\right)$ must be

$$MRP_{S.L,V=0} = \frac{SHP_{Cruise}}{N_{eng}} \times \left(\frac{1}{LR_{cruise}}\right) \quad \text{where the lapse rate } (LR_{cruise}) = \frac{MCP_{\text{available at cruise altitude, OAT \& speed}}}{MRP_{S.L,V=0}}$$

VERTICAL TAKEOFF EQUATIONS

1. Assume that in hover, all engines (N_{eng}) are operating at engine Maximum Rated Power (MRP) at altitude and OAT.
Let DL be the download factor, FM be the figure of merit, N_{props} be the number of proprotors, and D be diameter.
Then approximate the total engine shaft horsepower required to takeoff vertically at altitude and OAT from

$$\text{Total Hover Power Req.} = SHP_{VTOL} = \left[\frac{(DL\times GW)^{3/2}}{550\times FM\times\sqrt{2\times\rho\times N_{props}\times\frac{\pi}{4}\times D^2}}\right]\left[\frac{1}{\eta_{xmsn}\times(1-C_{Install})}\right] + SHP_{acc}$$

Therefore, the engine manufacturer's maximum rated power at sea level standard and zero speed $\left(MRP_{S.L,V=0}\right)$ must be

$$MRP_{S.L,V=0} = \frac{SHP_{VTOL}}{N_{eng}} \times \left(\frac{1}{LR_{VTOL}}\right) \quad \text{where the lapse rate } (LR_{VTOL}) = \frac{MRP_{\text{available at hover alt. \& OAT}}}{MRP_{S.L,V=0}}$$

Figure 2. Fundamental aircraft performance equations.

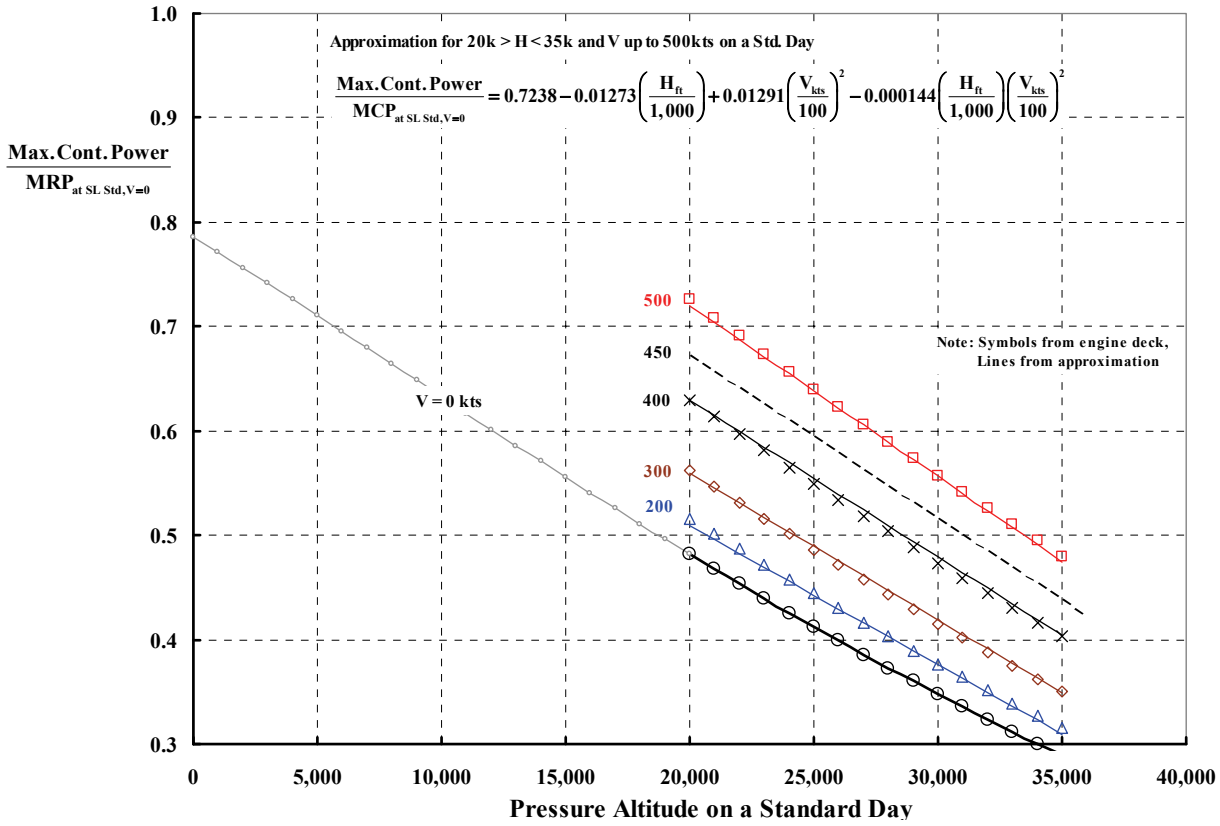

Figure 3. Typical turboshaft *maximum continuous power* lapse rates on a standard day.

denoted by ($MRP_{SL,\ V\ =\ 0}$). It is well understood that engines lose power output capability with increasing altitude and also with temperature. This fact of life is referred to as a lapse rate with nominal engine behavior as shown in figure 3.

Note from figure 3 that cruise at altitude and speed is achieved with the engine running at maximum continuous power (MCP). However, an engine manufacturer typically rates the continuous power at about 0.8 times the maximum rated power at sea level and at zero speed (which can only be used for, say, about 5 minutes). It is worth noting from figure 3 that high speed can offset the lapse rate at zero speed, which means a smaller installed engine.

The VTOL takeoff equation provided in figure 2 is based on the well known ideal momentum theory that

$$(2)\quad RHP_{VTOL} = \frac{T}{550\ FM}\sqrt{\frac{T}{2\rho A}}$$

whereupon

$$(3)\quad SHP_{VTOL} = [RHP_{VTOL}]\left[\frac{1}{\eta_{xmsn}\left(1-C_{Install}\right)}\right] + SHP_{acc}\ .$$

It is very important to remember that the engine lapse rate for hover is usually quite different from that given for cruise in figure 3. You see this immediately from figure 4; the maximum rated power is reduced by about 15 percent when the engine is operating at an outside air temperature (OAT) of 95°F versus 59°F, which is the manufacturer's generally accepted reference temperature. Of course, operating at pressure altitudes above sea level further reduces

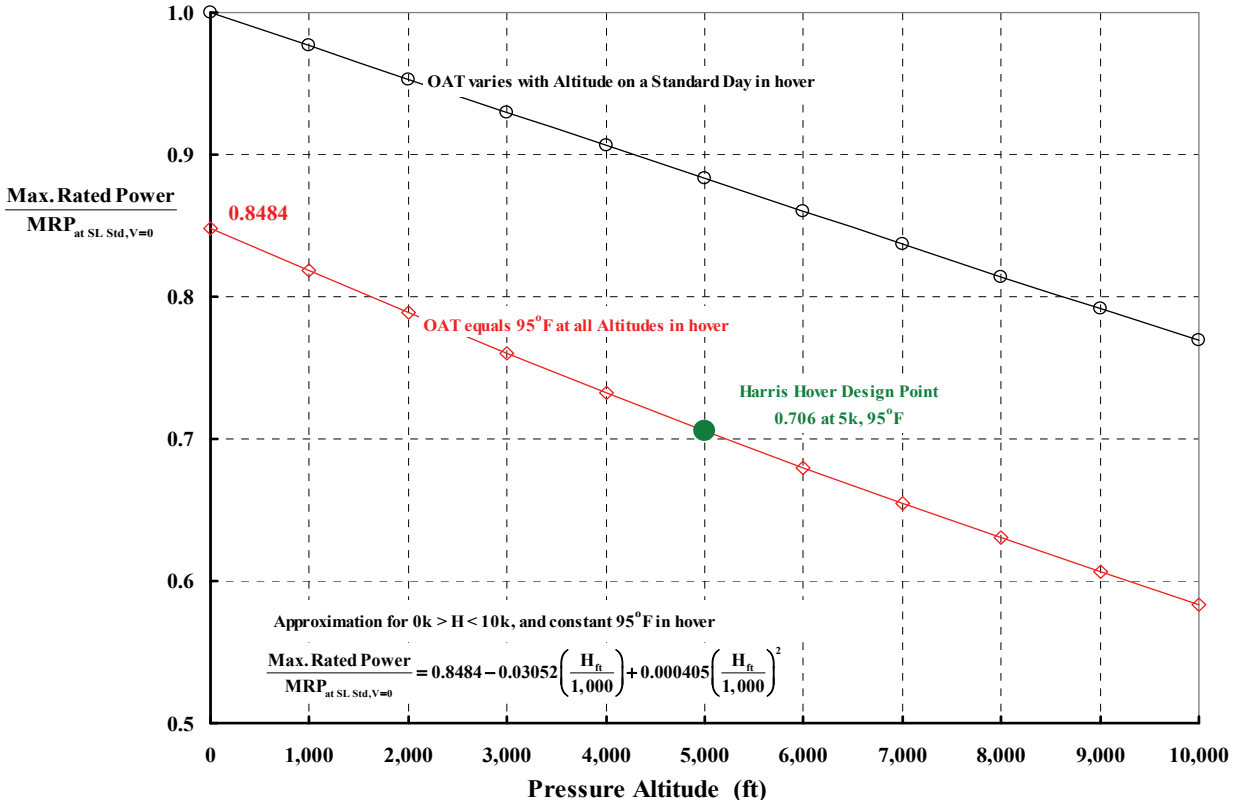

Figure 4. Typical turboshaft *maximum rated power* lapse rates on a standard day with 95°F outside air temperature.

power available. Thus, designing for VTOL at 5,000 feet and with an OAT of 95°F means that the uninstalled engine must have a sea level standard day rating ($MRP_{SL,\ V\ =\ 0}$) about 1.46 (i.e., 1/0.706) times the SHP_{VTOL} calculated previously.

A simple illustration for cruise calculations is very helpful to understand just how important an engine's lapse rate behavior is for correct engine selection. Figure 5 shows that Wayne Johnson's CAMRAD II program calculates a trend where total proprotor power (for the twin proprotor configuration) notably reduces as the cruise pressure altitude increases from 20,000 feet to 35,000 feet. The reduction comes from improving propulsive efficiency (η_{prop}) since the computation was made at constant proprotor thrust. The total engine shaft horsepower (shown as the blue line), which accounts for transmission and installation losses plus the accessory power, is several thousand horsepower more than CAMRAD II's calculated RHP. However, the trend of reduced power required with increasing pressure altitude is still evident.

Figure 5 shows that when the manufacturer's maximum rated power ($MRP_{SL,\ V\ =\ 0}$) needed to ensure that the shaft horsepower required to cruise at 425 knots at altitude is available, then the lowest cruise altitude is most favorable. The hover takeoff design point is the other consideration. Figure 5 points out that CAMRAD II's calculated RHP_{VTOL} (the solid black circle at 5,000 feet) must first be increased by about 2,000 horsepower to account for transmission and installation losses plus the accessory power (i.e., the solid blue triangle). Then the engine lapse rate factor for VTOL takeoff (LR_{VTOL}) must be applied, which leads to the solid red square point at 5,000 feet pressure altitude.

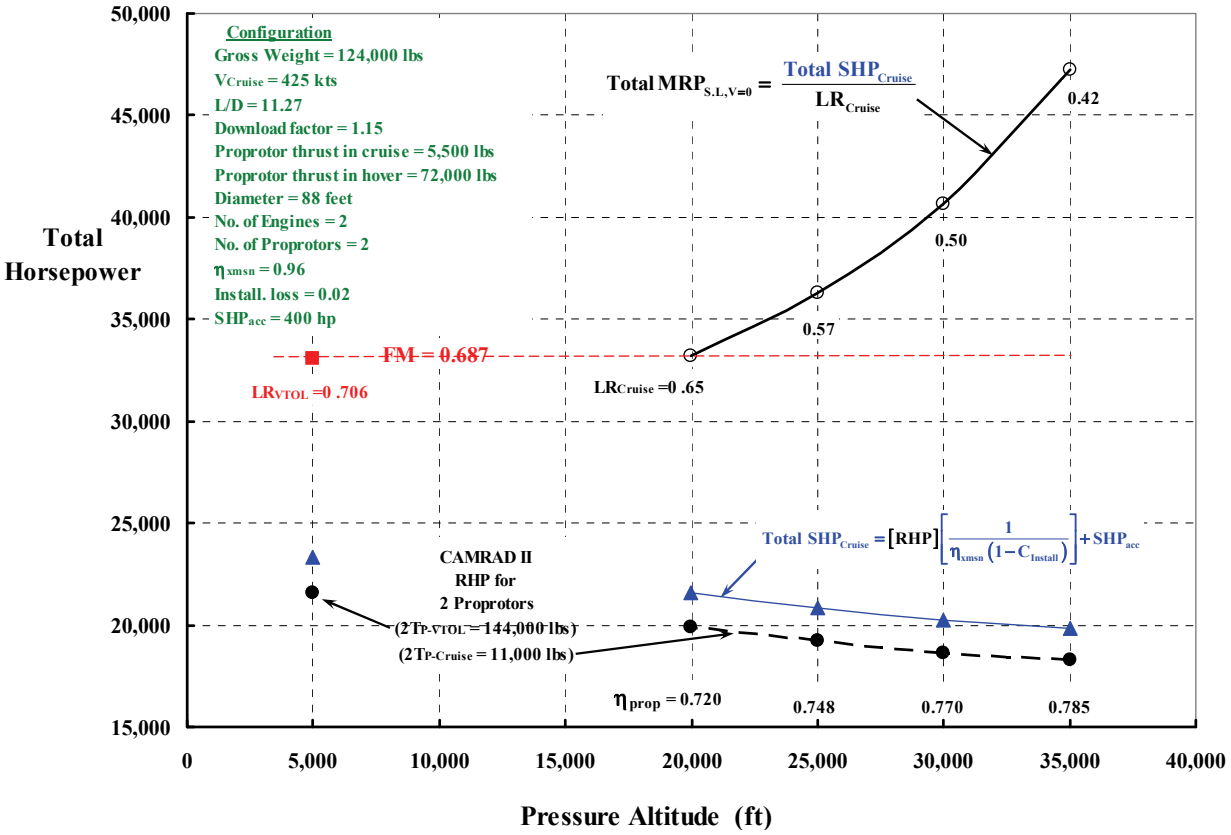

Figure 5. Cruise altitude is a very important parameter when choosing an engine's rated power (this is because of typical turboshaft engine lapse rates).

The illustration in figure 5 shows that the engine manufacturer must deliver two engines to the rotorcraft manufacturer. Each engine must be rated ($MRP_{SL,\ V\ =\ 0}$) at 16,500 shaft horsepower, and the maximum continuous rating (MCP) at sea level and zero speed must be on the order of 13,000 shaft horsepower so that the rotorcraft will cruise at 425 knots at a pressure altitude of 20,000 feet. This engine selection means that the power requirement for VTOL and cruise are well matched

However, cruising at 25,000 feet, which allows flying above even more bad weather, is generally preferred to cruising at 20,000 feet. Figure 5 shows that a cruise requirement of 425 knots at 25,000 feet would dictate more powerful engines than required for VTOL. The author believes the correct performance objective is to first minimize the amount of installed power, and secondly, to match the VTOL power requirement with the cruise power requirement.

The Primary Design Space

This design study was initiated using the elementary performance equations provide in figure 2. The inputs to these equations were, in the author's opinion, conservative relative to today's state of the art. It was felt that a proprotor Figure of Merit of 0.65 and a download factor of 1.15 coupled to an aircraft cruise lift-to-drag ratio of 13.5 with a proprotor propulsive efficiency of 0.75 would be a reasonable baseline starting point. Other key inputs chosen for this 120-passenger tiltrotor were:

Gross weight = 124,000 lb with a hover download factor of 1.15
Diameter = 88 feet
No. of engines = 2
No. of proprotors = 2
Transmission efficiency = 0.96
Installation loss = 0.02
SHP_{acc} = 400 hp

The results of these initial performance calculations are shown in figures 6, 7, and 8. It is immediately apparent from figure 6 that two engines, each having a maximum rated shaft horsepower of about 17,200 hp are required. At this $MRP_{SL,\ V\ =\ 0}$ this tiltrotor configuration will do vertical takeoffs and landings from a runway located at 5,000 feet pressure altitude with an OAT of 95°F. With this amount of installed power, the configuration should cruise continuously at 425 knots at a pressure altitude of 30,000 feet on a standard day.

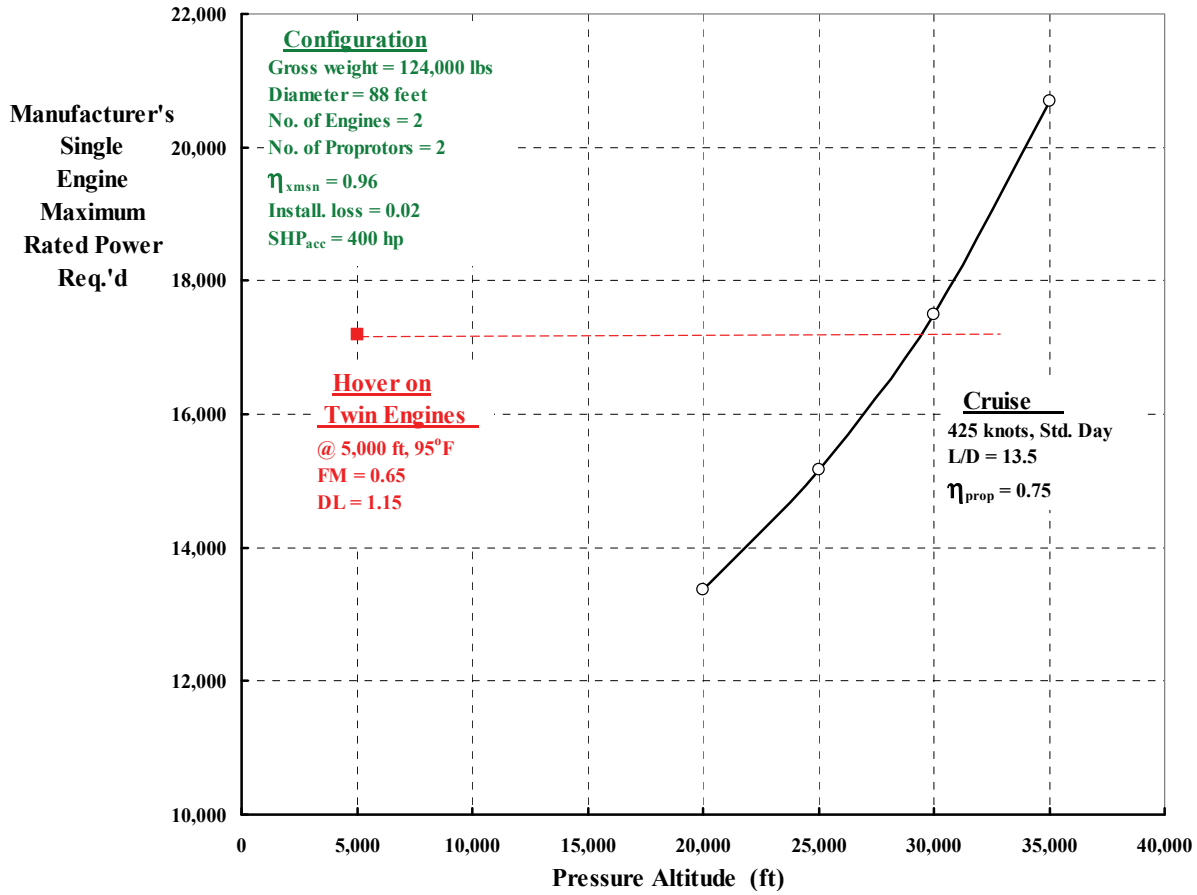

Figure 6. The smallest installed engine comes with a low cruise altitude.

The immediate follow-on questions were: (1) what happens with improved proprotors having better hover Figure of Merits; (2) how about changing the cruise speed, and (3) what improvement is obtained by increasing the configuration's cruise lift-to-drag (L/D) ratio. Answers to the first two questions are shown on figure 7. Clearly, increasing hover Figure of Merit leads to smaller engines (i.e., less installed power). Apparently, cruise speeds between 400 and 450 knots (holding the aircraft's design L/D ratio constant at 13.5) are relatively insignificant. However, the cruise altitude *is* significantly lowered as less power is installed with improving proprotor Figure of Merit while holding the design VTOL altitude at 5,000 feet and 95°F. Of course, an advantage to cruising at a lower altitude at 425 knots is that the cruise Mach number (M_{cr}) is lower, and therefore compressibility influences are more tractable. This means that high aircraft maximum L/D ratios are more easily obtained. This also means that proprotor propulsive efficiencies above 0.75 become a realistic objective.

The third question having to do with the aircraft's cruise L/D is answered with figure 8. Here you see that an increase in cruise L/D from 13.5 to 16 reduces the installed power requirement for cruise by about 3,000 shp per engine. However, it is clear that the choice of engine would be driven by the VTOL design point. This installed power for VTOL would be excessive for cruise. That is, a Figure of Merit equal to 0.75 means two engines each rated at $MRP_{SL,\ V\ =\ 0}$ of about 15,000 shp. The L/D-equals-16 configuration would cruise at 425 knots at 30,000 pressure altitude. Of course, by cruising at 25,000 feet and 425 knots the engines would be operating at a cruise power below the maximum continuous rating, and this would extend engine life and lower operating costs.

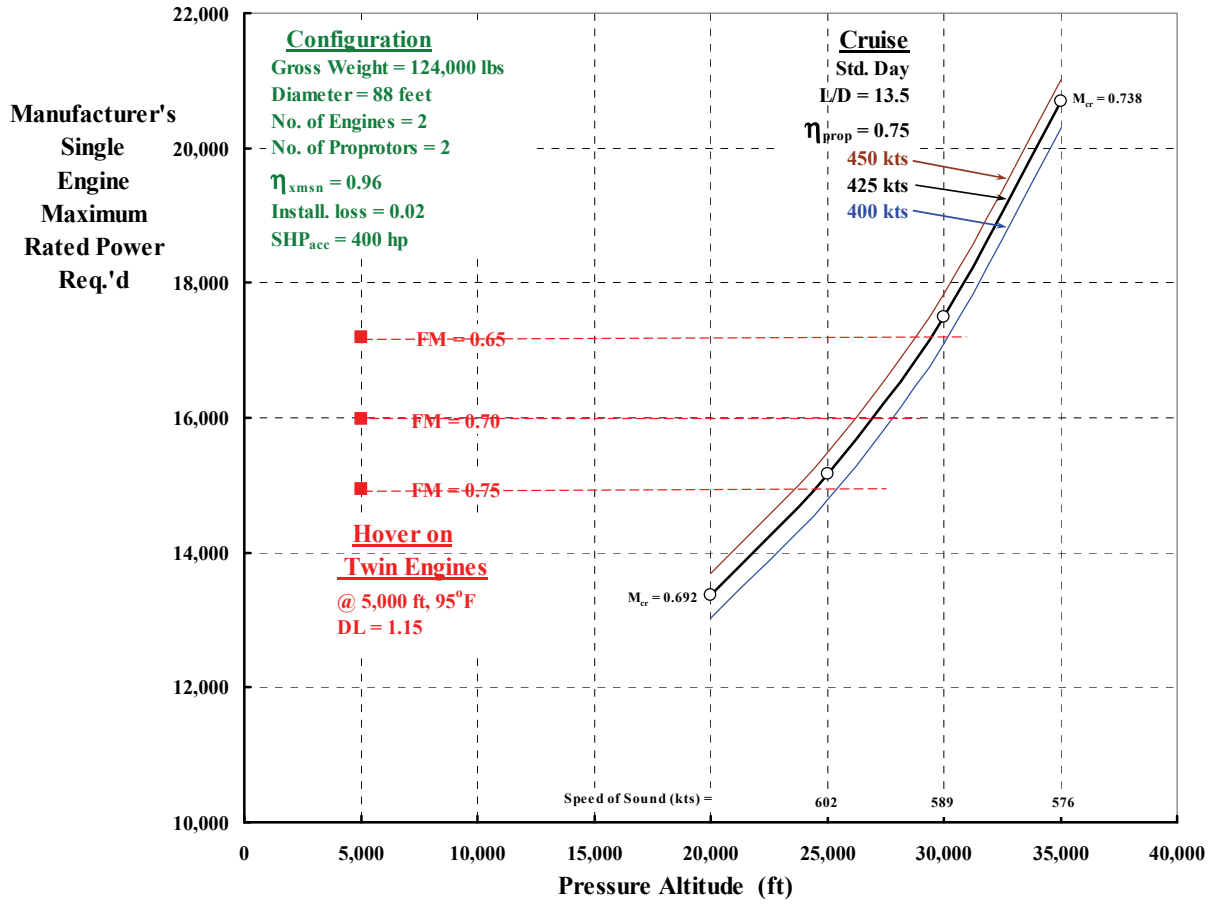

Figure 7. Cruise altitude is more influential than cruise speed for a given aircraft lift-to-drag ratio. *For a given rotor diameter*, the higher the FM the better.

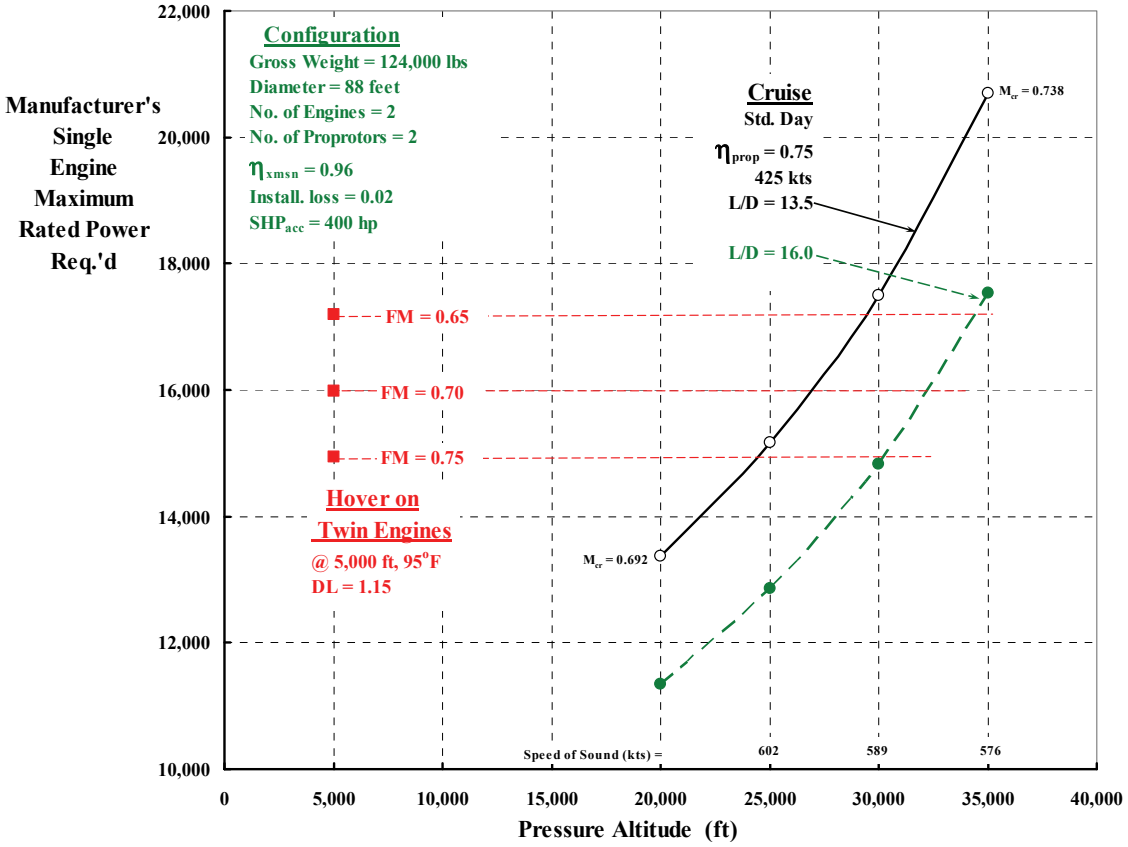

Figure 8. Maximizing aircraft lift-to-drag ratio is a key design objective.

Figure 8 raises an important point. Suppose the design takeoff criteria (say, from Denver on a day where the OAT is 95°F) were not a vertical takeoff. Rather, assume the design criterion was reduced to a short running takeoff (i.e., a STOL). Then the installed power could be based on cruising. For example, the L/D-equals-16 configuration designed to cruise at 425 knots at 25,000 feet would require two engines, each having a $MRP_{SL,\ V\ =\ 0}$ of about 13,000 shp. As you know, both tiltrotor and tiltwing aircraft have demonstrated an ability to clear a 50-foot obstacle in 500 feet or less when takeoff is done with the thrust vectors at a 30- to 45-degree angle to the flight path. Therefore, the author believes that two configurations of the 120-passenger tiltrotor must be included in future design studies.

The conclusions reached from this preliminary design space study are shown in figure 9 and table 1. First note that data points for three regional, turboprop, fixed wing aircraft are shown with solid blue triangles. While the Saab 2000 never really caught on in the face of regional jet popularity, it was considered a very "modern" turboprop airplane. Until recently, it appears that the ATR 72 series has satisfied the needs of what small airlines all over the world want. Today, the Bombardier Dash 8 Q400 is a real competitor to the ATR 72-600 as judged from reference 2.

As to the large, 120-passenger civil tiltrotor (LCTR-2005) presented in reference 1, figure 9 shows—with the solid red circle—that increasing the power loading by 50 percent from the Dash 8 Q400 and Saab 2000 levels, yields an aircraft that can hover on three of its four engines at the 5,000 feet, 95°F VTOL design condition. This LCTR-2005 configuration would cruise comfortably at 350 knots at 30,000 feet.

The preliminary sizing study completed this year has yielded the points shown in green on figure 9. These 120-passenger civil transports are identified as LCTR-2016, configurations 1 and 2. The LCTR-2016-1 is designed to takeoff vertically at 5,000 feet and 95°F. This configuration is conservatively expected to cruise at 425 knots with an L/D of 13.5. The LCTR-2016-2 is designed to takeoff as a STOL in 500 feet (or less) and then cruise at 425 knots with an L/D of 16.0. The author believes that a cruise L/D of 16 is a reasonable target. Finally, the design space falls within the green rectangle shown on figure 9.

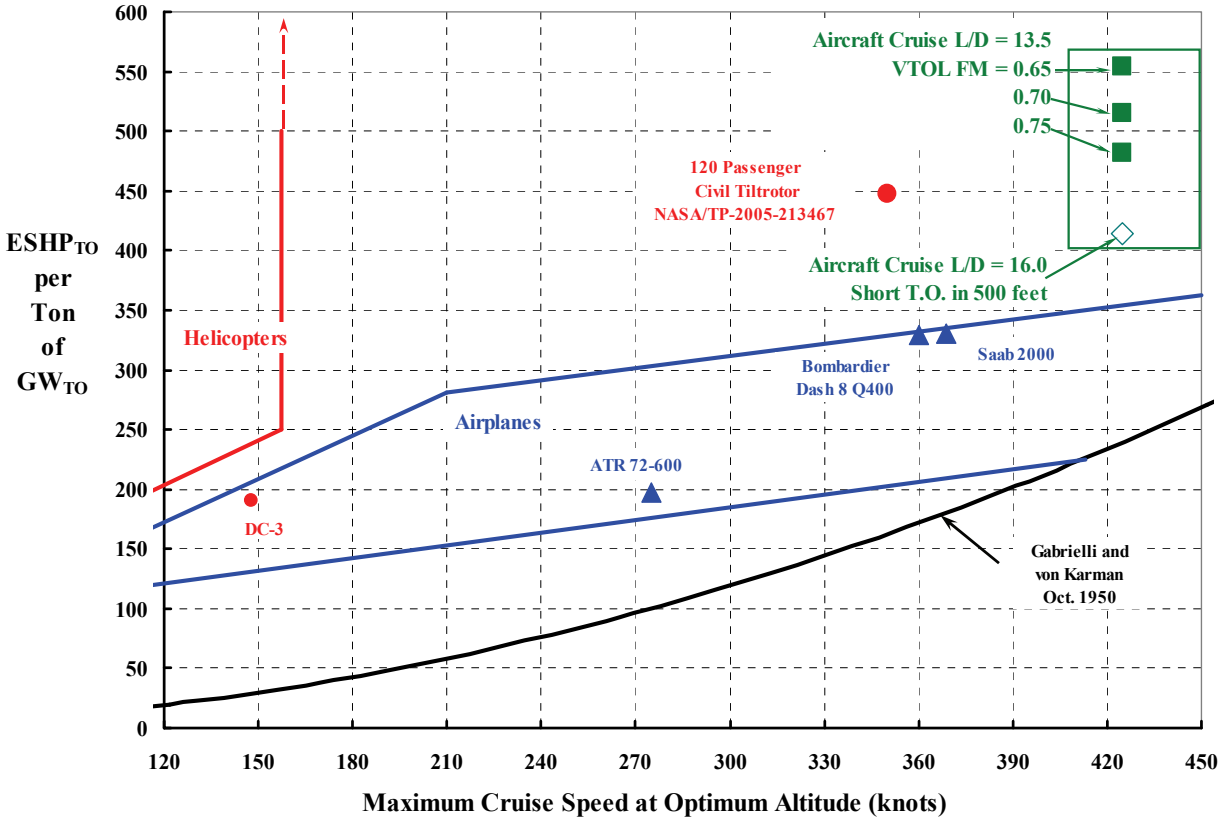

Figure 9. Designing for STOL may be better than designing for VTOL.

Table 1. Aircraft Characteristics

Item	Saab 2000	ATR72-600	Dash 8 Q400	LCTR-2005	LCTR-2016-1	LCTR-2016-2
Passengers	50	70	78	120	120	120
Takeoff distance (ft)	4,265	4,373	4,266	0	0	500
Cruise speed (kts)	370	275	360	350	425	425
Cruise altitude (ft)	25,000	20,000	25,000	30,000	27,000	25,000
Cruise L/D	na	na	na	15.0	13.5	16.0
Engines	AE 2100A	PW 127M	PW150A	tbd	tbd	tbd
No. of engines	2	2	2	4	2	2
$MRP_{SL, V=0}$ (SHP)	4,152	2,475	5,071	6,914	16,000	13,000
Propellers	Dowty	HamStd568F	Dowty R408	Rotorcraft	Rotorcraft	Rotorcraft
Prop. diameter (ft)	12.5	12.9	13.48	88.7	88.0	88.0
TOGW (lb)	50,265	50,706	61,700	123,562	124,000	124,000
Operating WE (lbs)	30,424	29,346	37,886	80,701	tbd	tbd
Wingspan (ft)	81.25	88.75	93.25	105.0	tbd	tbd
Wing area (ft^2)	600.0	626.6	679.2	1,545.0	tbd	tbd

PROPROTOR DESIGN

In their 2005 report (ref. 1), Johnson, Yamauchi, and Watts settled on two, 88.7-foot-diameter proprotors for their 120-passenger large civil tiltrotor (LCTR). Each proprotor had four blades attached to a hingeless hub and was designed to operate at 650 feet per second tip speed in hover and 350 feet per second in cruise. They found that each of the four turboshaft engines needed to have a two-speed gearbox so that the engines would operate at 100 percent RPM both in hover and in cruise. The choice of four engines was made so their design could hover out of ground effect at 5,000 feet (OAT of 95°F) with one engine inoperative (OEI). After considerable parametric studies, they found satisfactory blade chord, twist, and airfoil radial distributions were "an optimum twist of –32 deg inboard and –30 deg outboard, and an optimum taper of 0.8 (tip/root chord)." This planform geometry for their 123,562-pound-gross-weight aircraft is shown in figure 10a. The chord at the 3/4-radius station was 3.06 feet. They designed for a hover C_T/σ of 0.1557, which gave a nominal solidity (σ) of 0.0881.

The LCTR-2005 study chose to design the blade for minimum weight. With the assistance of some structural design work done at Penn State (ref. 3), they arrived at very thick airfoils as shown in figure 10b. A single blade's weight (with advanced composite materials) is quoted as 745 pounds because of the thick airfoil geometry.

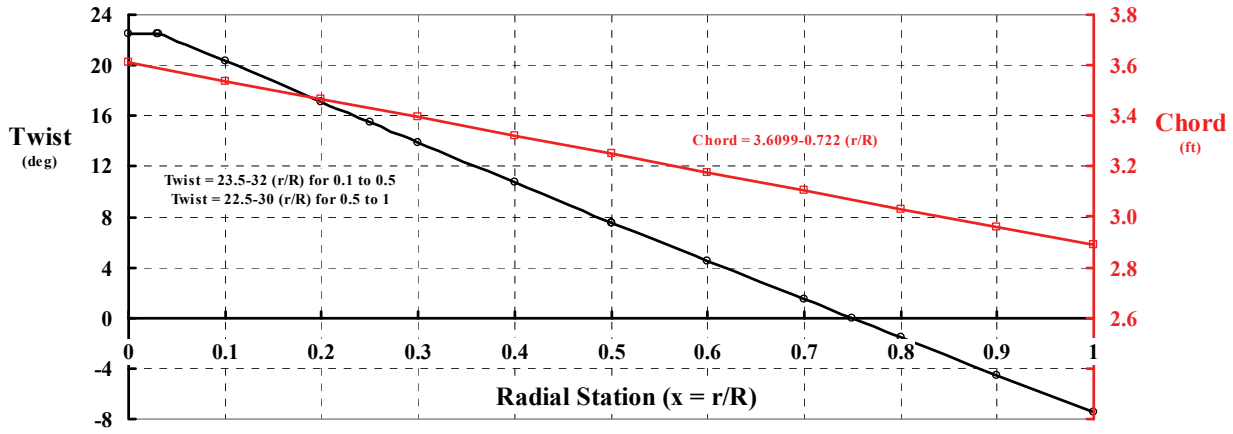

Figure 10a. LCTR-2005 blade geometry.

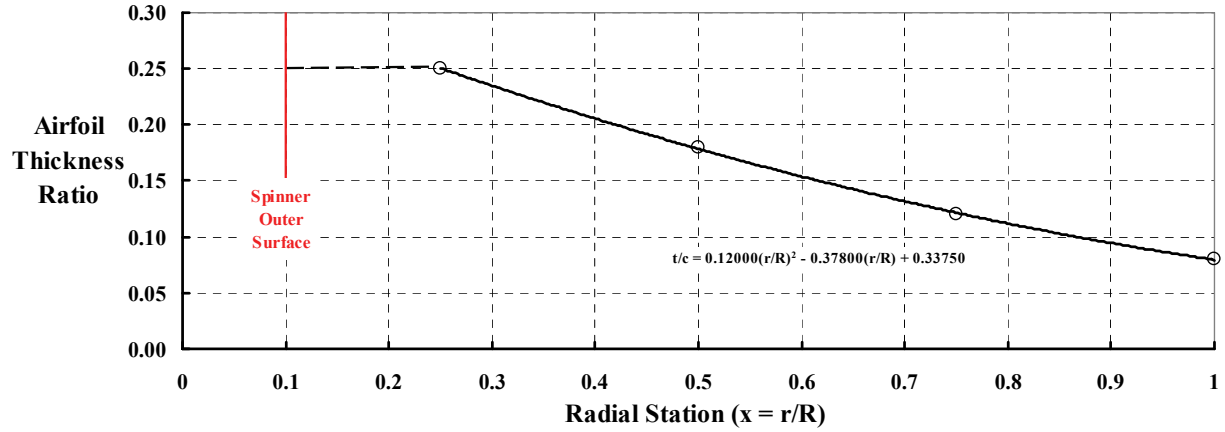

Figure 10b. LCTR-2005 blade airfoil thickness ratio distribution.

In this study of an LCTR-2016, it was elected to first strive to maximize the proprotor's propulsive efficiency (η_P), the objective being an efficiency of 0.8 at 425 knots with an 88.0-foot-diameter, four-bladed configuration. To meet this objective, it was immediately concluded that those airfoils found suitable for the 2005 LCTR design had to be replaced with supercritical airfoils. The immediate sources for aerodynamic characteristics of supercritical airfoils are references 4 through 10. Symmetrical airfoils in the NASA SC(2) 00xx series were found to be an acceptable initial choice. Additionally, it was determined that a lower solidity design having a cruise tip speed of 300 feet per second or less was going to be required.

Design Fundamentals

The design approach was based on two criteria:

1. The lift distribution must shoot for minimizing induced power, and
2. The chord and twist distribution must minimize profile power.

Help was provided first by Kenneth Hall at Duke University who used his rotor / proprotor performance optimizer (ref. 11) to find the lift distribution that minimized induced power for a four-bladed, 88-foot-diameter proprotor, at just one flight condition. He kindly computed the case and sent back the input/output data in table 2. The bound circulation and lift distribution for one blade contributing a thrust of 1,250 pounds is shown in figure 11. The induced axial, circumferential (i.e., swirl), and radial velocities for this case are shown in figure 12. The blade's lift distribution was computed from the fundamental relationship

$$(4) \qquad \frac{dL}{dr} = \rho V_r \Gamma_r = \left(\tfrac{1}{2}\rho V_r^2\right) c_r C_\ell \qquad \text{where } V_r = \sqrt{\left(V_{FP} + v_{axial}\right)^2 + \left(\Omega r + v_{circum}\right)^2}\,.$$

Keep in mind that the proprotor's total horsepower required ($RHP_{req'd.}$), when calculated by the energy method and with Hall's results, becomes

$$(5) \qquad \begin{aligned} RHP_{req'd.} &= RHP_{induced} + RHP_{useful} + RHP_{profile} \\ &= \frac{86,591}{550} + \frac{5,000 \times 717.3}{550} + 0 = 6,678\,\text{hp}\,. \end{aligned}$$

This result shows just how lightly loaded a proprotor is in cruise because the induced horsepower is only 157 hp while the useful horsepower (TV) is 6,521 hp. This leads to a propulsive efficiency ($T_P V_{FP}/RHP_{req'd.}$) of 0.976.

Table 2. Input/Output Data

Number of blades	4	
Radius	44	ft
Altitude	35,000	ft
Tip speed	350	ft/sec
Thrust	5000	lb
Velocity	717.3	ft/sec
Density	0.00072413	slug/ft^3
Coefficient of thrust	0.00927	na
Advance ratio	2.04943	na
Useful power	3,586,500	ft-lb/sec
Induced power	86,591	ft-lb/sec
Total power	3,673,091	ft-lb/sec
Efficiency	0.976	na

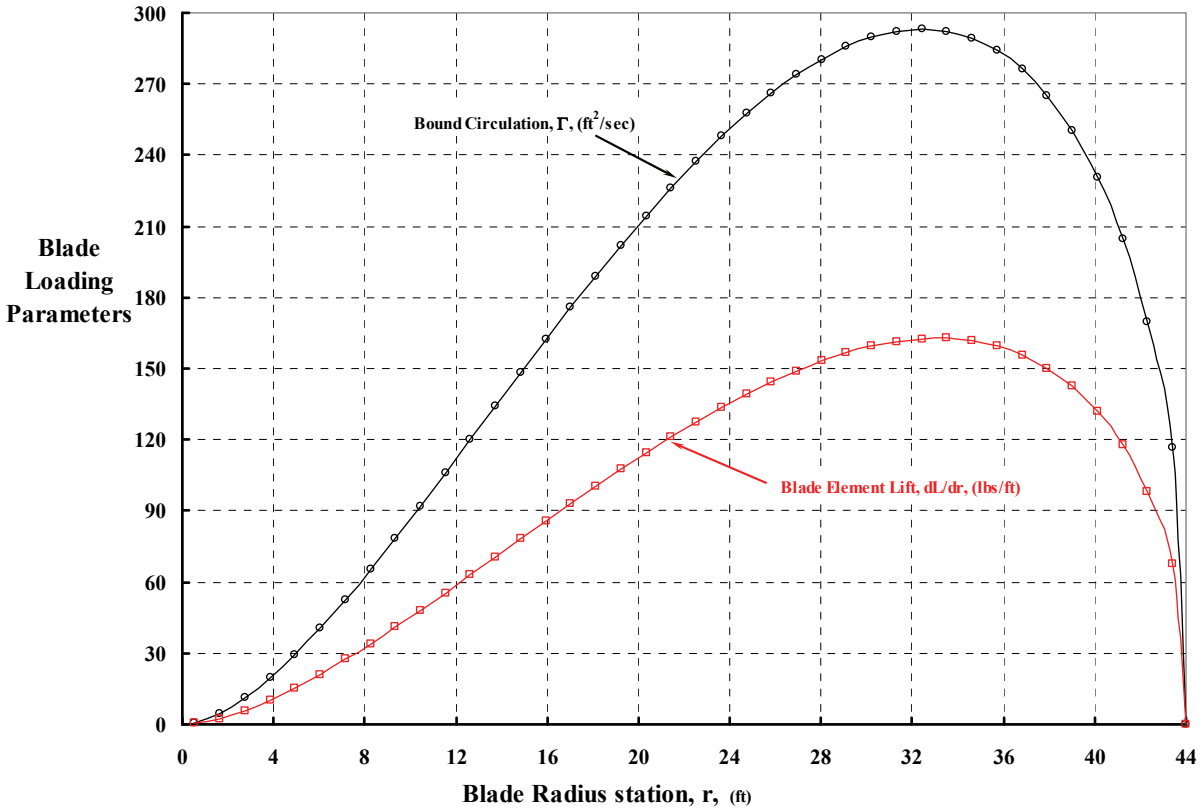

Figure 11. Kenneth Hall's optimum loading distributions.

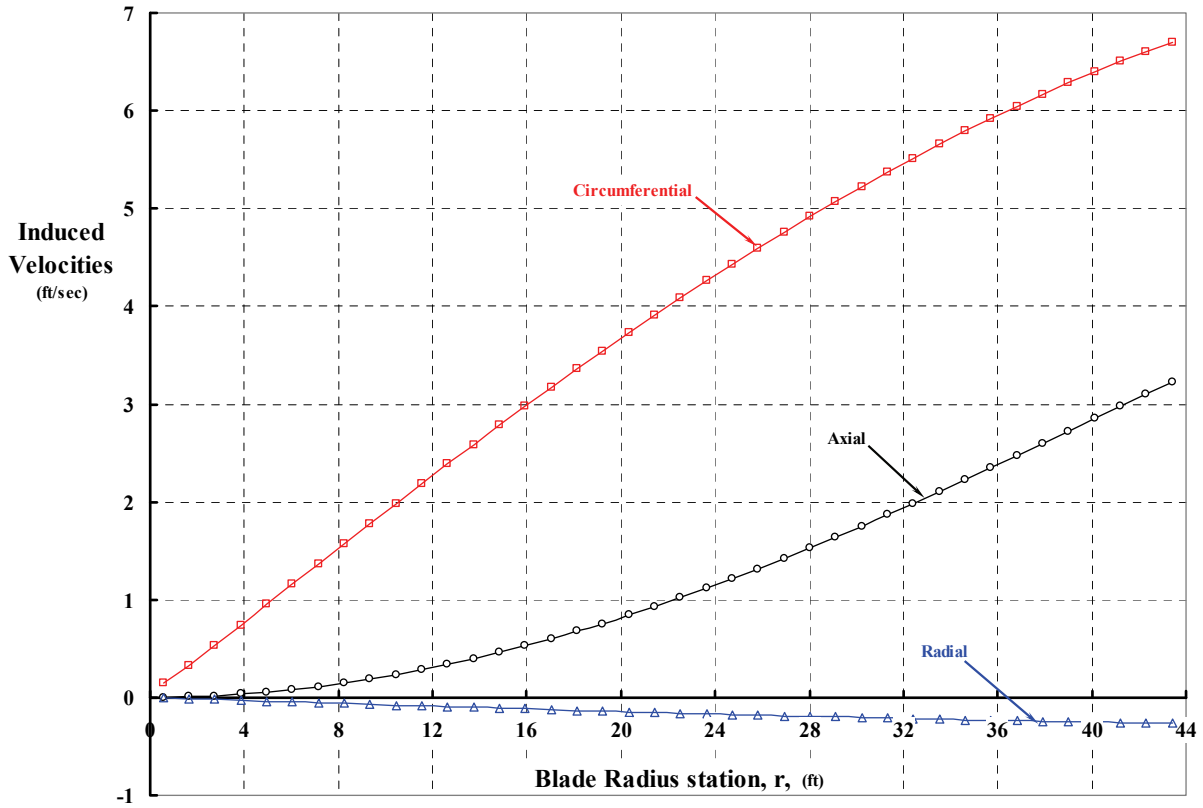

Figure 12. Kenneth Hall's induced velocities computed with optimum loading distributions.

Of course, this ideal propulsive efficiency is considerably reduced when the profile power is included. It is quite easy to make a first-order estimate of this profile power without ever knowing either a blade's twist or chord. Simply assume that every blade element will operate at a constant lift-to-drag (L/D) ratio of, say, 30. On this basis, you have

$$\frac{dD}{dr} = \frac{dL/dr}{L/D} \tag{6}$$

and the profile power is calculated as

$$RHP_{profile} = \frac{1}{550}\int_0^R \frac{dD}{dr} V_r dr = \frac{1}{550(L/D)}\int_0^R \frac{dL}{dr} V_r dr\,. \tag{7}$$

Figure 13 shows the radial distribution of blade element profile horsepower when a constant airfoil L/D of 30 is assumed. Completing the integration gives a profile power for four blades of 793 hp. Therefore, the total rotor horsepower required to produce the ideal thrust of 5,000 pounds is

$$\begin{aligned} RHP_{req'd.} &= RHP_{induced} + RHP_{useful} + RHP_{profile} \\ &= \frac{86,591}{550} + \frac{5,000 \times 717.3}{550} + 793 = 7,471\,\text{hp} \end{aligned} \tag{8}$$

and the propulsive efficiency has dropped to 0.872, assuming that each blade element airfoil is operating at a lift-to-drag ratio of 30.

It must immediately be understood that the thrust of 5,000 pounds assumed that there was no airfoil drag included in the computation. That is, the thrusting component of blade element lift

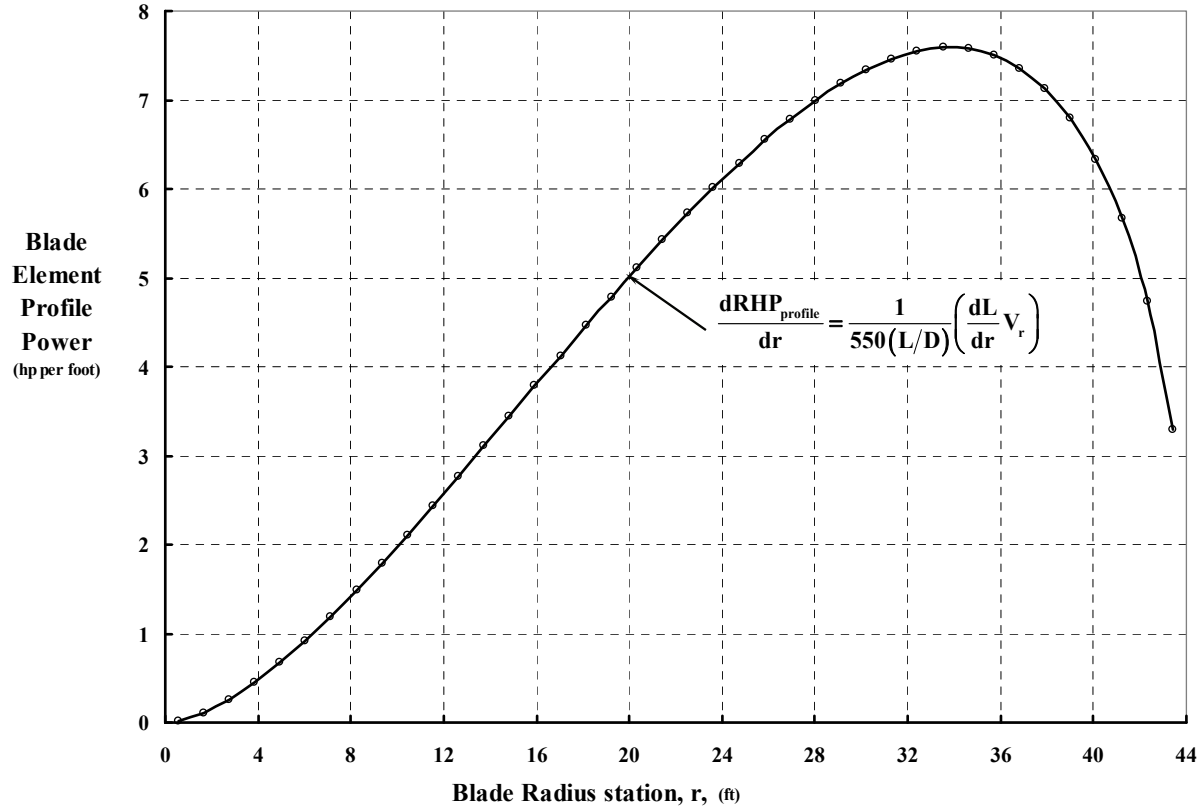

Figure 13. Airfoil L/D is the driving factor for a given design thrust.

is reduced by the negative thrusting component of airfoil drag. This classical sketch illustrates this vector problem. Blade element thrust is calculated as

(9) $$\frac{dT}{dr} = \frac{dL}{dr}\cos\phi_r - \frac{dD}{dr}\sin\phi_r .$$

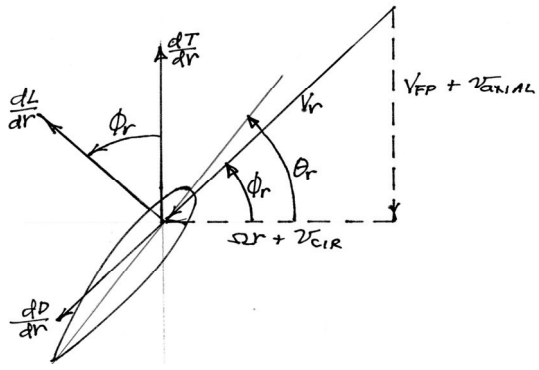

With Kenneth Hall's dL/dr distribution from figure 11 you have thrust due to blade element lift as

(10) $$T_{lift} = \int_0^R \frac{dL}{dr}\cos\phi_r dr = 5{,}000 \text{ lbs} .$$

The thrust due to blade element drag is, of course, just

(11) $$T_{drag} = -\int_0^R \frac{dD}{dr}\sin\phi_r dr = -\int_0^R \frac{dL/dr}{L/D}\sin\phi_r dr .$$

If the airfoils are all operating at the same lift-to-drag ratio (say 30, as in this example), then the thrust due to blade element drag is computed as

(12) $$T_{drag} = -\frac{1}{L/D}\int_0^R \frac{dL}{dr}\sin\phi_r dr \quad \text{where the inflow angle } \phi_r = \arctan\frac{V_{FP} + v_{axial}}{\Omega r + v_{cir}} .$$

Figure 14 provides the radial distributions of dL/dr cos ϕ_r, and dL/dr sin ϕ_r divided by airfoil L/D. Also shown is the inflow angle (ϕ_r).The integration of the thrust due to airfoil drag gives T_{drag} = – 547 pounds. Therefore, the total rotor horsepower required becomes

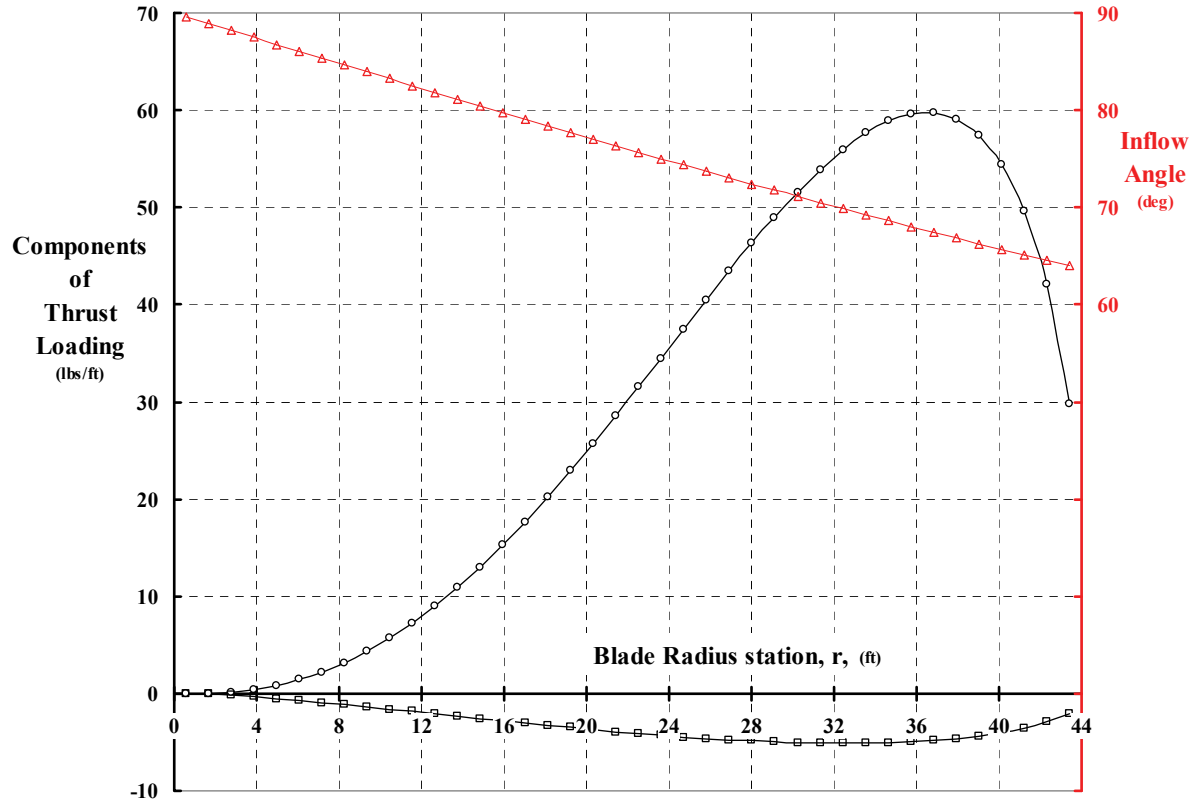

Figure 14. Thrust loss due to airfoil drag is not to be ignored.

(13) $$\mathrm{RHP}_{\mathrm{req'd.}} = \frac{86,591}{550} + \frac{(5,000-547)\times 717.3}{550} + 793 = 6,758\,\mathrm{hp}$$

and the propulsive efficiency now becomes

(14) $$\eta_P = \frac{\left(T_{\mathrm{lift}} + T_{\mathrm{drag}}\right) V_{FP} / 550}{\mathrm{RHP}_{\mathrm{req'd.}}} = \frac{(5000-547)\,717.3/550}{6,758} = \frac{5,807}{6,758} = 0.859\,.$$

Based on this simple proprotor aerodynamics performance analysis, it appears that a propulsive efficiency on the order of 0.75 to 0.8 should be attainable for the assumed configuration. To repeat, this proprotor configuration has four blades and a diameter of 88 feet. The cruise tip speed is 350 feet per second, and the twin proprotor tiltrotor is cruising at 425 knots at 35,000 feet pressure altitude on a standard day. A constant airfoil L/D of 30 has been assumed.

There are several points to keep in mind about the above analysis.

1. The optimum bound circulation provided by Kenneth Hall implies a rigid helical wake, much as Goldstein used in his work. A free wake such as that used by Johnson in CAMRAD II and by the U.S. Army's Reserve Component Automation Systems (RCAS) will account for blade vortex to blade interference in the very near wake, and this distorts the bound circulation. A different set of induced velocities are created, and the lift and drag loadings on the blade suffer.

2. The use of a constant airfoil L/D is a very unreasonable assumption at the ends of the blade. Airfoils have practical drag polars of the form

(15) $$C_d = C_{do} + \delta_1 C_\ell + \delta_2 C_\ell^2\,,$$

and parameters such as angle of attack, Mach number, and Reynolds number are very influential when trying to estimate the lift and drag coefficients; never mind the importance of selecting the correct airfoil to begin with. Because of the existence of C_{do}, no airfoil along the span can have less drag than

(16) $$\frac{dD}{dr} = \left(\tfrac{1}{2}\rho V_r^2\right) c_r C_{do}\,.$$

The proprotor is so lightly loaded compared to conventional propellers that the proprotor detailed design problem is keyed to minimizing the chord at the blade's root and over the tip region while staying within structural feasibility.

3. The inboard region of the blade has an aerodynamic environment severely influenced by the spinner that houses the hub and control subsystems. The flow around the spinner raises the local blade element velocity near the blade's root end by something on the order of 1.15. This means that helical Mach numbers near the blade root and at the blade tip are of the same order of Mach number. Thus, thin airfoils near the root (on the order of 0.15 thickness to chord ratios desired for performance) may not provide enough volume for structural and aeromechanic requirements. It appears that outboard of the 0.75 radius station the aerodynamicist has more freedom in both chord and airfoil thickness ratios. Airfoils with large pitching moments must be avoided because proprotor blades are easily twisted by aeromechanic loads.

4. The question of optimizing proprotors for cruise is an interesting one. Because the induced power is very small in comparison to the ideal power (i.e., $T_P V_{FP}$), it appears that a quite adequate optimizing objective is to get the most thrust for a given amount of profile power ($RHP_{profile}$). Stated in equation forms, the optimizing objective is

$$(17) \qquad \text{Maximize} \quad \frac{T_P}{RHP_{profile}} = \frac{b\int_0^R \left(\frac{dL}{dr}\cos\phi_r - \frac{dD}{dr}\sin\phi_r\right)dr}{\frac{b}{550}\int_0^R \frac{dD}{dr}V_r dr}$$

where the number of blades is denoted as (b). The first thing to notice here is that getting each blade element to produce thrust leads to rewriting the thrust equation in the following form:

$$(18) \qquad \begin{aligned} T_P &= b\int_0^R \left(\frac{dL}{dr}\cos\phi_r - \frac{dD}{dr}\sin\phi_r\right)dr = b\int_0^R \frac{dL}{dr}\cos\phi_r\left(1 - \frac{\frac{dD}{dr}\sin\phi_r}{\frac{dL}{dr}\cos\phi_r}\right)dr \\ &= b\int_0^R \frac{dL}{dr}\cos\phi_r\left[1 - \frac{1}{(dL/dD)_r}\tan\phi_r\right]dr \end{aligned}$$

Of course, two things are a given in this thrust equation: first, every blade element should be operating at a positive dL/dr, and second, the inflow angle (ϕ_r) lies between 0 and plus 90 degrees in cruise flight. Most informatively, if every blade element is to contribute its fair share to the blade's integrated thrust, then it is clear that

$$(19) \qquad \left[1 - \frac{1}{(dL/dD)_r}\tan\phi_r\right] > 0 \qquad \text{or} \quad (dL/dD)_r > \tan\phi_r \qquad (dL/dD)_r > \frac{V_{FP} + v_{axial}}{xV_t + v_{cir}}.$$

Consider the following numerical result. Suppose the wake-induced velocities V_{axial} and V_{cir} are assumed small enough that their contributions are zero. With this assumption, it is fair to say that $(dL/dD)_r > V_{FP}/xV_t$. Now suppose the cruise flight condition is V_{FP} = 425 knots = 718 feet per second with the proprotor tip speed (V_t) at 300 feet per second. Then $(dL/dD)_r > 2.39/x$, and as the blade's root end is approached, say x = r/R = 0.1, it appears that the root end airfoil must have an $(dL/dD)_r > 23.9$. At the blade's tip where x = r/R = 1.0, airfoils operating at relatively poor lift-to-drag ratios *might* be tolerated.

PROPROTOR CONCEPTUAL DESIGN RESULTS TO DATE

The first iteration of a proprotor for the LCTR-2016 has been completed. This iteration would not have been possible without Wayne Johnson's considerable help. Wayne ran a number of cases with his CAMRAD II program using C81 airfoil tables obtained with C81Gen/ARC2D. The key results of this first iteration are discussed next.

This cruise performance study concentrated on proprotor diameters of 88.0 feet down to 76.0 feet and pressure altitudes from 20,000 to 35,000 feet. The tip speed for all configurations was held constant at 300 feet per second, and all configurations had four blades. Figure 15 defines the chord and twist while figure 16 provides the airfoil thickness ratio arrived at after considerable detailed trade studies. This geometry remained the same for all configurations regardless of diameter. This means that the proprotor's hover thrust and torque weighted solidities vary with diameter according to

(20) $$\sigma_{thrust} = \frac{b}{\pi R}\left[\frac{3}{1-x_c^3}\int_{xc}^{1} c_x x^2 dx\right] = \frac{4}{44\pi}[3.756] = 0.1087 \qquad \sigma_{torque} = \frac{b}{\pi R}\left[\frac{4}{1-x_c^4}\int_{xc}^{1} c_x x^3 dx\right] = \frac{4}{44\pi}[3.667] = 0.1061$$

Two cruise design thrust values were selected. The first assumed the aircraft would cruise at a lift-to-drag ratio of 11.27, which gives a total aircraft drag of about 11,000 pounds using the assumed gross weight of 124,000 pounds. Therefore, each of the two proprotors must contribute a design thrust of 5,500 pounds. The second design thrust of 3,875 pounds was based on the aircraft cruising at an L/D of 16.0.

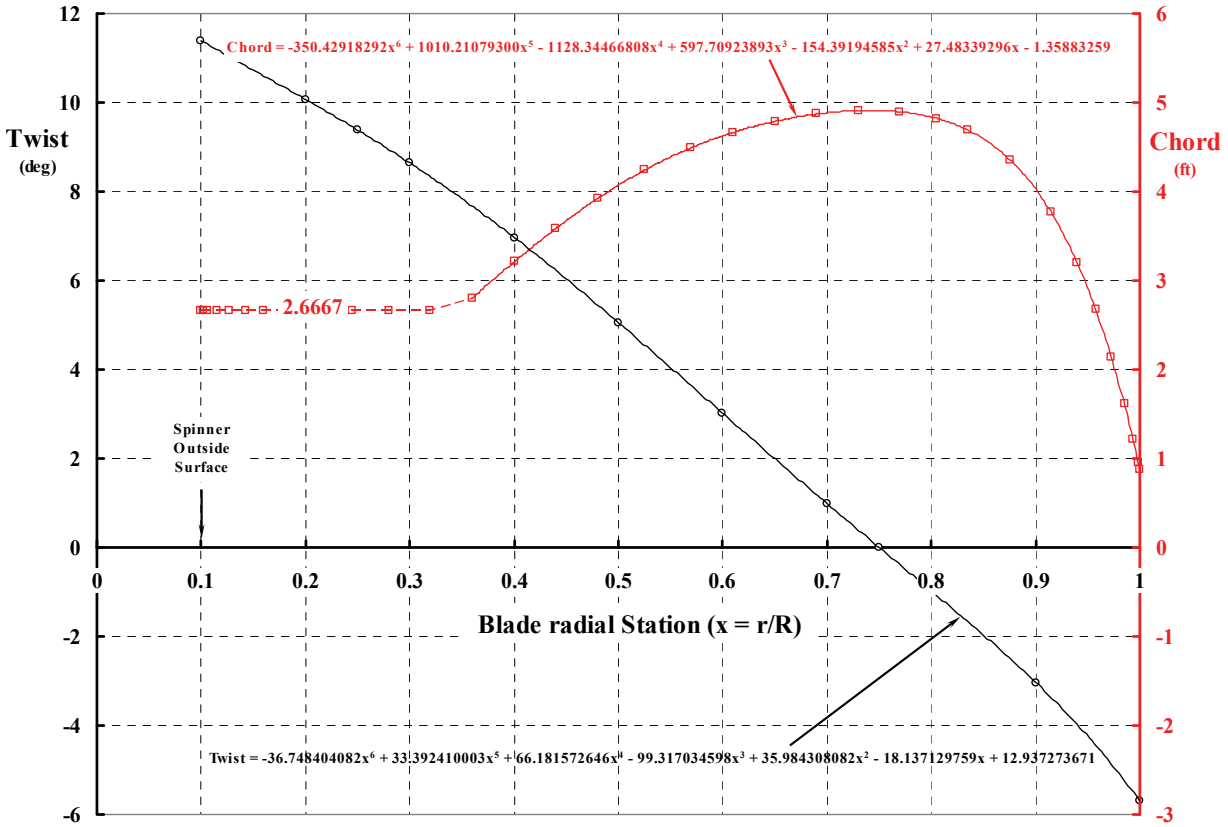

Figure 15. Design 1's twist and chord blade geometry is well suited for cruise.

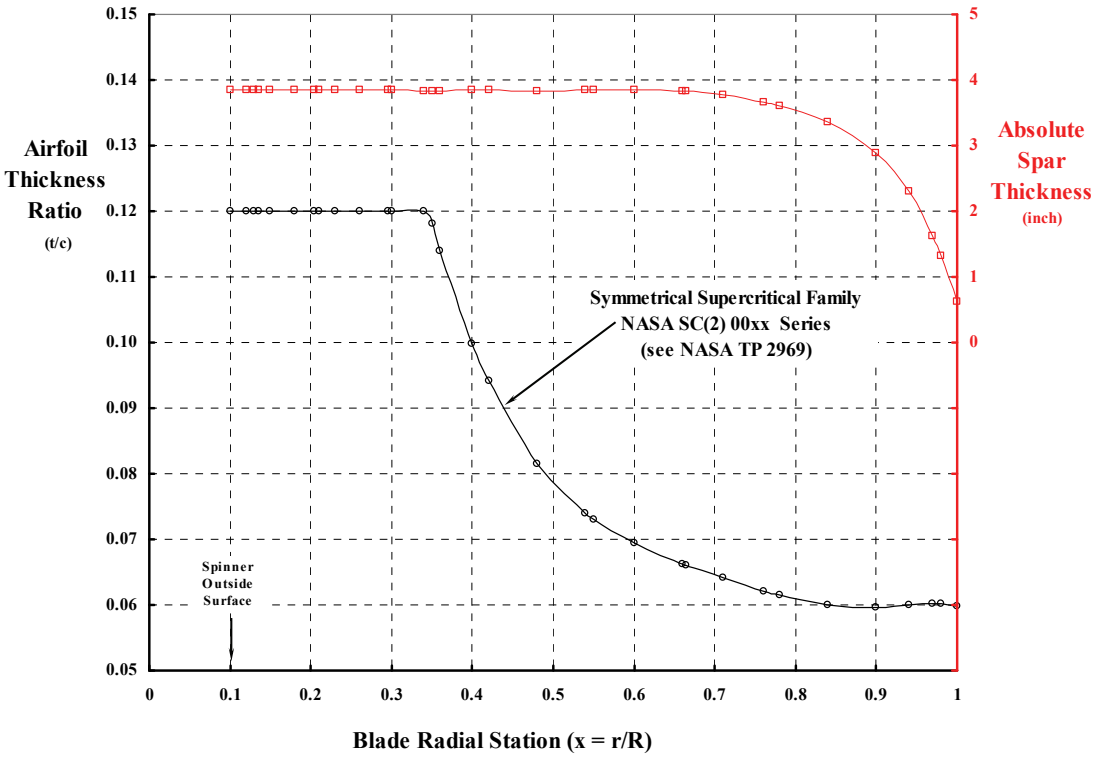

Figure 16. Design 1's airfoil thickness ratio and spar thickness blade geometry is well suited for cruise.

The performance calculations were made by Wayne Johnson with his CAMRAD II program. For the cruise calculations, the blade was divided into 32 radial stations. Because CAMRAD II requires airfoil lift, drag, and pitching moment data, a C81 deck was prepared for each of the 32 radial stations based on one given operating condition. The chosen condition leads to distributions of Reynolds and Mach numbers shown in figure 17. As a first approximation, the four baseline airfoils were assigned to the radial spans shown in figure 17.*

As mentioned earlier, the NASA SC(2)-00xx series of airfoils were chosen for this proprotor conceptual design study. The aerodynamic characteristics given to CAMRAD II in C81 deck format are included here in Appendix B. The airfoil lift coefficient and associated lift-to-drag-ratio behavior are shown in figures 18, 19, 20, and 21. The airfoil data was computed with C81Gen/ARC2D at the specific Reynolds and Mach numbers shown in figure 17. Optimum airfoil characteristics are shown in figure 22.

The airfoil summary properties shown in figure 17 were used as a key barometer of where each of the four airfoils should be placed along the blade's radius. Keeping in mind the structures' requirements, the absolute blade spar thickness shown in figure 16 was able to be maintained while tailoring the distribution of airfoil thickness ratio as shown.

*Of course, CAMRAD II computations at any other operating condition and blade chord and airfoil geometry require a completely new set of C81 decks, which were not prepared at this time. A more careful refinement of the proprotor blades' aerodynamics depends on a much more extensive C81 airfoil data set from which the CAMRAD II program could draw upon. Note that, in the author's view, proprotor design in much further detail would be greatly helped if comprehensive codes such as CAMRAD II and RCAS had a direct connection to the CFD program and calculated the airfoil aerodynamics directly. Using OVERFLOW to help the design process would be even better because a configuration would be modeled quite accurately.

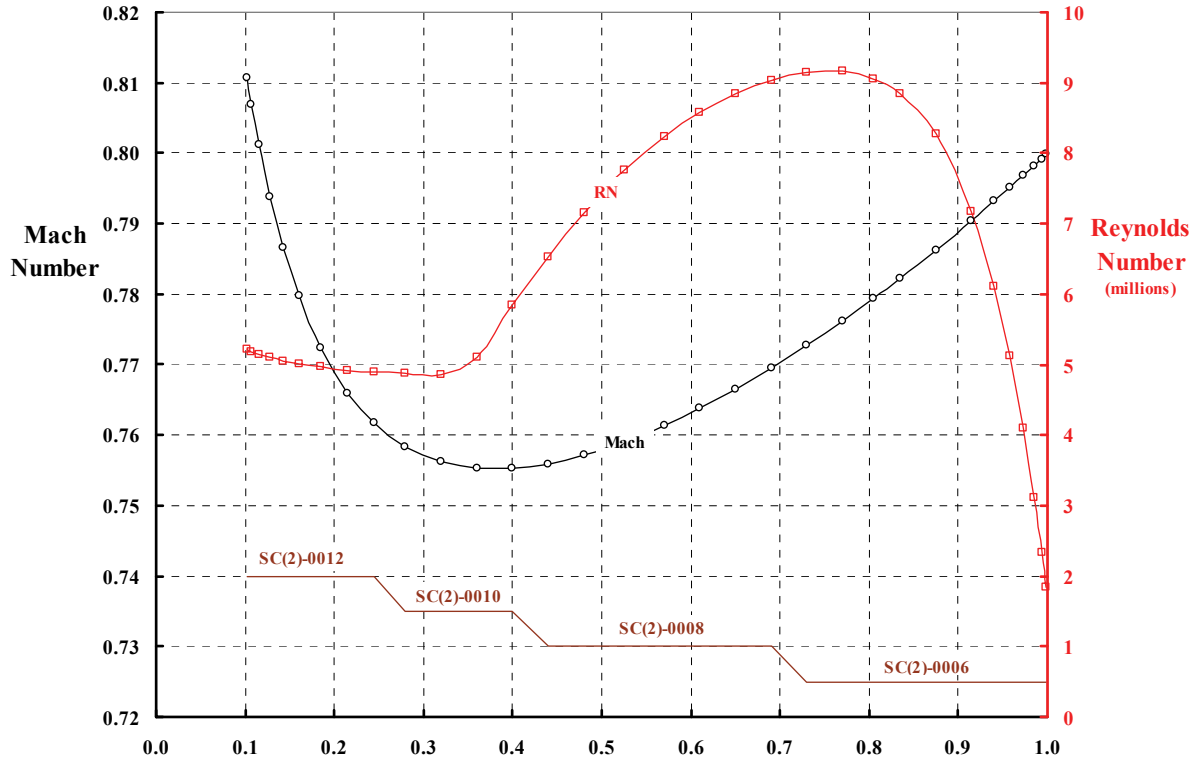

Figure 17. Design 1 blade element operating at Mach and Reynolds number conditions.

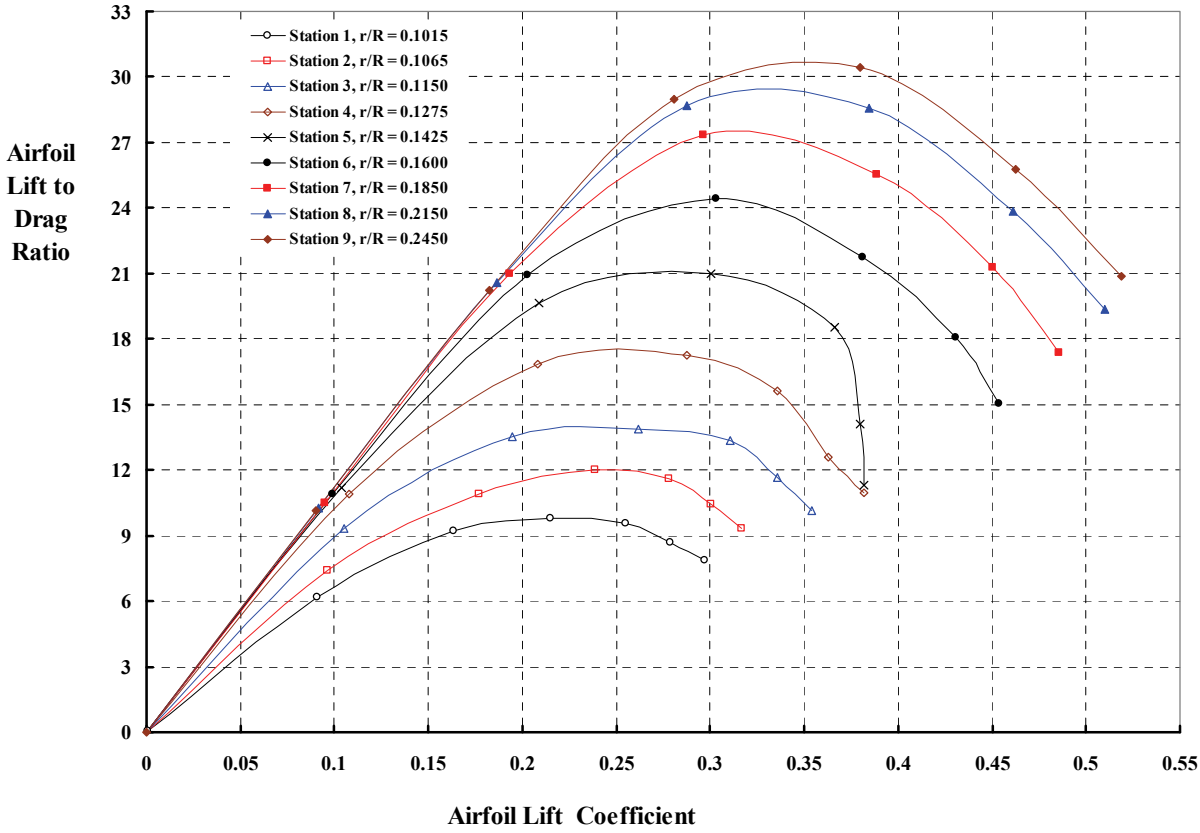

Figure 18. NASA SC(2)-0012 aerodynamic characteristics (fully turbulent model).

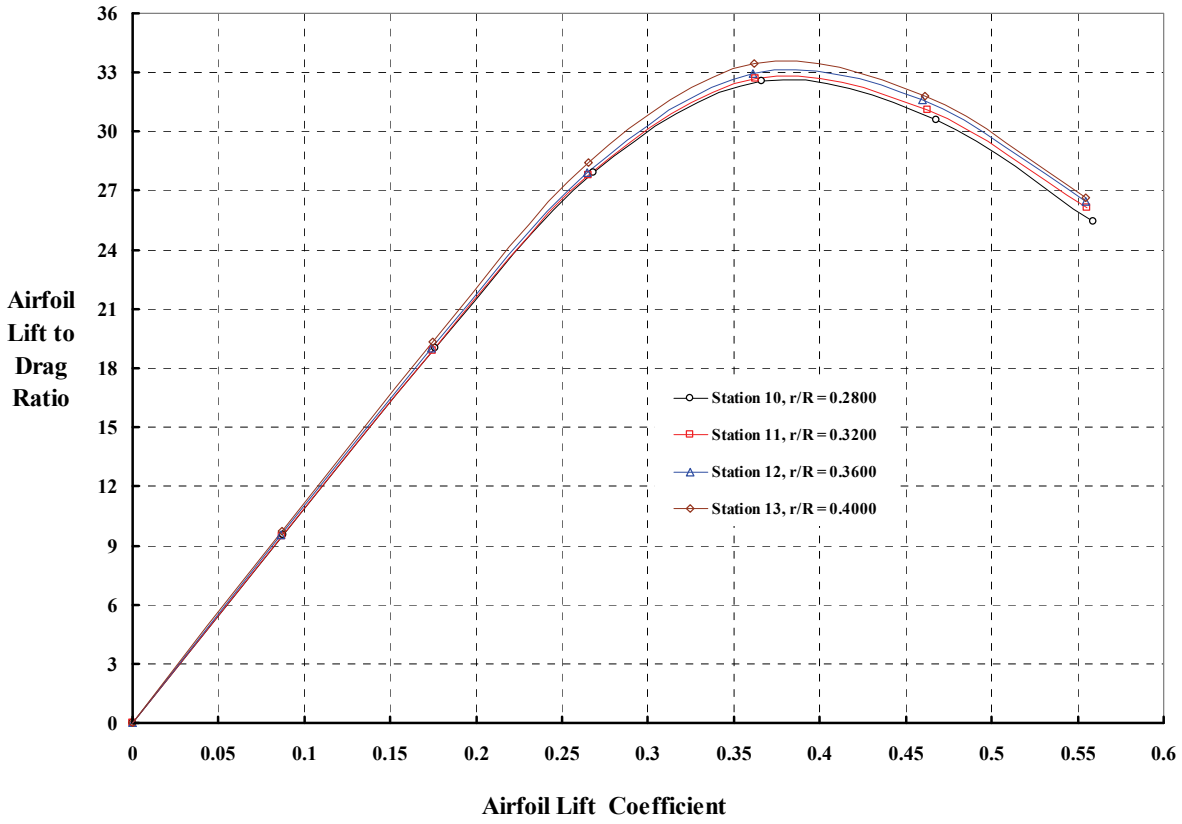

Figure 19. NASA SC(2)-0010 aerodynamic characteristics (fully turbulent model).

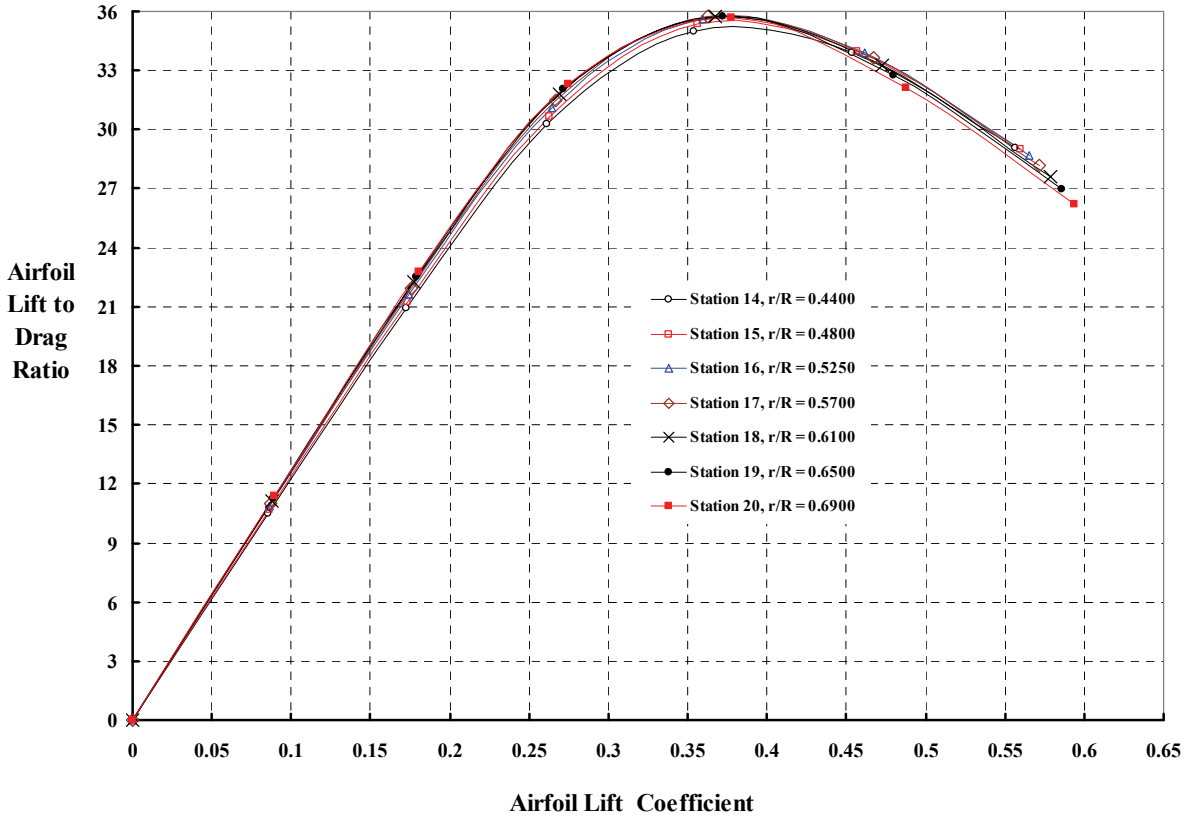

Figure 20. NASA SC(2)-0008 aerodynamic characteristics (fully turbulent model).

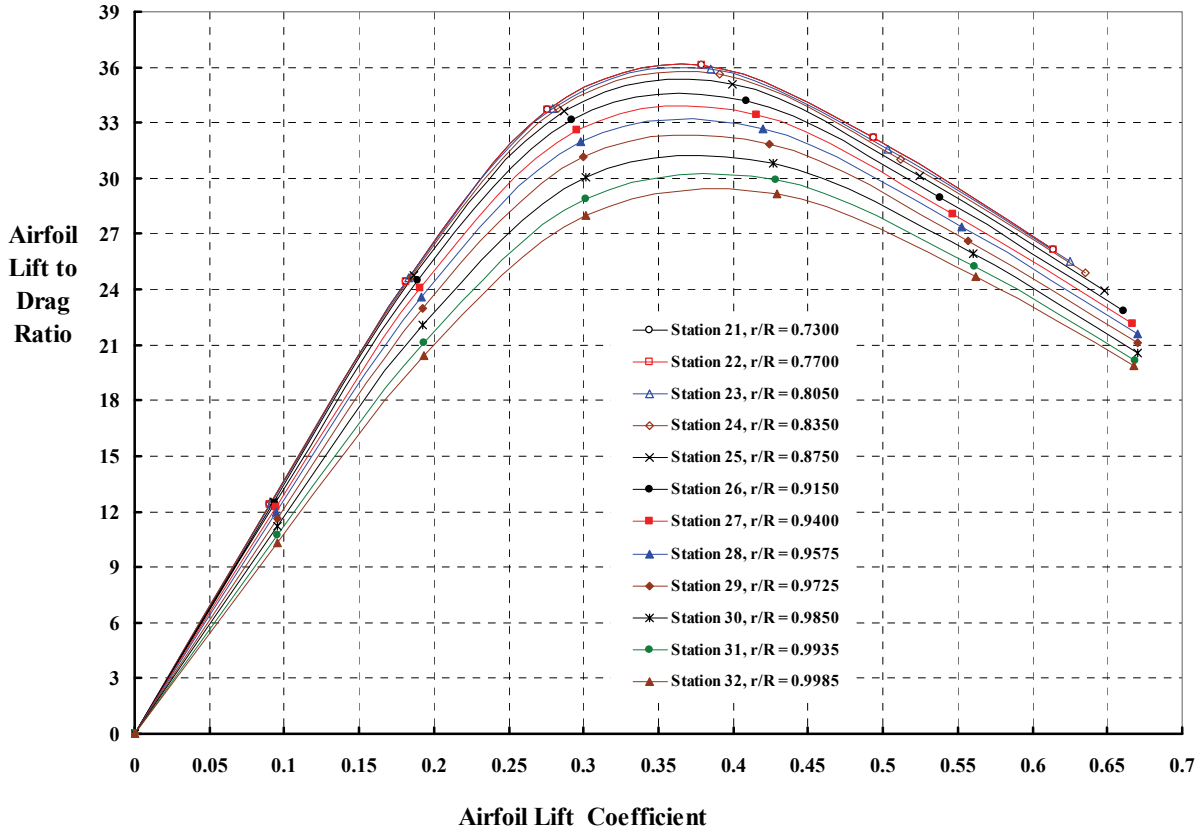

Figure 21. NASA SC(2)-0006 aerodynamic characteristics (fully turbulent model).

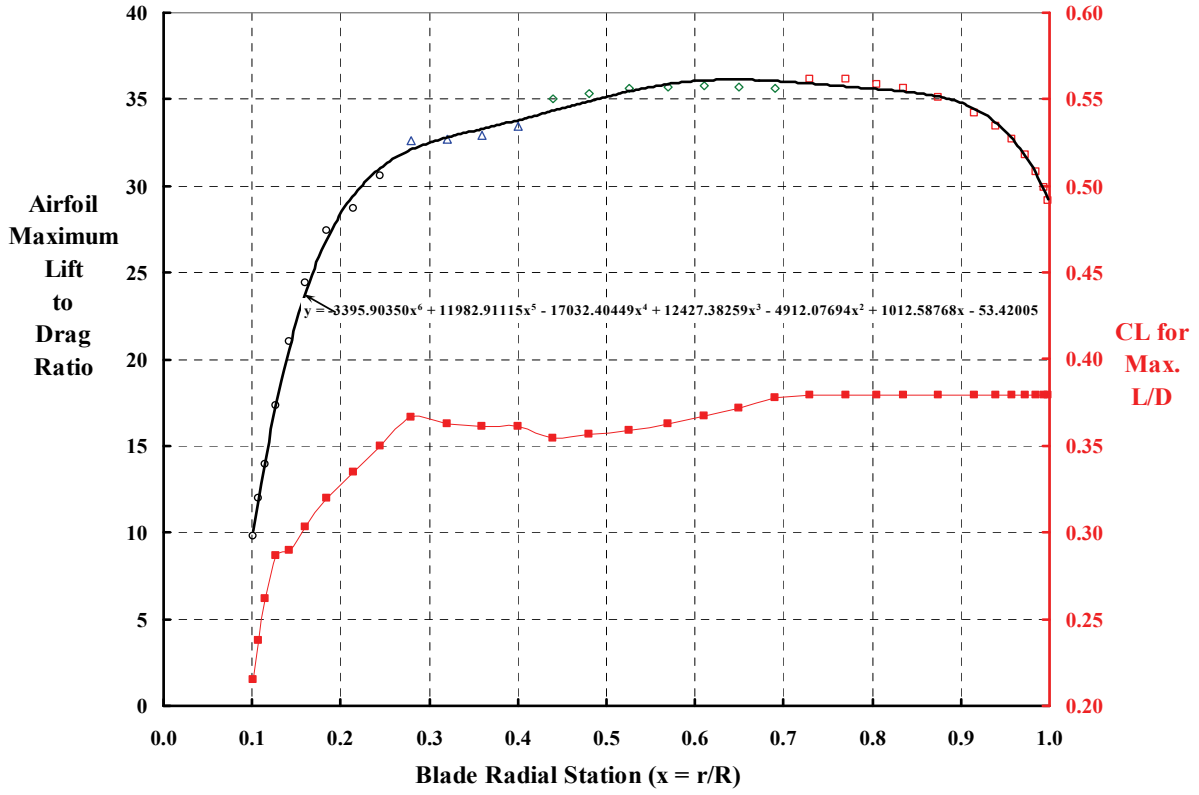

Figure 22. Optimum airfoil aerodynamic characteristics to shoot for (fully turbulent model).

Hover performance calculations by CAMRAD II were also wanted for this study. C81Gen/ARC2D was used to obtain airfoil lift, drag, and pitching moment for the blade geometry defined in figures 15 and 16, but at a tip speed of 800 feet per second. This calculation was made for the 5,000-foot pressure altitude and an OAT of 95°F design condition. The airfoil force and moment data used for the hover CAMRAD II calculation is shown in Appendix C.

The output from CAMRAD II (provided by Wayne Johnson) clearly showed the estimated performance for this first proprotor design, should it have any diameter in the range between 76 and 88 feet and at pressure altitudes from 20,000 to 35,000 feet in cruise. Figure 23 shows a single proprotor's horsepower required (RHP) in hover at 5,000 feet and OAT of 95°F, versus a single proprotor's cruise horsepower required assuming a gross weight of 124,000 pounds and a cruising speed of 425 knots with two design thrusts.

The single proprotor RHP was then used to find the required engine size (i.e., $MRP_{SL,\ V=0}$). These results are shown in figure 24. As noted earlier, the adjustment made to get from RHP to $MRP_{SL,\ V=0}$ must account for the estimated engine lapse rates shown in figures 3 and 4, and the aircraft configuration defined as:

Gross weight = 124,000 lb with a hover download factor of 1.15
No. of blades per proprotor = 4
Hover tip speed = 800 fps
Cruise tip speed = 300 fps
No. of engines = 2
No. of proprotors = 2
Gearbox configuration = two-speed (one each per engine)
Transmission efficiency = 0.96
Installation loss = 0.02
SHP_{acc} = 400 hp

It was concluded from figure 24 that each of the two proprotors must be at least 88 feet in diameter. If the airframe has a poor cruise lift-to-drag ratio on the order of 11 to 12, then the design cruise altitude is probably 20,000 feet, and each engine must have an $MRP_{SL,\ V=0}$ of 16,500 shp so that both hover and cruise design conditions are met. This is not a completely satisfactory solution because the horsepower per ton of gross weight is about

$$\frac{ESHP_{TO}}{GW_{TO}\text{ in tons}} = \frac{2\times 16,500}{124,000/2,000} = 532$$

since the horsepower to hover is rather large (in part because the Figure of Merit equals 0.687). This suggests that the proprotor designed for cruise has compromised performance in hover.

If the airframe cruise lift-to-drag ratio were on the order of 16 (typical of turbofan and turboprop civil airliners), then an aircraft cruising at 425 knots at 25,000 feet would only need engines rated at 14,000 shp each, whereupon

$$\frac{ESHP_{TO}}{GW_{TO}\text{ in tons}} = \frac{2\times 14,000}{124,000/2,000} = 452\,.$$

This means that the proprotor's performance must be improved so that the hover RHP per proprotor at 5,000 feet, OAT of 95°F is on the order of 9,100 hp—assuming the diameter remains at 88 feet. Achieving a Figure of Merit of 0.75, without impairing cruise performance, appears to be a necessary next step in the study.

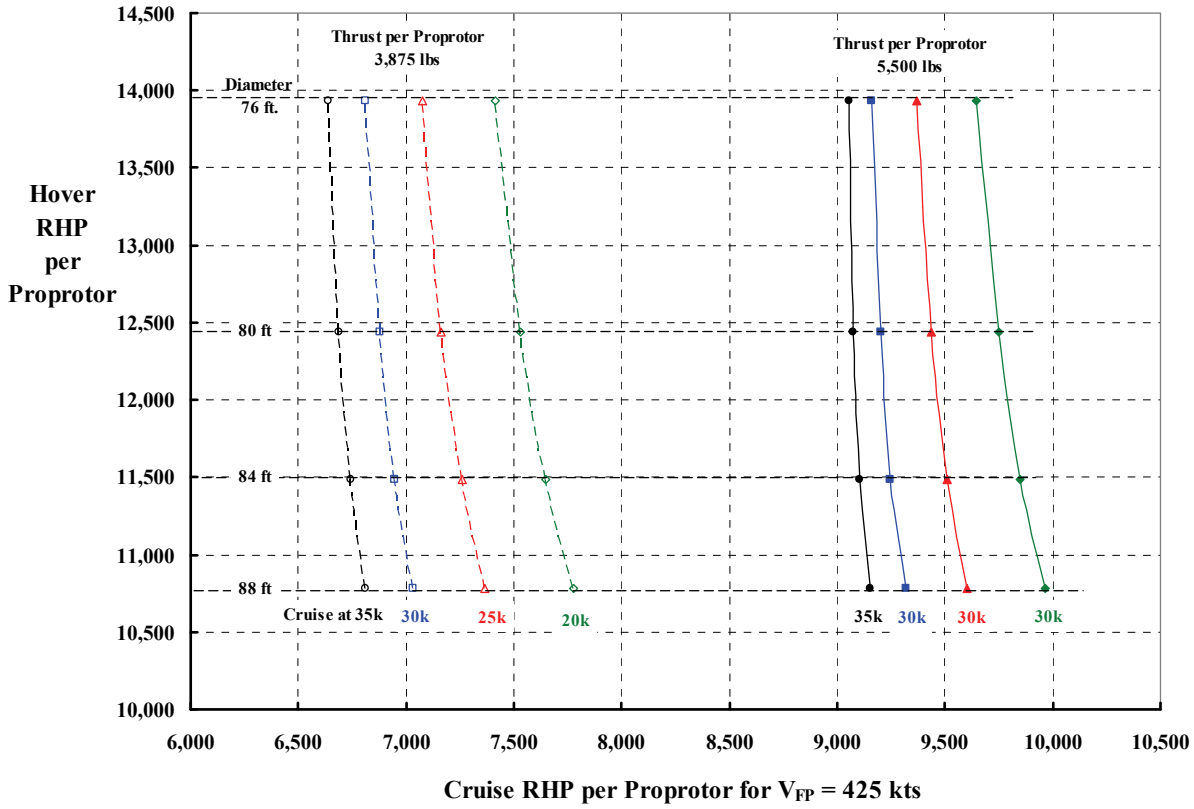

Figure 23. Proprotor performance trends.

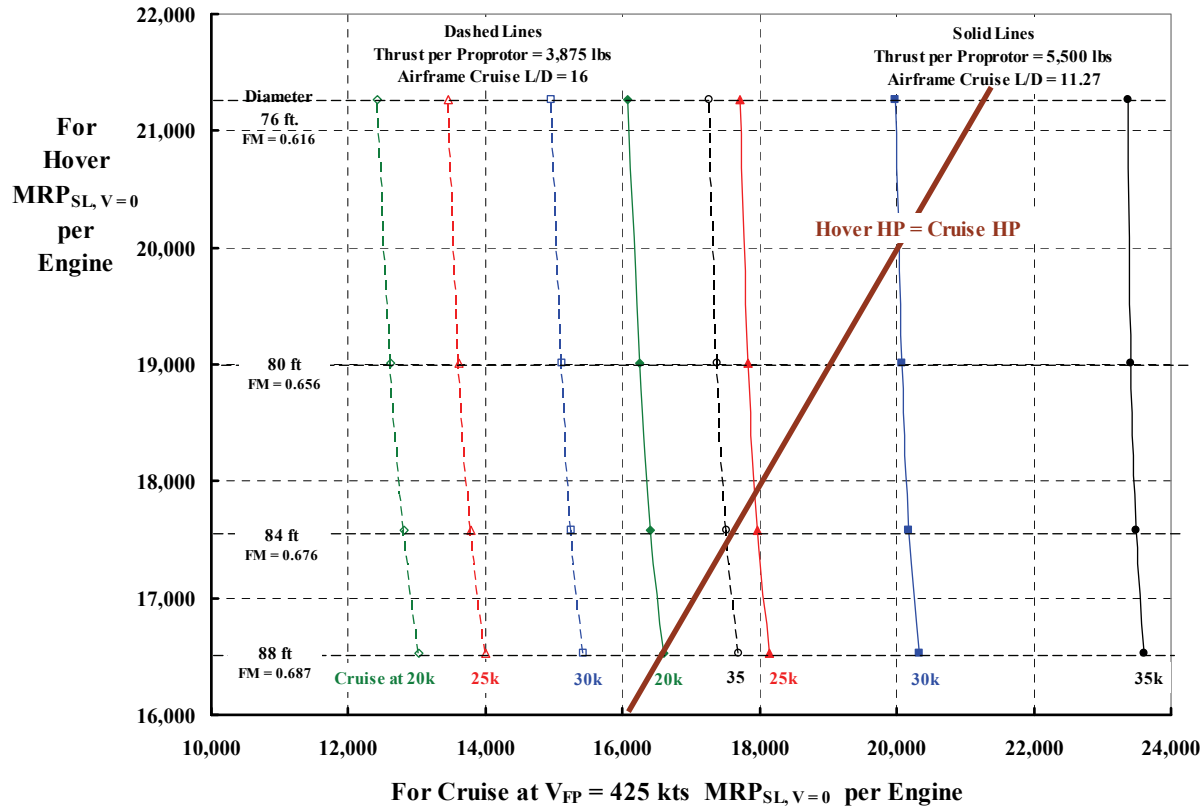

Figure 24. Maximum installed power trends.

Of particular interest was how each of the four blades was loaded in cruise versus the loading in hover. To pursue this investigation, two of the 88-foot-diameter proprotors were selected (with a tip speed of 300 feet per second) cruising at 25,000 feet and propelling an aircraft having an L/D of 16.0. The hover condition was 5,000 feet, 95°F, and the tip speed was 800 feet per second. The radial distribution of several key aerodynamic parameters was studied, beginning with the lift coefficient and Mach number parameters. The contrast in these two fundamental parameters is quite stark as figure 25 shows. Two facts immediately become apparent from figure 25:

1. In cruise, the blades are so lightly loaded that the maximum lift coefficient along a blade is below 0.2. But the airfoils should be operating at a lift coefficient of at least 0.35 to obtain the maximum lift-to-drag ratio as figure 22 indicates.

2. In hover, the trailing blade vortices are creating a downwash/upwash flow environment outboard of the 0.75 radius station. This blade-to-blade vortex interference drives the lift coefficient to very high values outboard of the 0.85 radius station, which is where the SC(2)-0006 was placed. Figure C-4 in Appendix C (or even figure 21) shows that this airfoil is only adequate if the lift coefficient is below, say, 0.5, considering the Mach number over this portion of the span.

The blade element forces (i.e., dT/dr and $dD_{inplane}/dr$) were the second parameters studied. These two forces are shown in figures 26 and 27. The thrust loading reflects the fact that the thrust in hover is 13 times the thrust in cruise, and this, of course, is the typical proprotor design

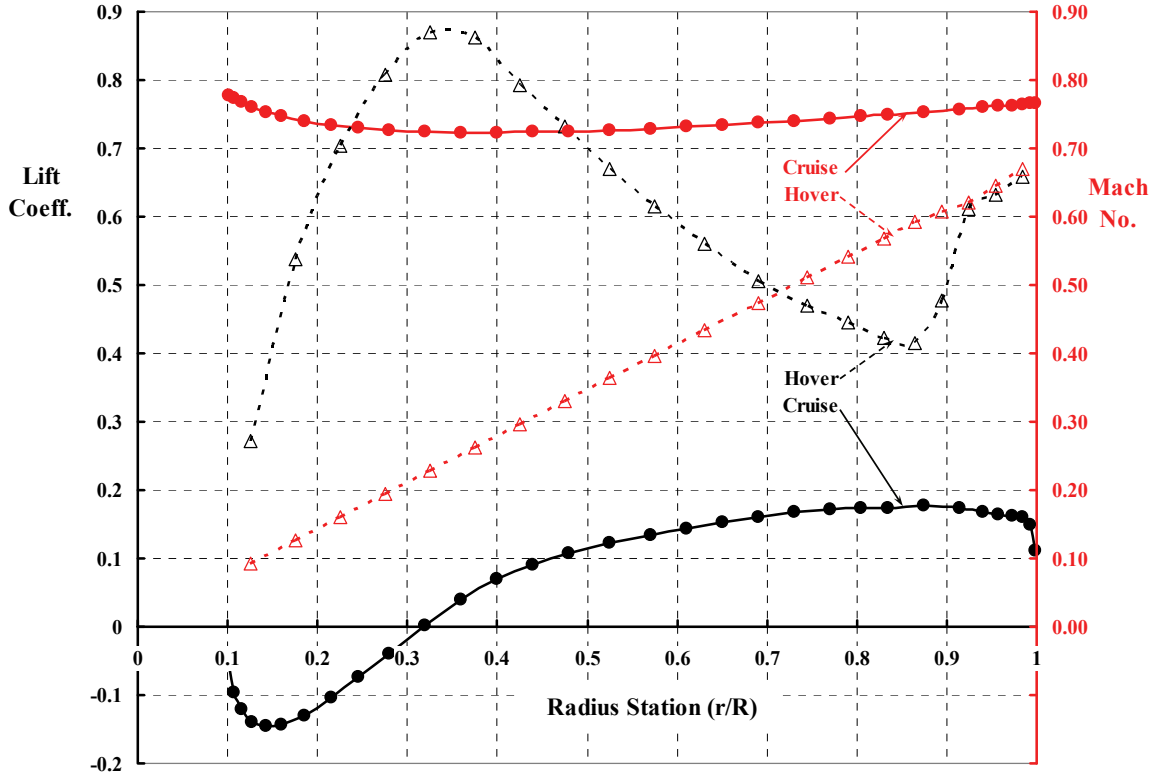

Figure 25. LCTR-2016 proprotor design 1—blade element lift coefficient and Mach number in cruise at 425 kts at 25,000 ft, a tip speed of 300 fps, and a thrust of 3,787 lb per proprotor. Hover data at 5,000 ft, 95°F, a tip speed of 800 fps, and a thrust of 72,000 lb per proprotor. This configuration has four blades.

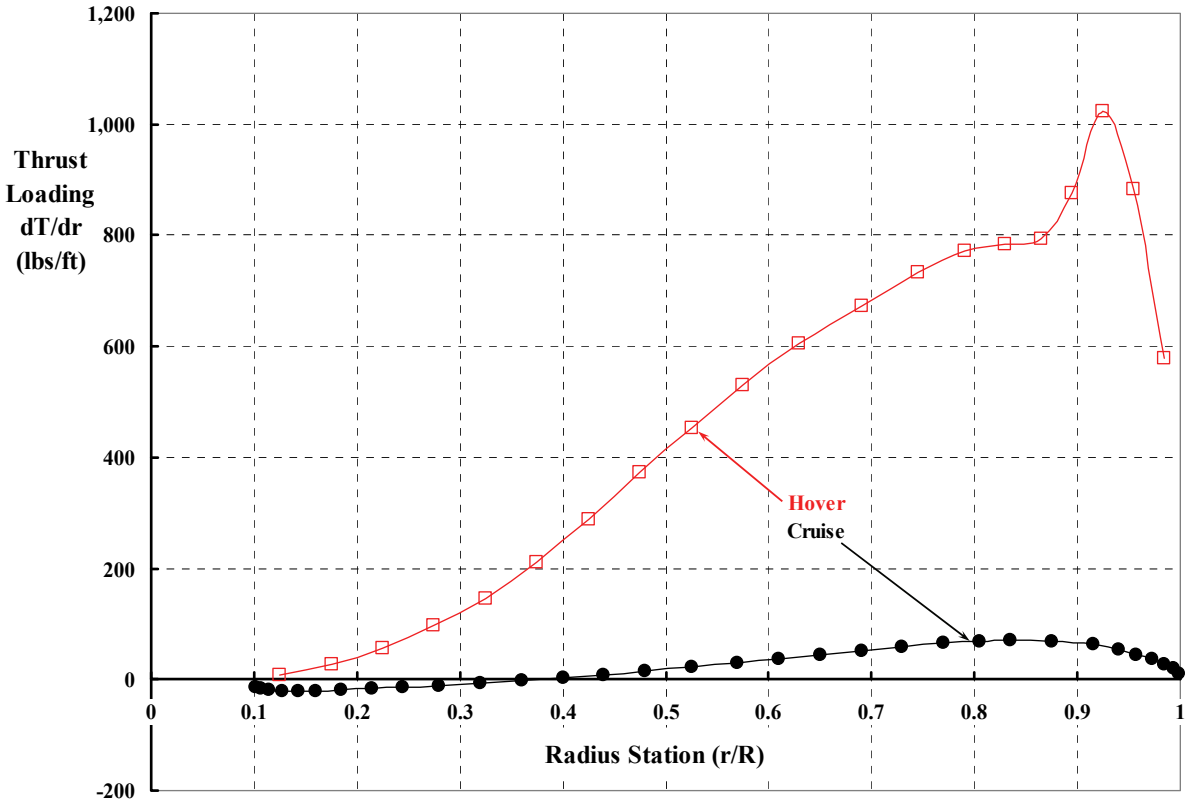

Figure 26. LCTR-2016 proprotor design 1—blade element thrust loading.

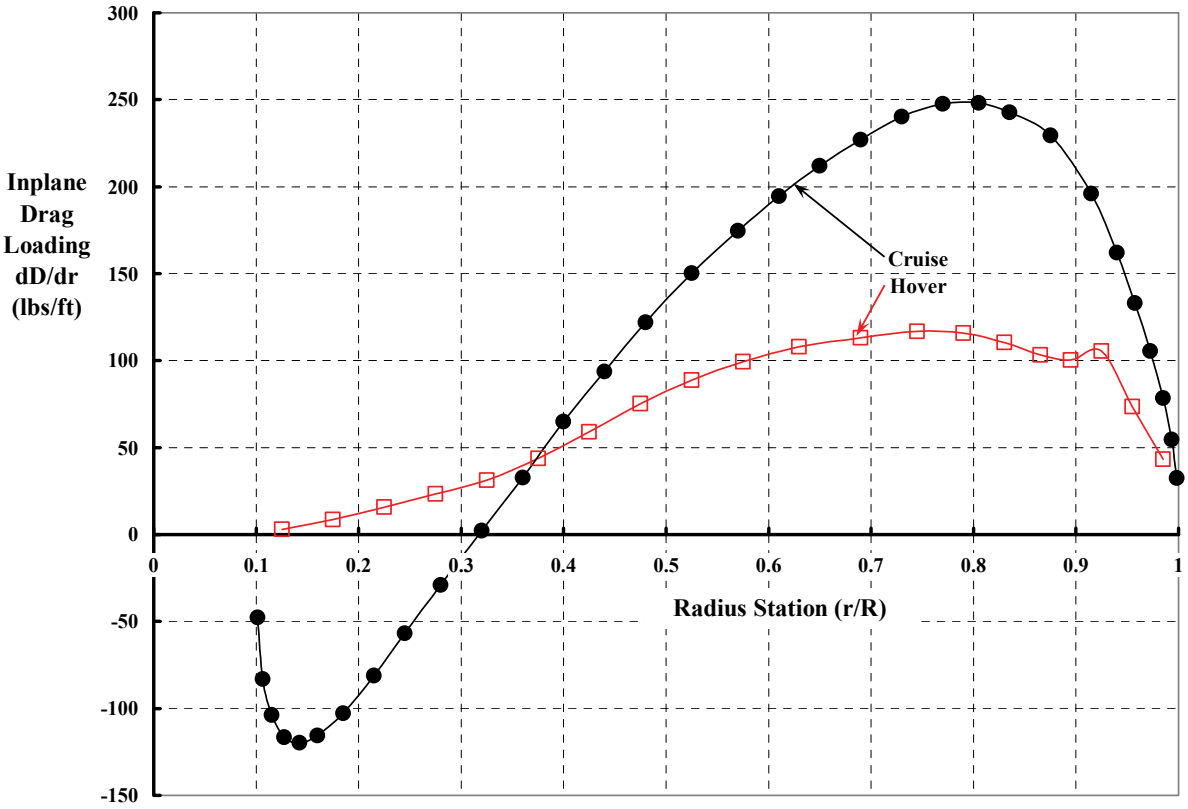

Figure 27. LCTR-2016 proprotor design 1—blade element inplane drag loading.

problem. That is, in cruise the well designed tiltrotor aircraft has a lift-to-drag ratio on the order of 16 to 18. But in hover, the lift-to-drag ratio is the equivalent of 1.0.

The more interesting data is shown in figure 27 because it raises the question of what axial force and torque should the proprotor's drive shaft be designed for. The simple table seen here illustrates this issue.

Flight Condition	Single Proprotor Thrust (lb)	Proprotor Shaft Horsepower Required	Tip Speed (ft/sec)	Proprotor Shaft Torque (ft-lb)
Hover	72,000	10,785	800	326,250
Cruise	3,787	7,364	300	594,100

It is clear that hover will determine the LCTR-2016 proprotor design 1 axial strength required. But note that while hover requires the most shaft horsepower, the high tip speed leads to a relatively low torque when compared to the strength require in the shaft for cruise. These types of differences exist all the way through the drive train until the turboshaft engine's output shaft is reached. Keep in mind that the LCTR-2016's design requires a two-speed gear box so that each turboshaft engine is operating at 100 percent RPM in either hover or cruise.

The last set of parameters examined were the key induced velocities created by the wakes from the four blades and the bound circulation along the blade span that created the induced velocities. Figure 28 shows the inplane velocities that make up what is known as

(21) $V_{inplane} = \Omega r + V_{cir}$ or nondimensionally $U_T \equiv \frac{V_{inplane}}{\Omega R} = \frac{r}{R} + \frac{V_{cir}}{\Omega R}$.

Here, the circumferential velocity (V_{cir}) is frequently called swirl in rotorcraft terms. It is clear from CAMRAD II's free wake analysis that near the blade's root, swirl increases the inplane velocity above the velocity due to blade rotation (Ωr). Then, by the 0.4 radius station, swirl has become negligible. However, swirl is reducing the nominal inplane velocity over the blade's outboard span.

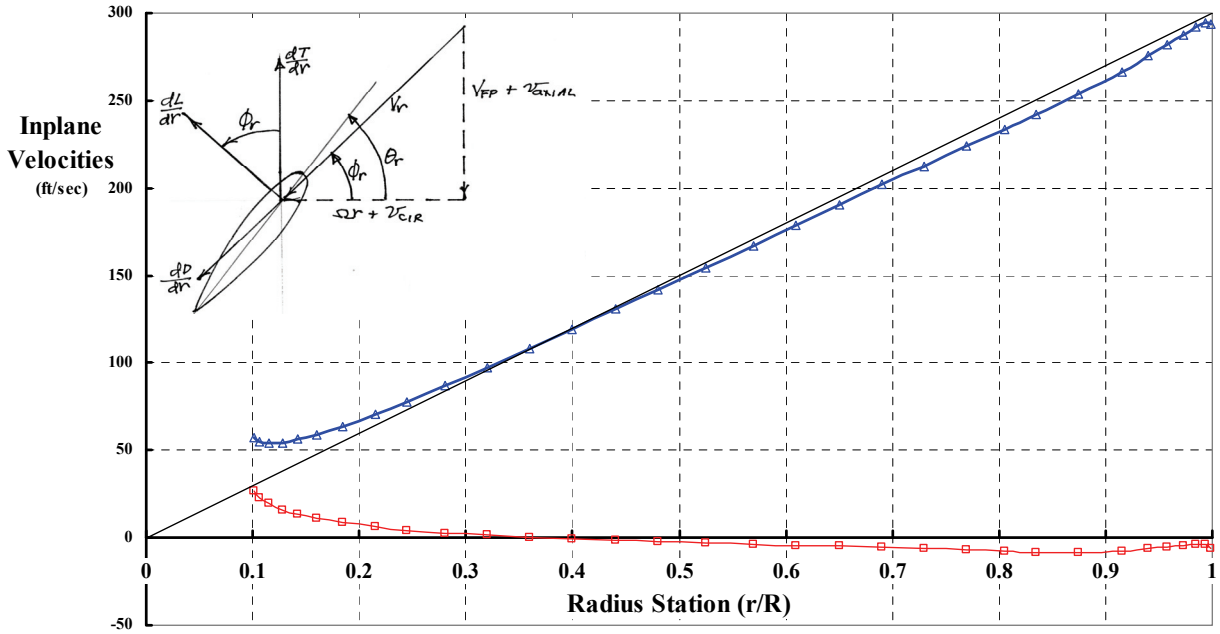

Figure 28. Induced velocity is an important component of inplane velocity (cruise flight), particularly near the blade's root.

The axial velocity is affected not only by wake-induced velocity but also by the spinner and nacelle. This is apparent from figure 29. CAMRAD II was chosen to model the spinner and nacelle as an ellipsoid 8 feet in diameter and 26.4 feet long. The proprotor hub was placed 8.8 feet aft of the ellipsoid's nose. The interference velocity created by the nacelle and spinner was calculated assuming just potential flow. The spinner's portion of the ellipsoid was assumed to not be rotating. It was quite interesting to note that the wake-induced axial velocity, as figure 29 shows, was of little consequence inboard of the 0.4 radius station. More importantly, the spinner significantly increases Mach number for the airfoils inboard of the 0.4 radius station. This point was made abundantly clear by Ethan Romander in reference 12.

The conclusion is that this first cut at a proprotor design for a 425-knot, 120-passenger LCTR-2016 should incorporate some changes for a second try. The changes to investigate are: (1) decrease the cruise tip speed from 300 feet per second to as low as 250 feet per second, (2) dispense with the SC(2)-0006 airfoil over the blade's outboard span and instead use the SC(2)-0008, and (3) lower the tip speed in hover from 800 feet per second to as low as 750 feet per second. The chord distribution need not be changed, but the twist distribution should be carefully reevaluated. The LCTR-2016 design flight conditions of cruise at 425 knots at 25,000 feet with a thrust of 3,787 pounds per proprotor and hover at 5,000 feet, 95°F, with a thrust of 72,000 pounds per proprotor should remain. Four blades should continue to be the baseline.

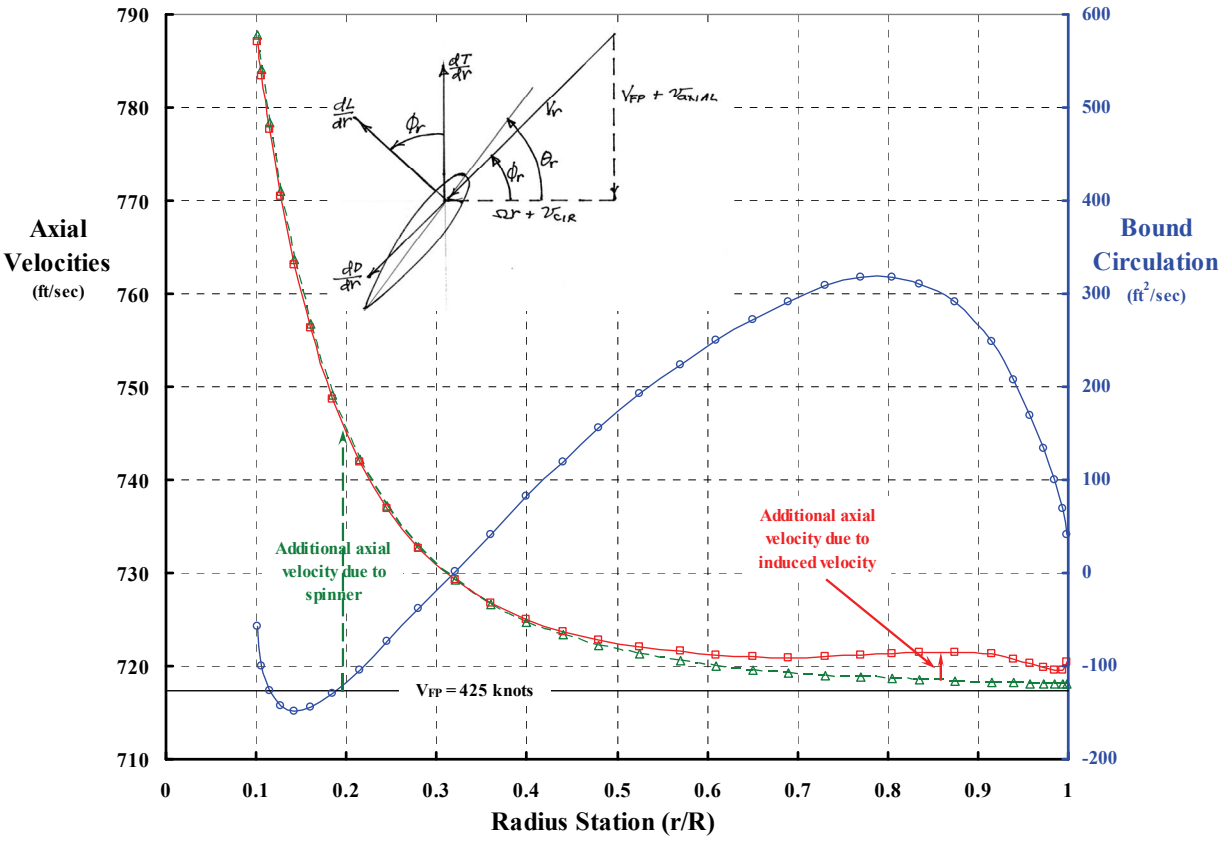

Figure 29. Flow about the spinner creates a major distortion in the axial flow environment that blade airfoils see (cruise flight).

AIRFRAME DESIGN

In their 2005 design study (ref. 1), Johnson, Yamauchi, and Watts estimated a 120-passenger, large civil tiltrotor (LCTR) would have a cruise lift-to-drag ratio on the order of 15 to 16. They envisioned this LCTR configuration as sketched in figure 30. Somewhat later, Wally Acree reported (ref. 13) on a design study of a 90-passenger civil tiltrotor identified as the LCTR2 (fig. 31). Since then an unpowered, small-scale model representative of the smaller, 90-passenger LCTR2 was built and tested in the NASA Ames 7- by 10-foot low-speed wind tunnel. This was an experimental program jointly conducted by NASA and the U.S. Army. The Army's interest was to obtain airframe aerodynamics for a configuration they called the HETR, which had a cargo fuselage. NASA's interest was in a passenger fuselage. Because of a money shortage, both Army and NASA configurations used the Army's HETR wing.* Therefore, the configuration used in the NASA portion of the test is referred to as the LCTR2 + HETR wing. Figure 32 shows this NASA configuration installed in the 7- by 10-foot wind tunnel.

Colin Theodore (et al.) reported on the NASA portion of the program in January 2014 (ref. 14). A test data report is currently in preparation. Key dimensions of this approximately 0.06-scale LCTR2 + HETR wing model are provided in figures 33a, b, c, d, and table 3.

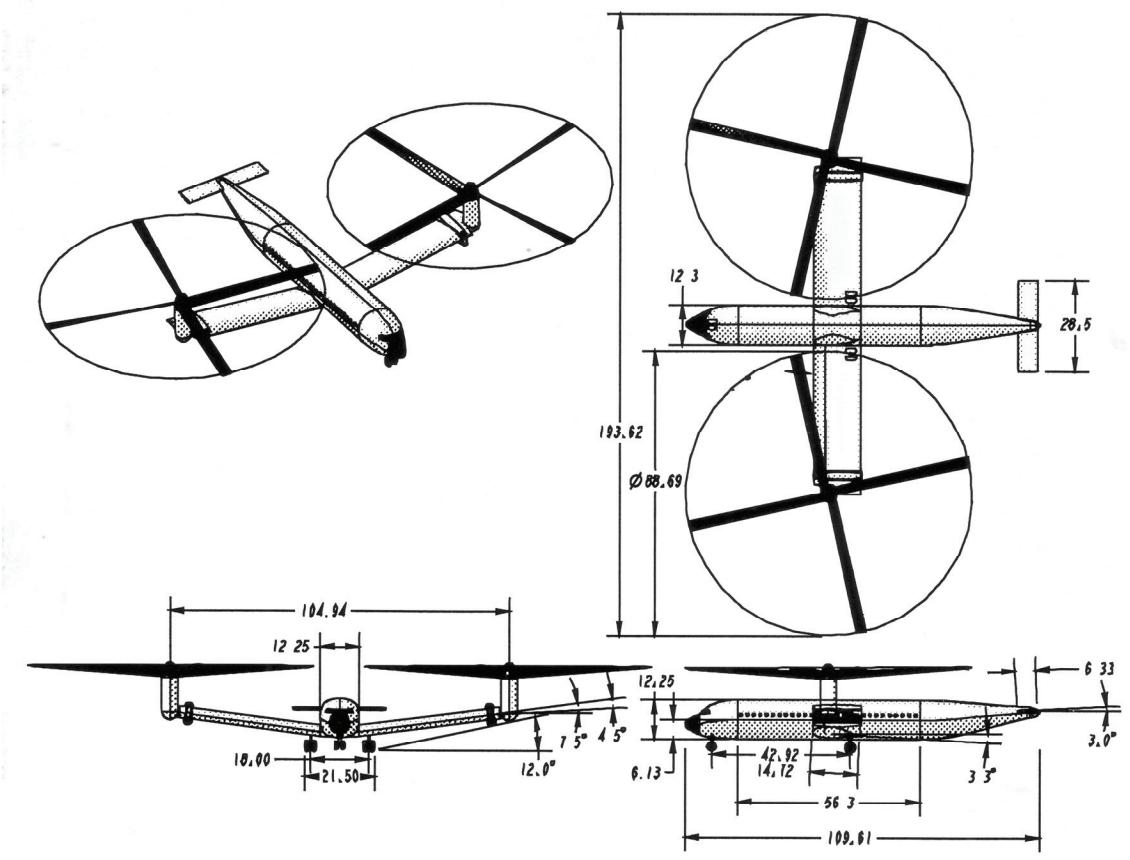

Figure 30. NASA 120-passenger LCTR-2005 (ref. 1).

* The HETR wing's 21-percent-thick airfoil and its coordinates have not, at present, been made available to the general public.

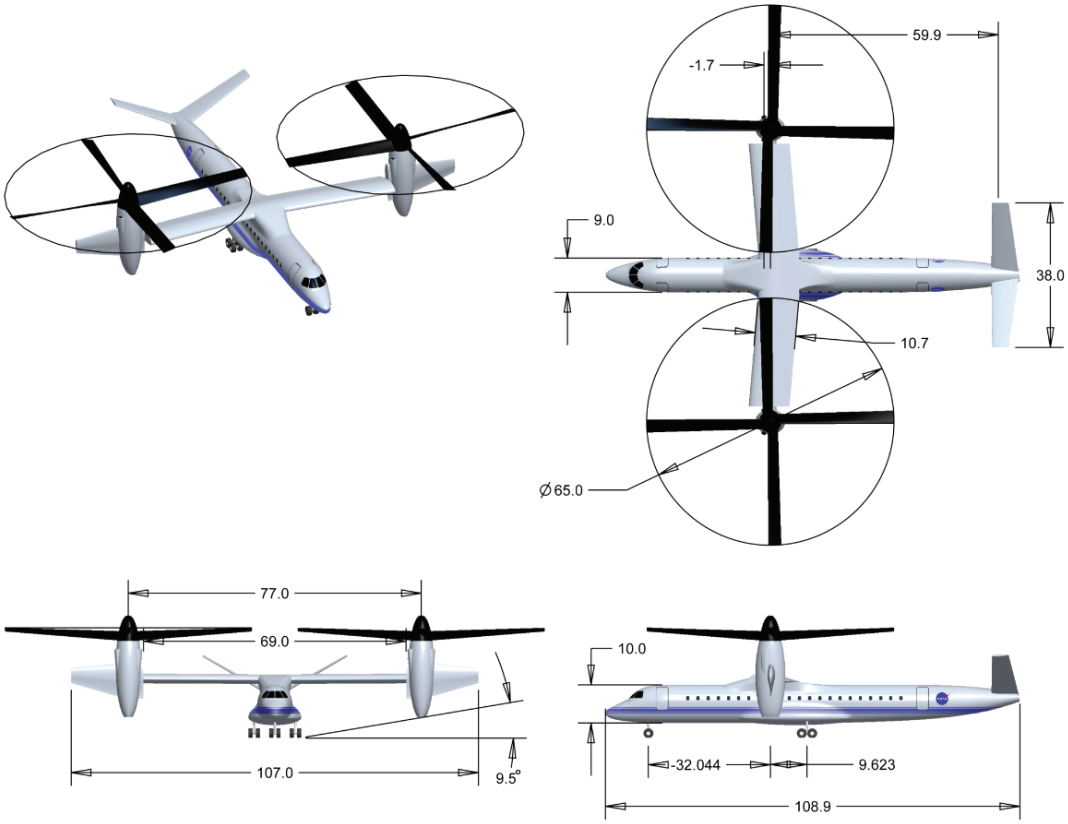

Figure 31. NASA 90-passenger LCTR2-2008 (ref. 13).

Figure 32. NASA 6%-scale LCTR2 body and tail planes + U.S. Army HETR wing in NASA Ames 7- x 10-foot low-speed wind tunnel.

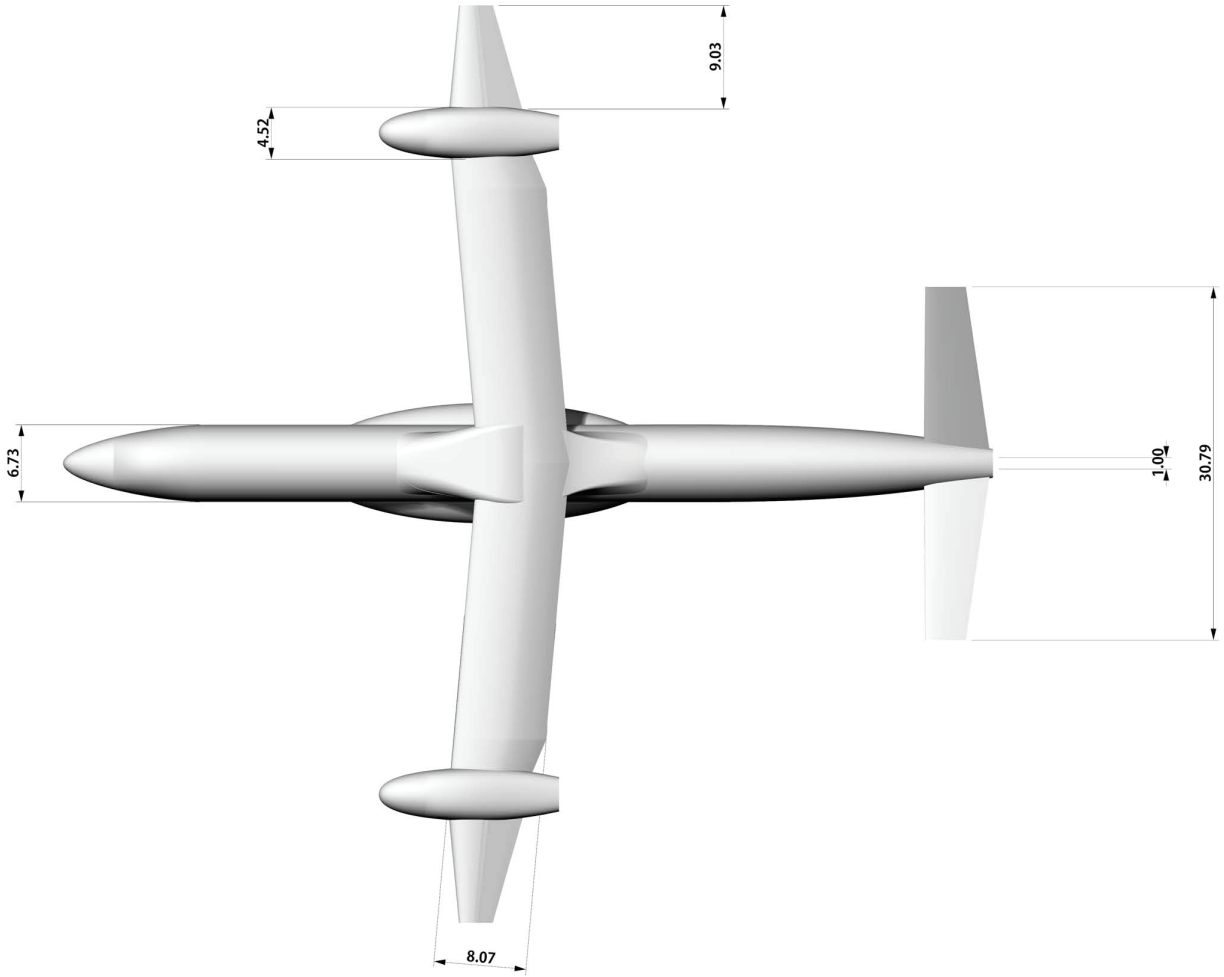

Figure 33a. NASA 6%-scale LCTR2 body and tail planes + U.S. Army HETR wing (top view).

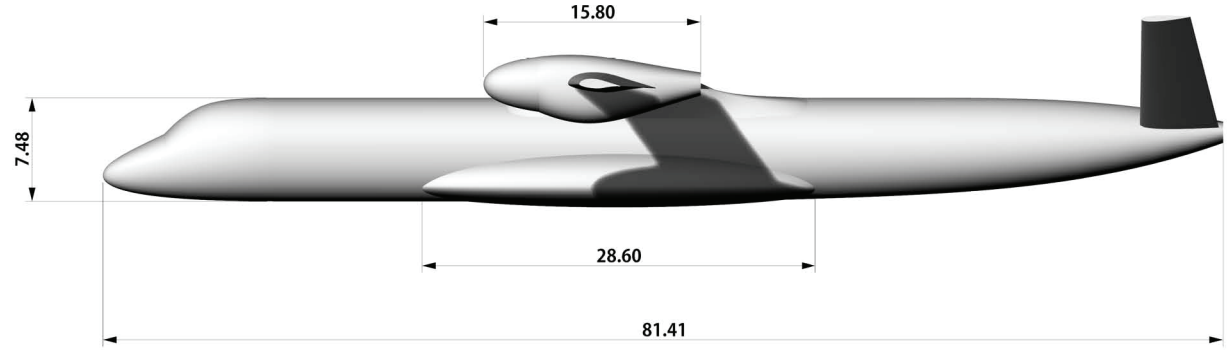

Figure 33b. NASA 6%-scale LCTR2 body and tail planes + U.S. Army HETR wing (side view).

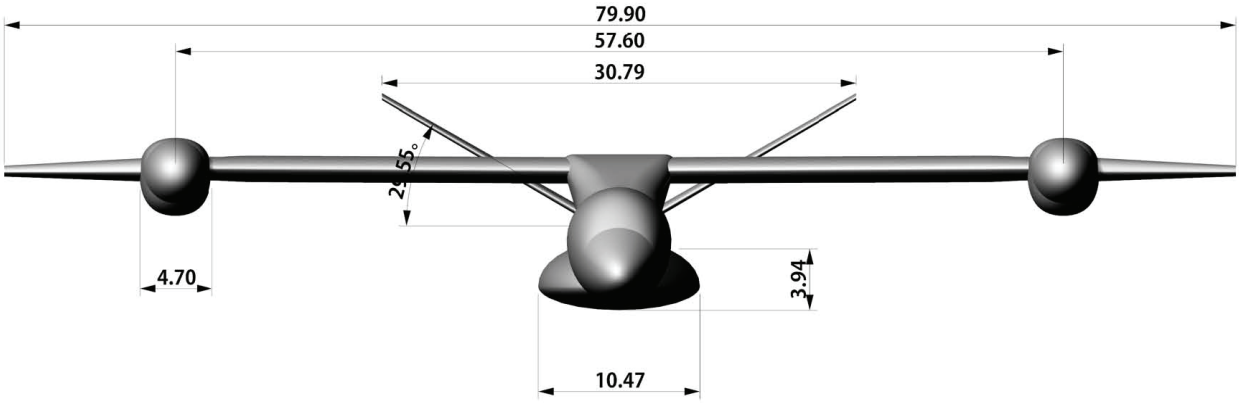

Figure 33c. NASA 6%-scale LCTR2 body and tail planes + U.S. Army HETR wing (front view).

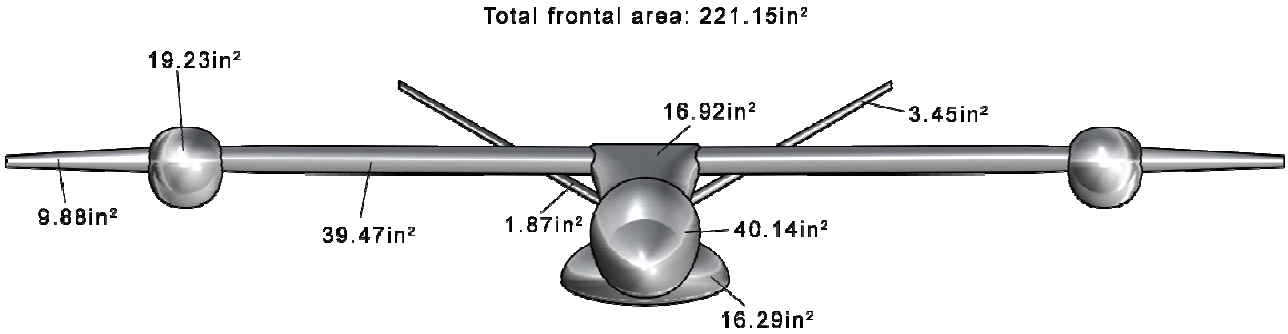

Figure 33d. NASA 6%-scale LCTR2 body and tail planes + U.S. Army HETR wing (frontal area).

Table 3. Key Dimensions of the LCTR2 + HETR Wing Model

Parameter	Dimensions
Wingspan (in./ft)	79.9/6.658
Wing area (in.^{2}/ft^2)	454.0/3.1528
Wing aspect ratio (b^2/S)	14.06
Inner wing chord (in./ft)	8.07/0.6725
Inner wing sweep (deg)	–5.0 (fwd)
Inner wing taper ratio	No taper
Inner wing Reynolds number at V = 285 fps	1,200,000

Preliminary experimental data for the LCTR2 + HETR wing are shown in figures 34 and 35. The derived fuselage plus tail planes drag-versus-lift data are shown in figure 36. It appears that the shoulder-mounted wing is a very high drag configuration similar to the MV-22B. This coupled with fuselage sponsons to house the retractable landing gear leads, in the author's opinion, to a less than attractive design approach for a civil tiltrotor. The 120-passenger LCTR design approach sketched in figure 30 is favored.

However, the 120-passenger 2005 LCTR's wing assumes a 21-percent-thick airfoil currently thought to be required to ensure freedom from whirl flutter and other aeromechanic instabilities. In the author's view, freedom from whirl flutter can be obtained, today, from a fly-by-wire control system. However, a mechanical coupling of nacelle motion to the proprotor's swashplate control system was discussed by Troy Gaffey in November of 1969 (ref. 15). A subsequent full-scale test of a 25-foot-diameter flight-worthy proprotor in the NASA Ames Large Scale Wind Tunnel included some test results showing how powerful controlling blade flapping could be in stabilizing whirl flutter (ref. 16). A model test demonstrating stabilization of whirl flutter using a fly-by-wire control system was reported by Mark Nixon (et al.) in May of 2003 (ref. 17). Therefore, cambered, supercritical airfoils such as the NASA SC(2)–0714 (a 14-percent-thickness-ratio airfoil) as discussed in reference 4 appears more attractive as a starting point for the wing of a 425-knot, 25,000-foot-altitude VTOL civil transport.

At the present time, there is no more detailed wing and nacelle configuration information to report. However, an airframe cruise lift-to-drag ratio of 16 at 425 knots at 25,000 feet altitude is believed feasible, since this is a cruise Mach number slightly below 0.71.

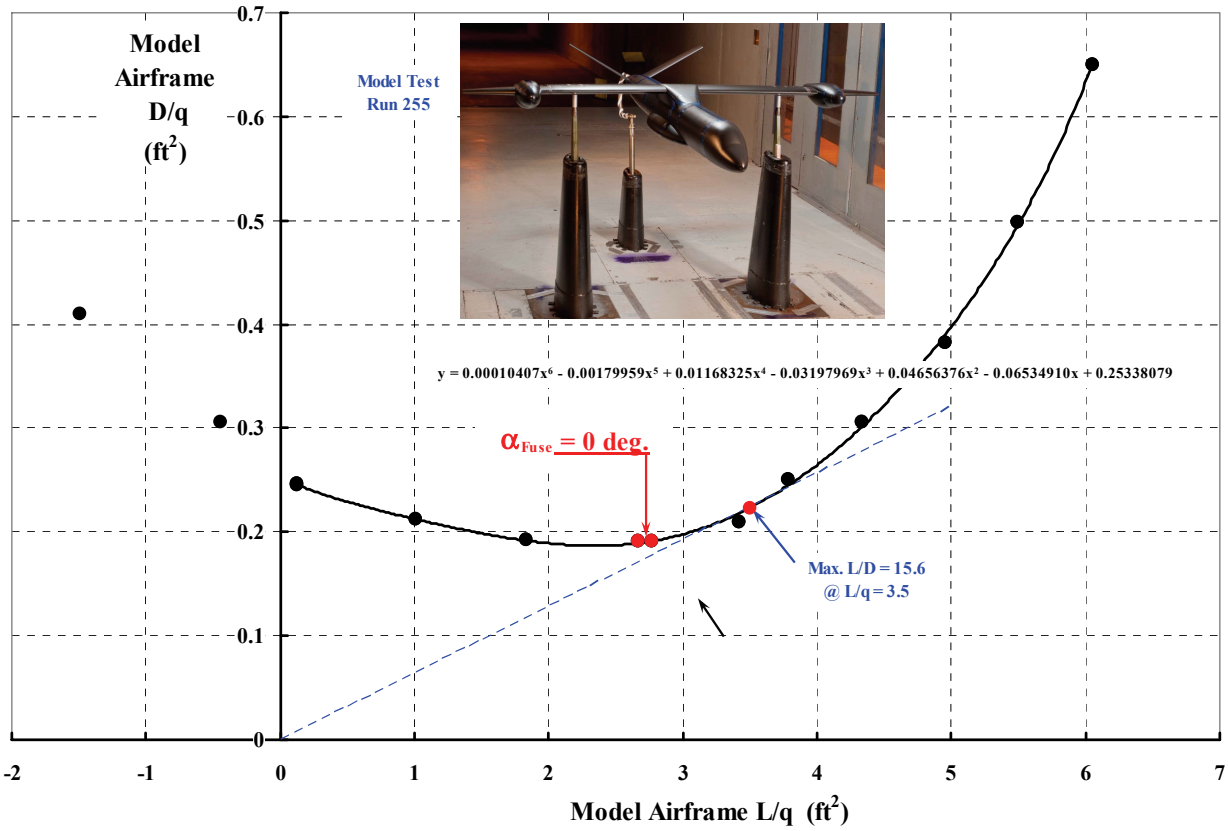

Figure 34. Preliminary NASA 6%-scale LCTR2 body and tail planes + U.S. Army HETR wing test data.

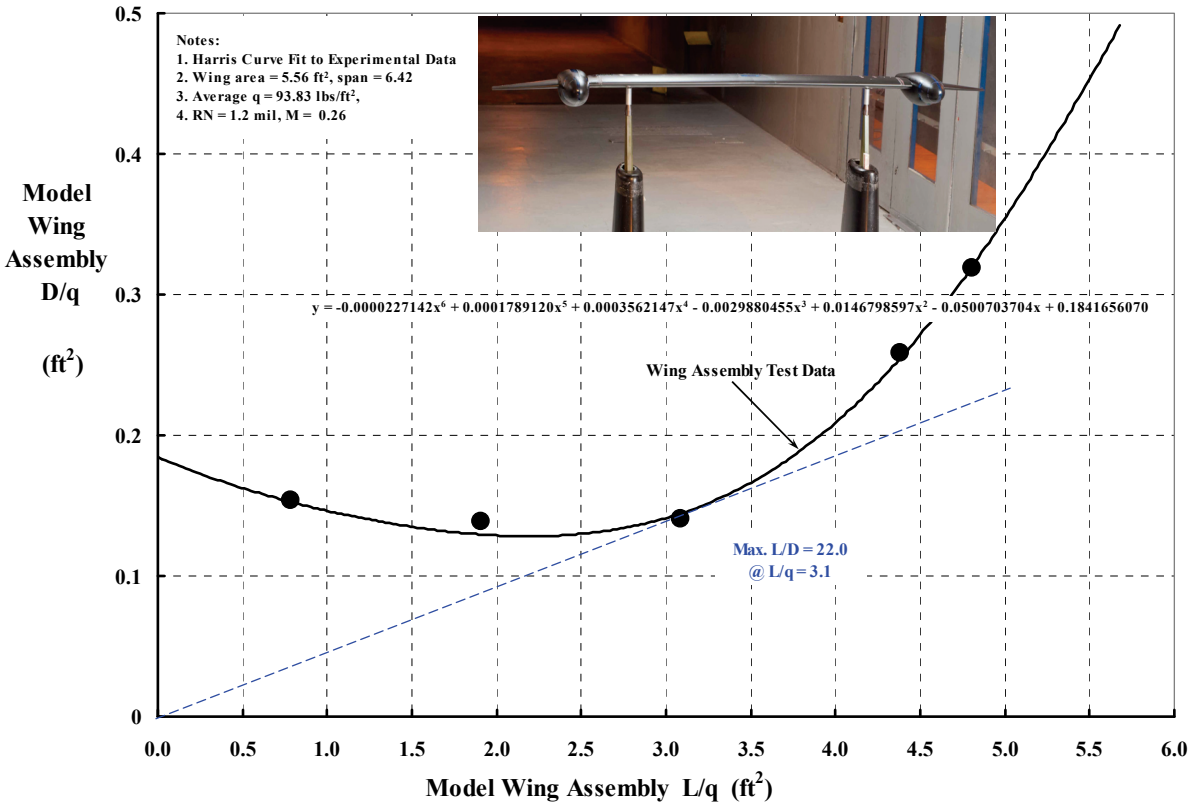

Figure 35. Preliminary HETR wing test data.

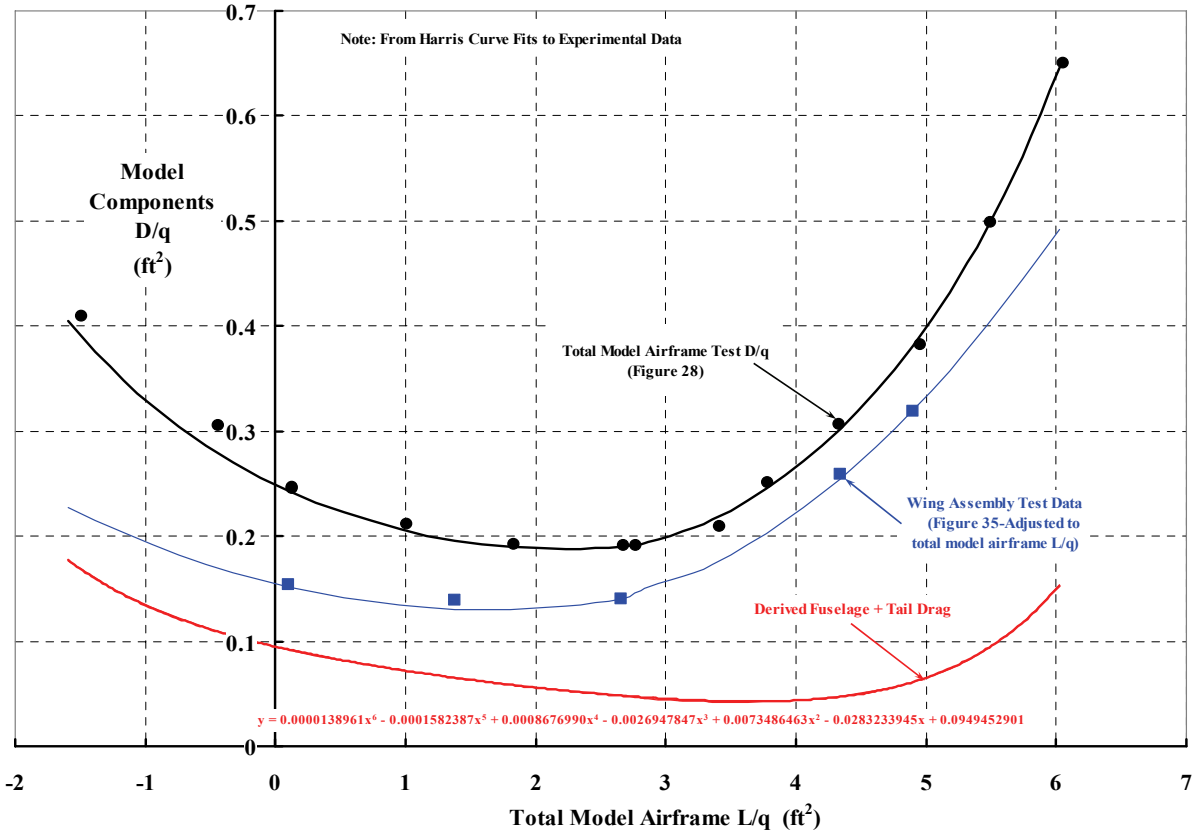

Figure 36. Preliminary derived data for fuselage plus tail planes of the 6%-scale LCTR2.

CONCLUSIONS

A 120-passenger VTOL civil transport capable of cruising efficiently at 425 knots and at 25,000 feet pressure altitude is worth pursuing with more concept and preliminary designing, and of course, wind tunnel testing. It is believed that:

1. Each of the two installed turboshaft engines must be rated at 14,000 shp for VTOL takeoff at sea level, standard day, which is an engine manufacturers' most often quoted standard condition.

2. Two-speed gearboxes are required so that an engine can operate at 100 percent RPM in both hover and cruise.

3. A takeoff gross weight of a 124,000-pound aircraft is rational during the conceptual design stage, albeit probably with a weight empty somewhat greater than that quoted for the 2005 LCTR (80,700 pounds) and, therefore, with less than the 2005 LCTR fuel capacity of 15,000 pounds.

4. The current proprotor geometry appears to be satisfactory for cruise but unsatisfactory for hover.

5. The wing airfoil thickness ratio must be no greater than 15 to 17 percent, which requires that whirl flutter and other aeromechanical instabilities must be overcome by the proprotor's control system in some fly-by-wire plus software manner.

6. Available (but preliminary) experimental data suggests that an airframe lift-to-drag ratio of 16 in cruise is a reasonable expectation.

7. A secondary configuration designed to takeoff and land as a STOL should be studied. This aircraft should meet a requirement of operating from a 500-foot runway located at 5,000 feet (on a day when the OAT is 95^{o}F). It should be assumed that the runway is surrounded by 50-foot-high obstacles.

In May of 1968, Ken Wernicke of Bell Helicopter presented a paper at the 24th Annual National Forum of the American Helicopter Society. The presentation was later publish in the Journal of the AHS and titled *Tilt Proprotor Composite Aircraft, Design State of the Art* (ref. 18). Ken's conclusion was that the "speed potential of the [tiltrotor] concept will permit its application to long-range missions with cruise speeds in the 400 knot range." The author believes Ken was quite correct in his assessment.

REFERENCES

1. Johnson, W.; Yamauchi, G.; and Watts, M.E.: NASA Heavy Lift Rotorcraft Systems Investigation. NASA/TP-2005-213467, Dec. 2005.

2. Anon.: Proud to Fly a Turboprop: Q400 vs ATR 72, http://theflyingengineer.com/proud-to-fly-a turboprop-q400-vs-atr72, article in The Flying Engineer.

3. Smith, E. and Zhang, J.: Structural Design of Composite Blade for Low Weight Rotor Systems. Penn State Rotorcraft Center of Excellence report dated Aug. 2005.

4. Harris, C. D.: NASA Supercritical Airfoils—A Matrix of Family-Related Airfoils, NASA TP 2969, March 1990.

5. Jenkins, R.V.; Hill, A.S.; and Ray, E.J.: Aerodynamic Performance and Pressure Distributions for a NASA SC(2)-0714 Airfoil Tested in the Langley 0.3-Meter Transonic Cryogenic Tunnel. NASA TM 4044, 1988.

6. Jenkins, R.V.: NASA SC(2)-0714 Airfoil Data Corrected for Sidewall Boundary-Layer Effects in the Langley 0.3-Meter Transonic Cryogenic Tunnel. NASA TP 2890, 1989.

7. Rivers, M.B. and Wahls, R.A.: Comparison of Computational and Experimental Results for a Supercritical Airfoil. NASA TM 4601, Nov. 1994.

8. Fulker, J.L.: Aerodynamic Data for Three Supercritical Aerofoils—RAE (NPL) 9515 and 9530, and RAE 9550, Parts I and II. Aeronautical Research Council R&M 3820, 1978.

9. Khalid, M. and Jones, D.J.: A Summary of Transonic Natural Laminar Flow Airfoil Development at NAE. National Aeronautical Establishment Note NAE-AN-65, May 1990 (also see DTIC AD-A225102).

10. Jenkins, R.V. and Adcock, J.B.: Tables for Correcting Airfoil Data Obtained in the Langley 0.3-Meter Transonic Cryogenic Tunnel for Sidewall Boundary-Layer Effects. NASA TM 87723, June 1986.

11. Giovanetti, E.B. and Hall, K.C.: A Variational Approach to Multipoint Aerodynamic Optimization of Conventional and Coaxial Helicopter Rotors. AHS 71st Annual Forum, Virginia Beach, VA, May 5–7, 2015.

12. Romander, E.: 3-D Navier–Stokes Analysis of Blade Root Aerodynamics for a Tiltrotor Aircraft in Cruise. AHS Vertical Lift Design Conference, San Francisco, CA, Jan. 18–20, 2006.

13. Acree, C.W.; Yeo, H.; and Sinsay, J.D.: Performance Optimization of the NASA Large Civil Tiltrotor. International Powered Lift Conference, London, UK, July 22–24, 2008.

14. Theodore, C.R. et al.: Wind Tunnel Testing of a 6%-Scale Large Civil Tiltrotor Model in Airplane and Helicopter Modes. Fifth Decennial AHS Specialists' Conference, San Francisco, CA, Jan. 22–24, 2014.

15. Gaffey, T.M.: Some Aspects of Control Feedback Stabilization of VTOL Proprotors. Aerospace Flutter and Dynamics Council Meeting, San Francisco, CA, Nov. 12–14, 1969.

16. Anon.: Advancement of Proprotor Technology: Task II-Wind Tunnel Test Results. NASA CR-114363, Bell Helicopter Company Report 300-099-004, 1971.

17. Nixon, M.W. (et al.): Aeroelastic Stability of a Four-Bladed Semi-Articulated Soft-Inplane Tiltrotor Model. 59th Annual National Forum of the AHS, Phoenix, AZ, May 6–8, 2003.

18. Wernicke, K.G.: Tilt Proprotor Composite Aircraft, Design State of the Art. Journal of the AHS, vol. 14, no. 2, April 1969.

APPENDIX A

F. D. Harris' Presentation at the AHS Technical Meeting on Aeromechanics Design for Vertical Lift
San Francisco, CA
January 20–22, 2016
AHS Paper

The V/STOL Performance Gap

- **How Big Is The Gap Anyway?**
- **What Have We Done To Fill It?**
  - **a. With VTOLs?**
  - **b. With STOLs?**
- **The Two Performance Goals I See.**
  - **a. What to do & how to start.**

Presented at the AHS Technical Meeting on
Aeromechanics Design for Vertical Lift
San Francisco, California
January 20-22, 2016

Franklin D. Harris
15505 Valley Dr.
Piedmont, OK 73078
(405) 373-0850/0587

Our "Rotorcraft" Industry Offers Only One (1) Product to Commercial Aviation Operators.

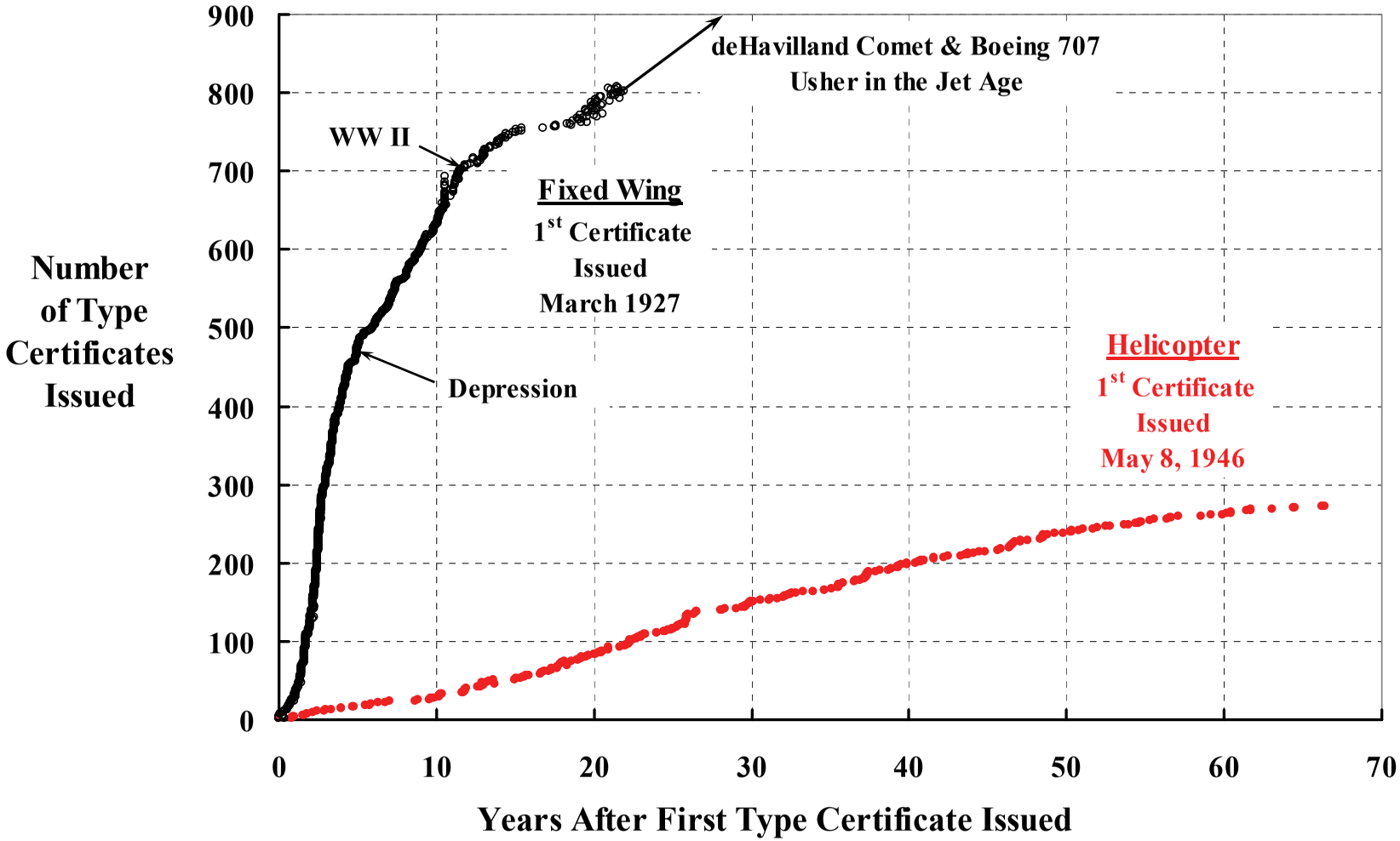

39

Gabrielli & von Karman's View in 1950 did not Portray the Helicopter as a Competitor to the Airplane.

Ref: Gabrielli, G.; and von Karman, T.: *What Price Speed.* Mechanical Engineering, Volume 72, October 1950.

Note: I have taken some liberty with their chart and also added a few points.

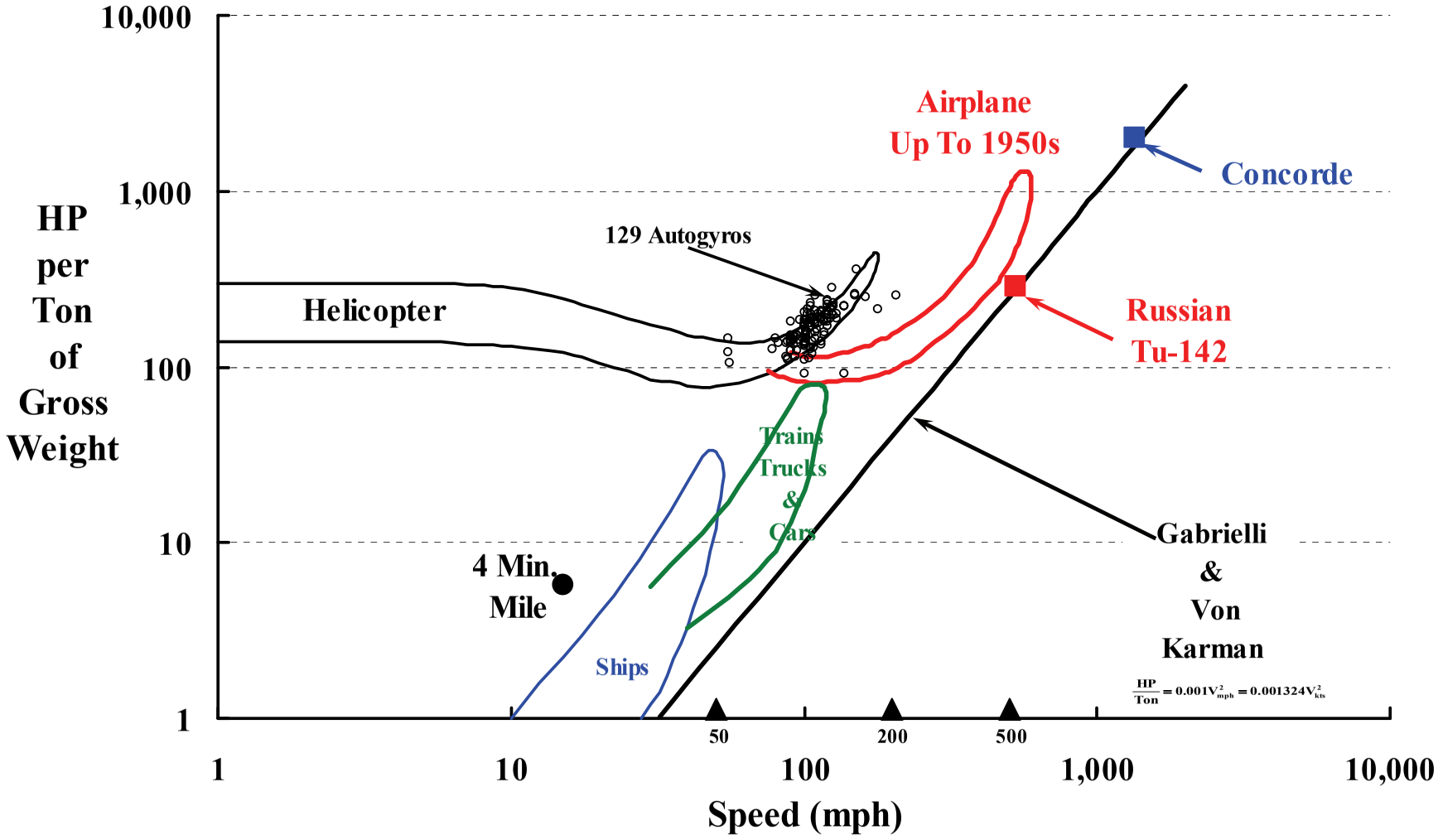

The Tupolev Tu-95/142 Bomber and Boeing B-52 were Comparable. The Aerospatiale/BAC Concorde was not Economical in Service.

Refs: 1. John Stroud, *Soviet Transport Aircraft Since 1945*, Funk & Wagnalls, New York, 1968
2. *Aerospatiale/BAC Concorde*, Flightpath - Premier Volume, Vol. 1, Summer 2003

1st flight of Tu-95 was in November of 1952
Maximum speed of about 510 knots
TOGW around 400,000 lbs
Weight empty around 198,000 lbs
Four NK-12MV, each rated at 14,795 eshp
18.375-ft-dia, 8-bladed, counter-rotating props
Takeoff distance 9,350 ft at S.L.
Wingspan of 177.5 ft
Wing sweep of 35 deg

1st Flight March 2, 1969
Entered service January 21, 1976
120 Passengers (2 + 2 abreast)
Began cruise at Mach 2 & 50,000 feet
Maximum TOGW of 418,500 lbs
Four Rolls-Royce/SNECMA Olympus 593
(Rated at 39,940 lbs thrust each for takeoff)
Runway requirement: same as Boeing 747
Wingspan of 84.0 ft
Wing sweep of 35 deg

Gabrielli & von Karman's 1950s View Using Linear Scales.

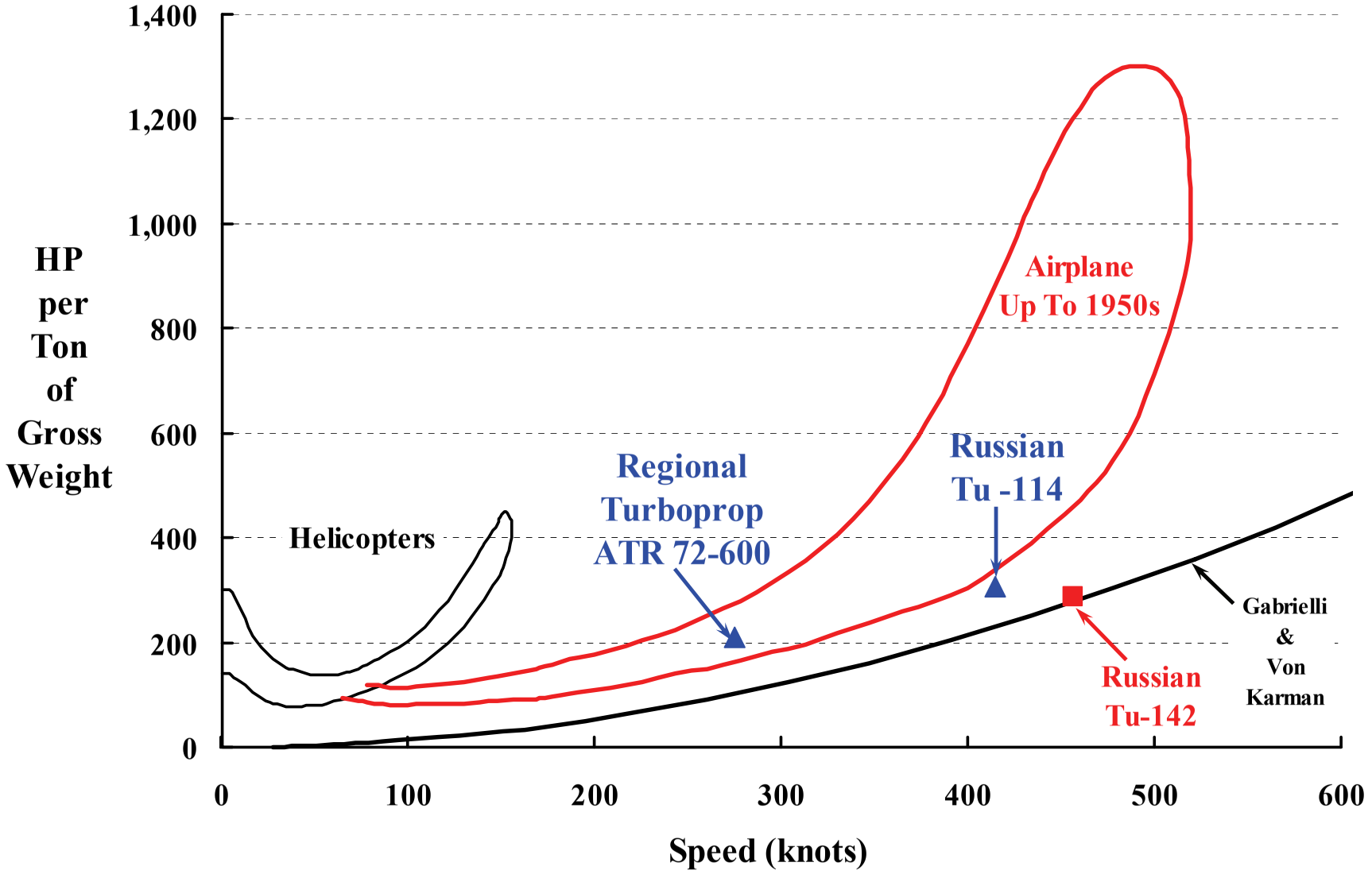

Here's My Update to Gabrielli & von Karman's 1950s View.

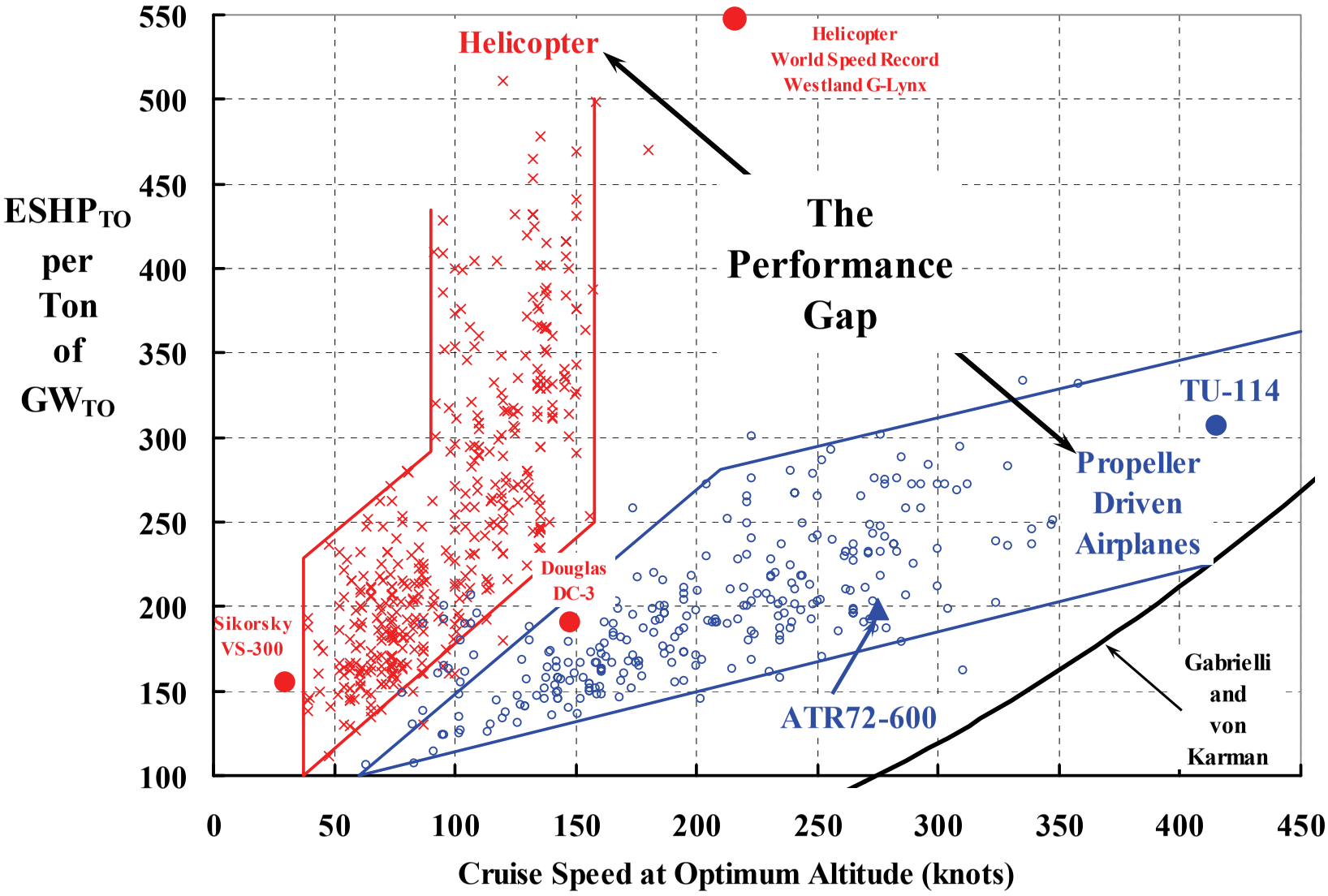

My Count of V/STOL Aircraft That Have Demonstrated at Least a Hint of Flight Worthiness.

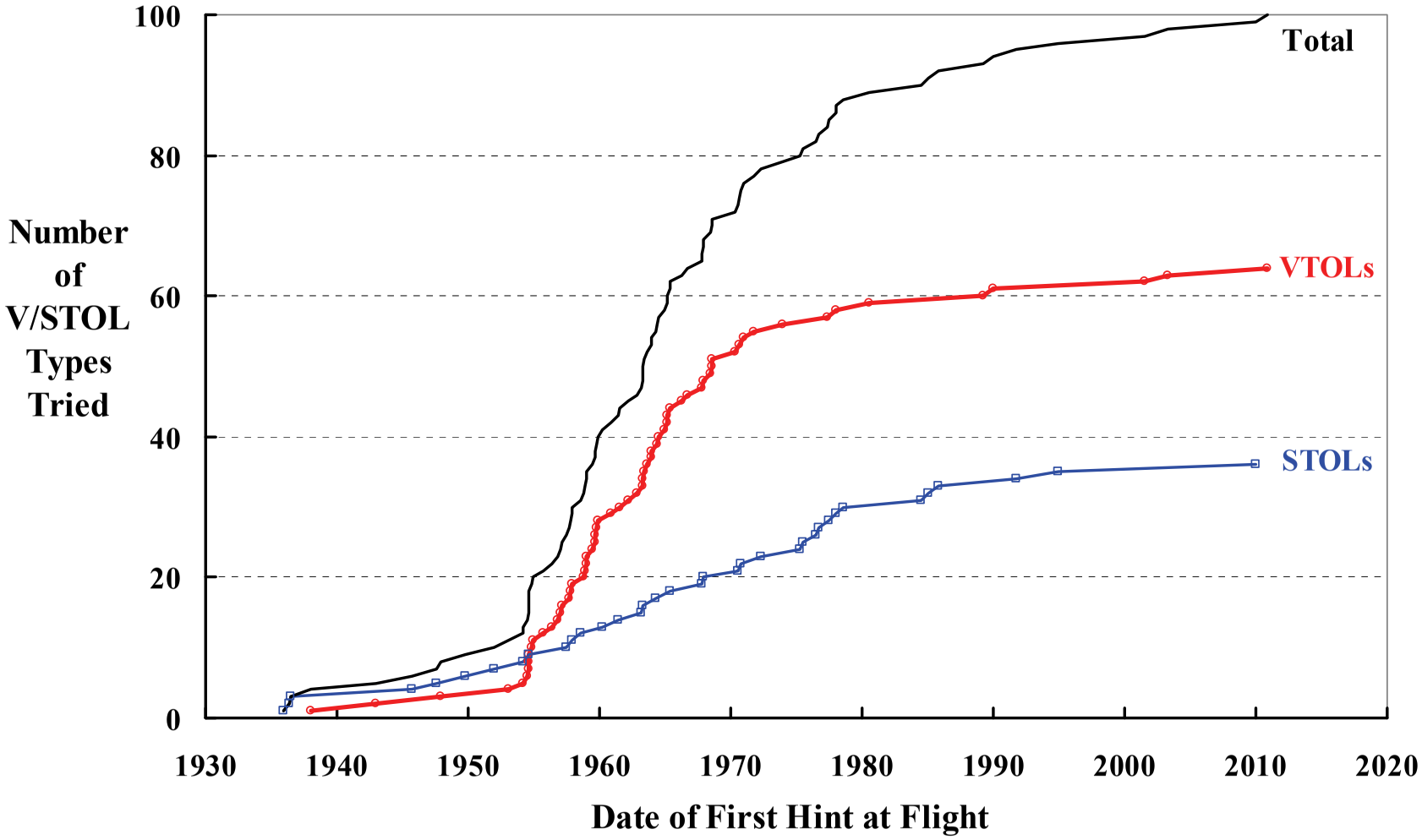

Sixteen Concrete Examples of V/STOL Aircraft after 65 Years of Trial and Error and Research and Development.

CLASS	AIRCRAFT	Total Takeoff ESHP (hp)	Gross Weight (lb)	Cruise Speed (kts)	ESHP/(GW) (hp per ton)	Weight Empty (lb)
Rotary Wing						
a. Compound	Fairey Rotodyne	5,600	33,000	161	339	22,000
	Sikorsky X2	1,630	6,100	260 est	534	5,000
	Eurocopter X^3	4,540	11,464	232 est	792	na
	Lockheed AH-56A	4,600	18,300	221	503	12,215
b. Tiltwing	Canadair CL-84	2,800	14,500	249	386	8,417
	LTV XC-142A	12,320	41,500	251 demo	594	25,552
c. Tiltrotor	Bell Boeing MV-22B	12,300	52,600	291	468	33,459
	Agusta Westland 609	3,880	16,800	275	462	10,483
Fixed Wing						
a. Propeller (piston)	de Havilland Caribou	2,900	28,500	158	204	18,260
	Fairchild C-123 B	5,000	54,000	166	185	30,900
b. Propeller (turboprop)	de Havilland Buffalo	6,266	49,200	250	255	23,197
	Breguet 941S	6,000	58,420	260	205	32,400
	Lockheed C-130H	16,200	155,000	300	209	74,000
c. Turbofan	Antonov An-72	21,372	67,240	388	636	42,000
	Boeing YC-14	108,636	225,000	370	966	116,397
	McDonnell YC-15	92,430	216,680	375	853	101,400

Tiltrotors Are Favored Today. Who Knows About Tomorrow.

Rotodyne, 1st Flt. Nov. 1957, 40 passengers

X2 Tech. Demo, 1st Flt. Aug. 2008, 2 crew

XC-142, 1st Flt. Sept. 1964, 32 troops (seated)

MV-22B, 1st Flt. March 1989, 24 troops (seated)

The Rotorcraft Industry's Eight Concrete VTOLs.

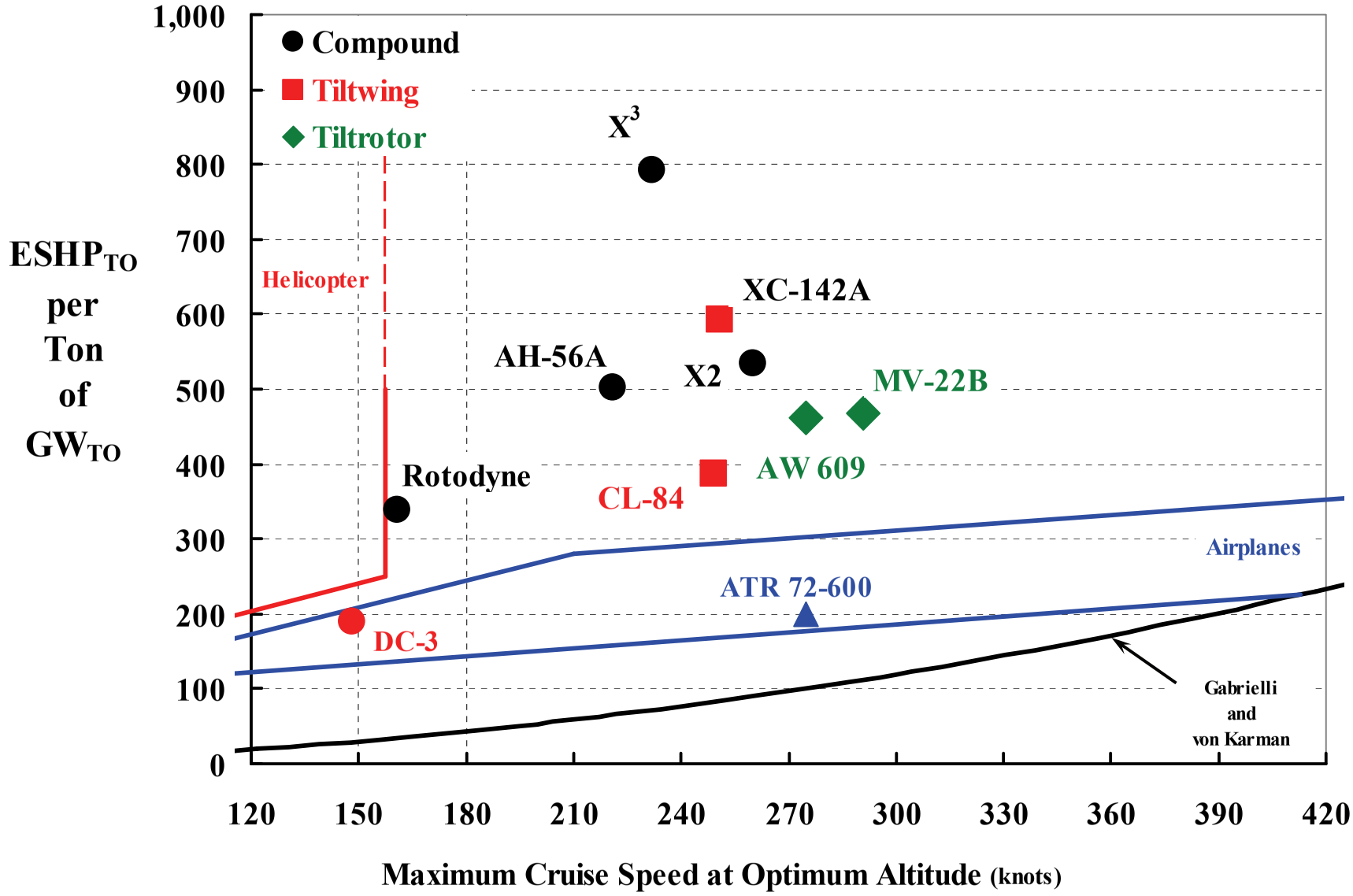

Turbofans Are Favored Today. Who Knows About Tomorrow.

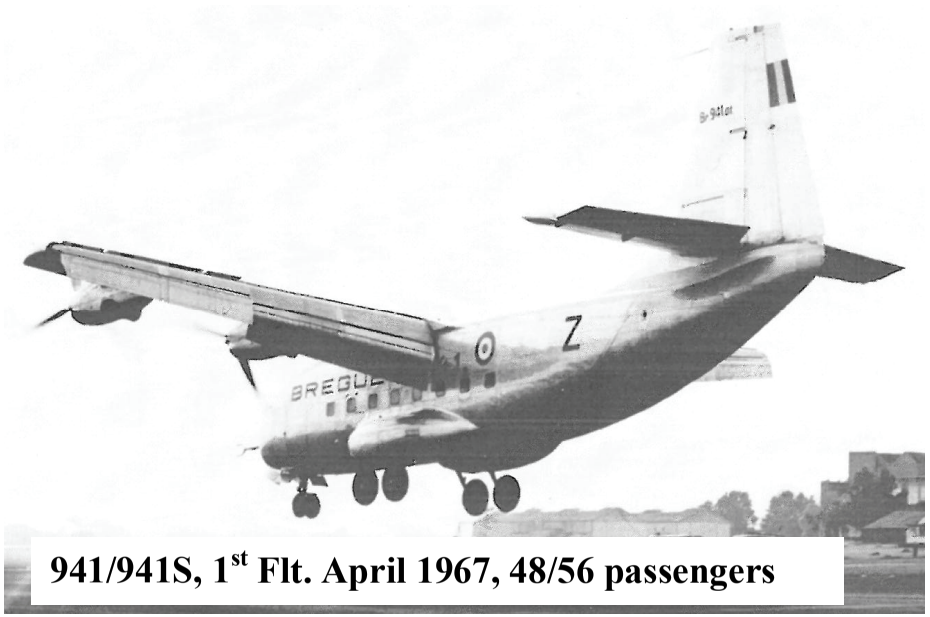

941/941S, 1st Flt. April 1967, 48/56 passengers

AN–72, 1st Flt. Dec. 1977, 52 passengers

YC-15, 1st Flt. Aug. 1976, 150 troops (seated)

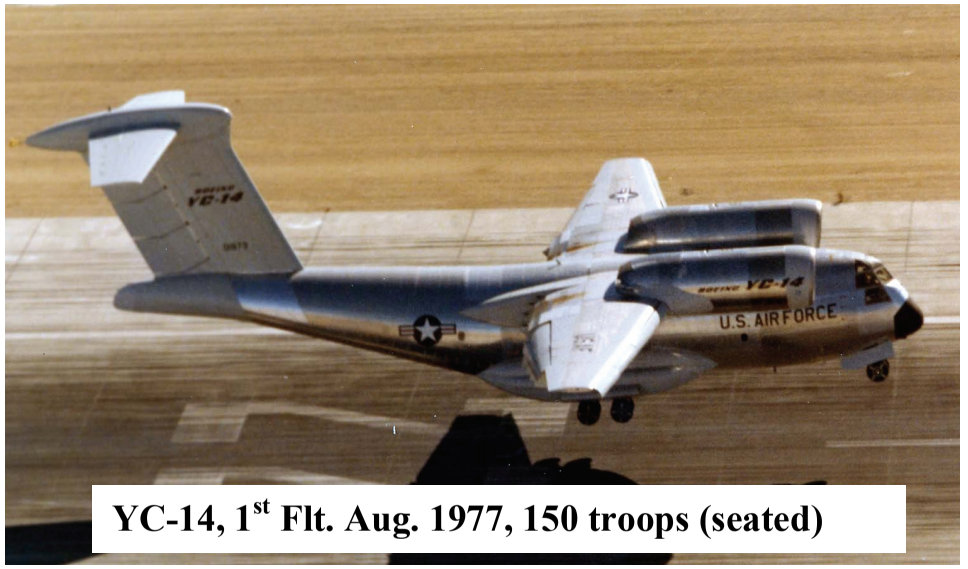

YC-14, 1st Flt. Aug. 1977, 150 troops (seated)

The Fixed Wing Industry's Eight Concrete STOLs.

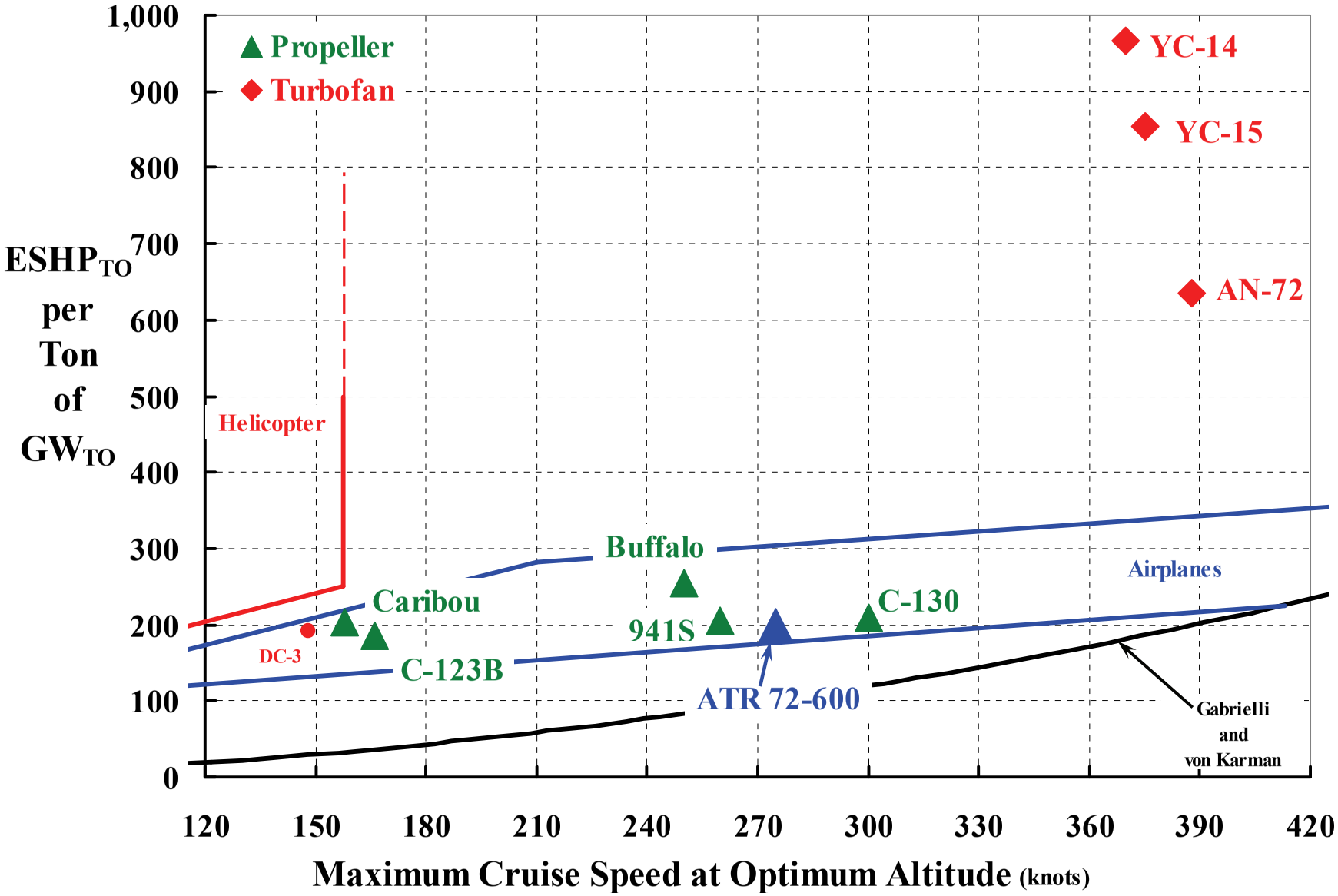

We've Made Substantial Progress With the R&D $$ We've Had.

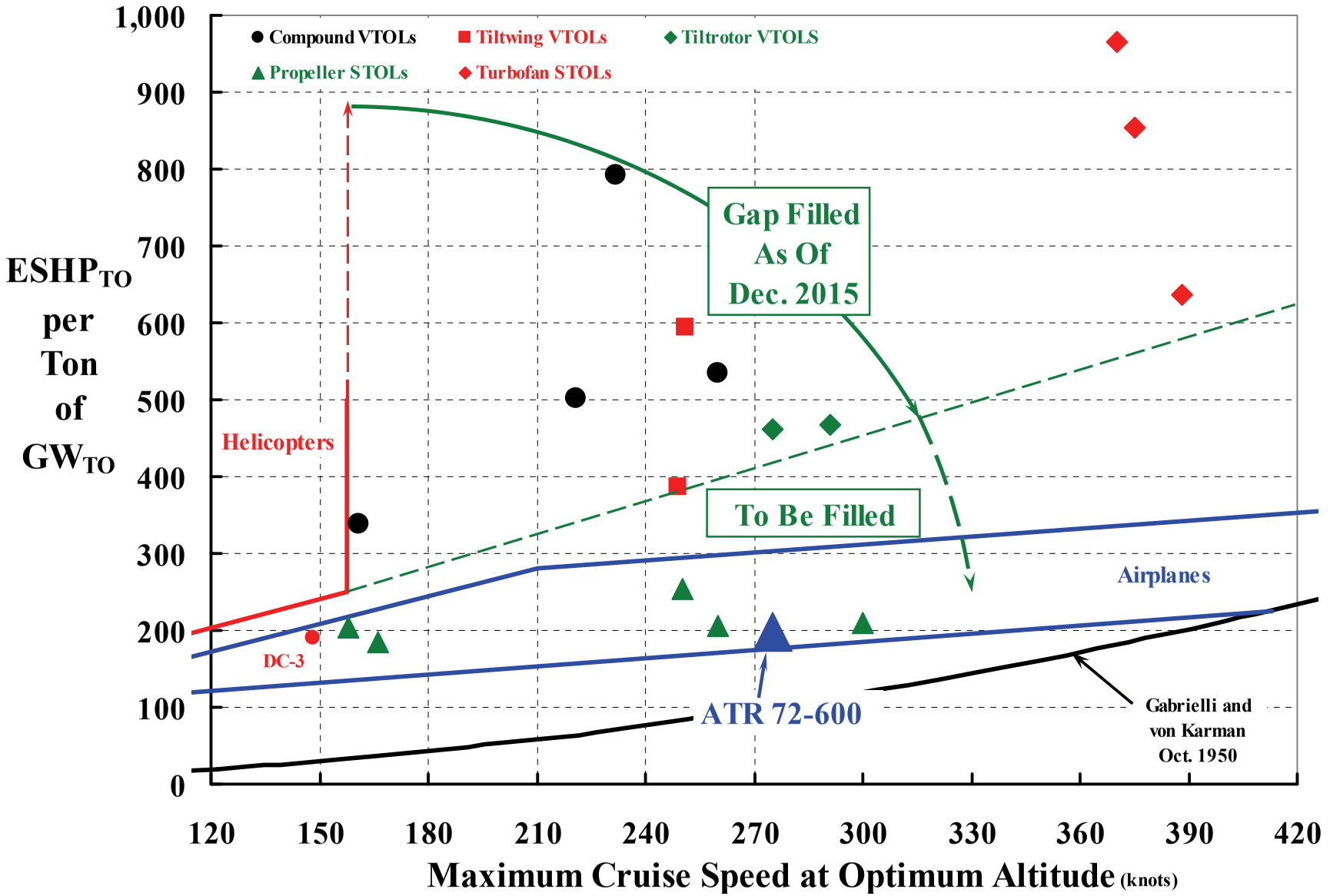

V/STOLs Should Takeoff and Land—*With Seats and Tanks Full*—From a Runway Located at Denver, Colorado on a 95°F Day. Aim for (a) and (b):

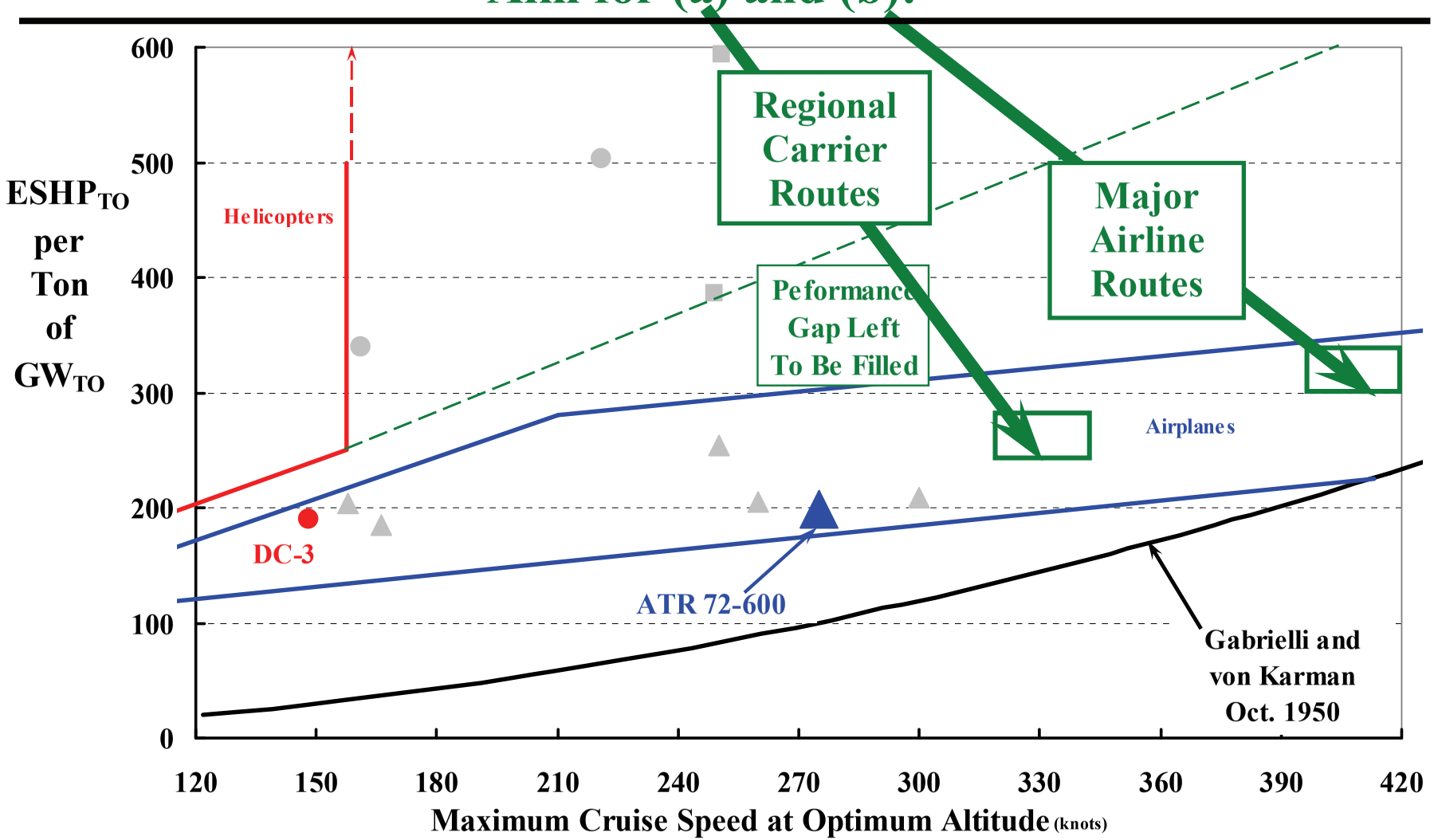

Why Aren't We Marketing a Competitor to Regional Turboprop Aircraft Like This 70-Passenger Fixed Wing?

- The ATR 72-600 first entered service in 1989 as the ATR 72-100.
- The – 600 is powered by two P&W Canada PW127M rated at 2,500 ESHP each.
- Its maximum takeoff weight (MTOW) is 50,265 lb.
- It cruises at 275 knots at 95% of MTOW on 5,000 ESHP burning fuel at 1,680 lb/hr.
- Its range with 70 passengers is 825 n.m. and its HP/Ton equals 209. It sells for $20 M in 2015.

Problem: The Europeans Have Taken the Lead on Commercial V/STOLs. What to Do About It and How to Start?

1. Reestablish our view that there is a need for commercial V/STOLs.
   a. Turn to our industry leaders and ask for their advocacy and their help.
   b. Survey all the Regional and Major Airlines to establish their current views about their future needs and how V/STOLs might help them make more profit. Give them a pitch about what we can offer. Ask them what V/STOL characteristics must be before they would consider any further discussion. Try to establish if VTOL or STOL is the better candidate.

2. Come home and do some engineering and make the rounds again until we have a little momentum.

3. Bet on the come and approach Cessna, ATR, Bombardier, Embraer, and Mitsubishi about putting a tiltrotor or tiltwing on a couple of their fuselages to make a demonstration article.

4. With respect to aeromechanics:
   a. The Regional configuration for 330 knots is feasible with today's technology.
   b. The Airliner configuration for 425 knots is not. It needs a lot of R&D. For instance:
      (1) The aero guys can get very competitive configurations if the wing airfoil has a $t/c < 0.17$.
      (2) Therefore, the burden falls on the aeroelastic stability guys to find stiffness and couplings that clear the flight envelope to Mach 0.85 for both a tiltrotor and a tiltwing.

5. If we can't solve the tiltrotor whirl flutter problem at high Mach number with wing airfoil $t/c < 0.17$, then turn to the tiltwing.

Backup Charts

The Tupolev Tu-114, a Long-Range Airliner, Was Derived From the Tu-95 Bomber.

Ref: Wikipedia

- Entered service in April 1961, and 32 were built and sold.
- World speed record of 462.857 kts over a 5000 kilometer course (with payload 0 to 25,000 kg).
- 170 sleeping berths plus a dining lounge (or seating for 224 passengers).
- Maximum takeoff weight (MTOW) at 385,800 lb. Weight empty 189,000 to 194,500 lb.
- Powered by four NK-12MV, each rated at 14,800 eshp.
- Cruised at 415 knots at turbojet altitudes with a HP/Ton equal to 307.

VTOLs—Edgewise Flying Rotors vs. Proprotors.

Ref: Harris, *The Path to the V-22.* NASA / Army Seminar, Ames Research Center, November 5, 2014

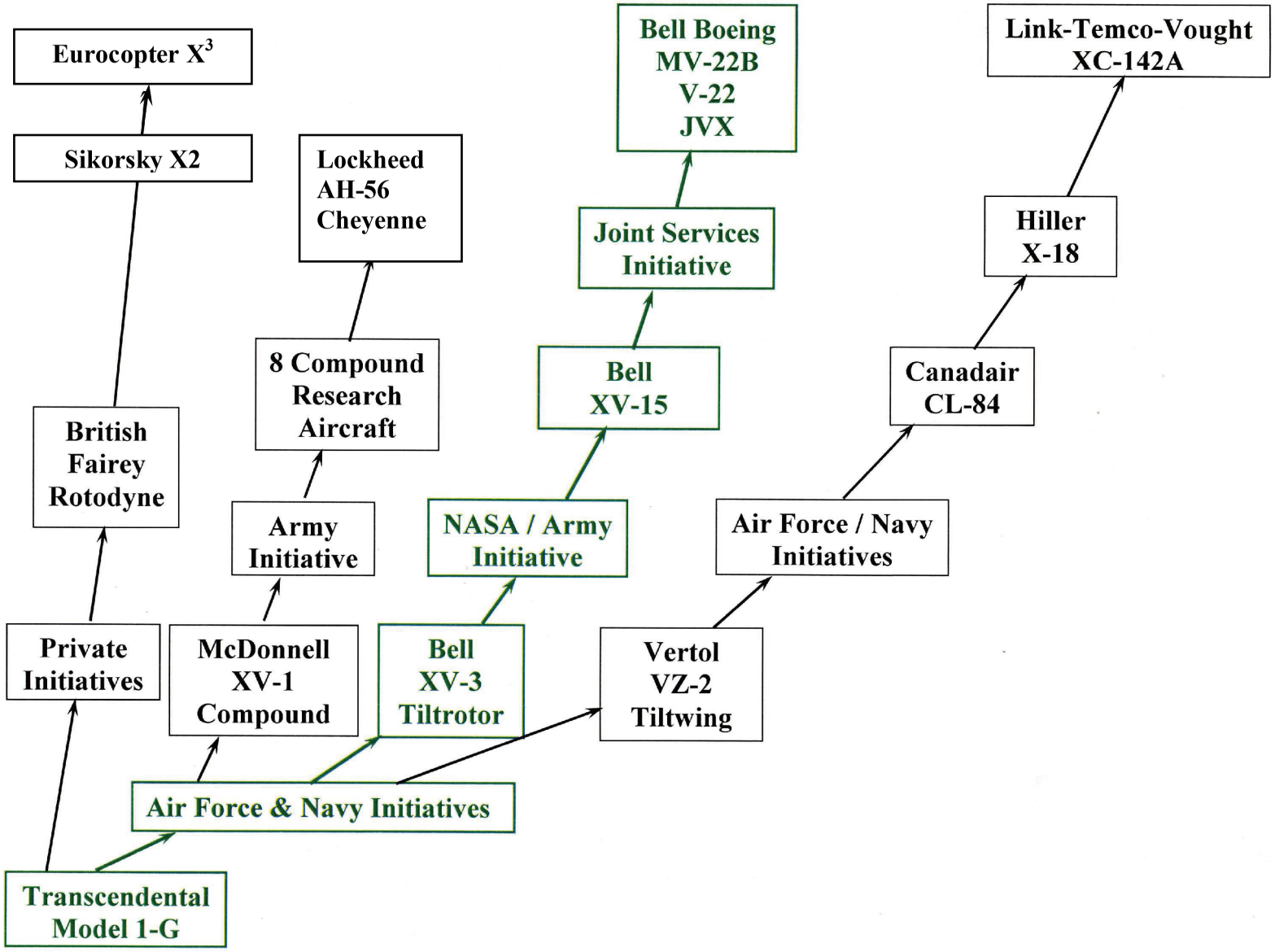

Incidentally, for the Army's Future Vertical Lift Program, the Russian Mi-12 Could Have Been a Compound Airplane, or a Tiltrotor, or even a Tiltwing.

Ref: John Stroud, *Soviet Transport Aircraft Since 1945*, Funk & Wagnalls, New York, 1968

When it first flew on July 10, 1968, Mil's Mi-12 (the Homer) was the largest helicopter in the world. The maximum STOL takeoff gross weight was 213,850 lb with a 27-ton payload. It was powered by four 6,500 eshp D-35VF turboshaft engines and lifted by two, five-bladed, 114.83-foot-diameter rotors. The maximum speed was 140 knots and it cruised at 130 knots. Civil version was designed for 170 passengers.

Note: Disc Loading was 10.3 lbs/ft^2.
At 20 lbs/ft^2, diameter = 82 ft.

My Concept Design Chart for VTOLs.

Ref: Harris, *High Speed Rotorcraft,* Presented at NASA/Army Seminar, NASA Ames Research Center, April 2013 (derivation in Volume III)

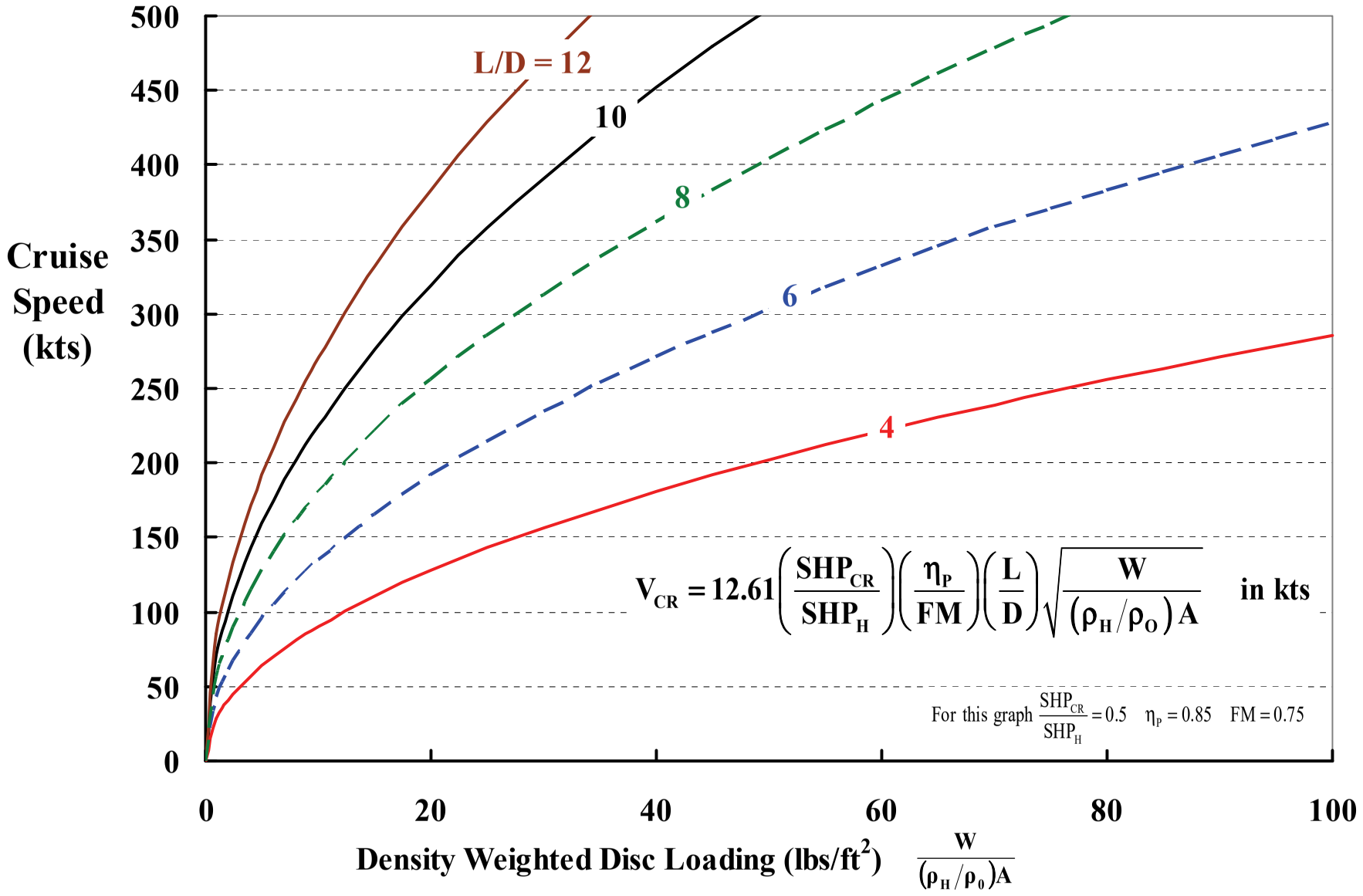

STOLs—Propellers vs. Turbofans.

Ref: Harris, *V/STOLs, Nine Decades of R&D – Few In Production.* NASA/Army Seminar, Ames Research Center, August 5, 2015

Note: Fighters in Gray

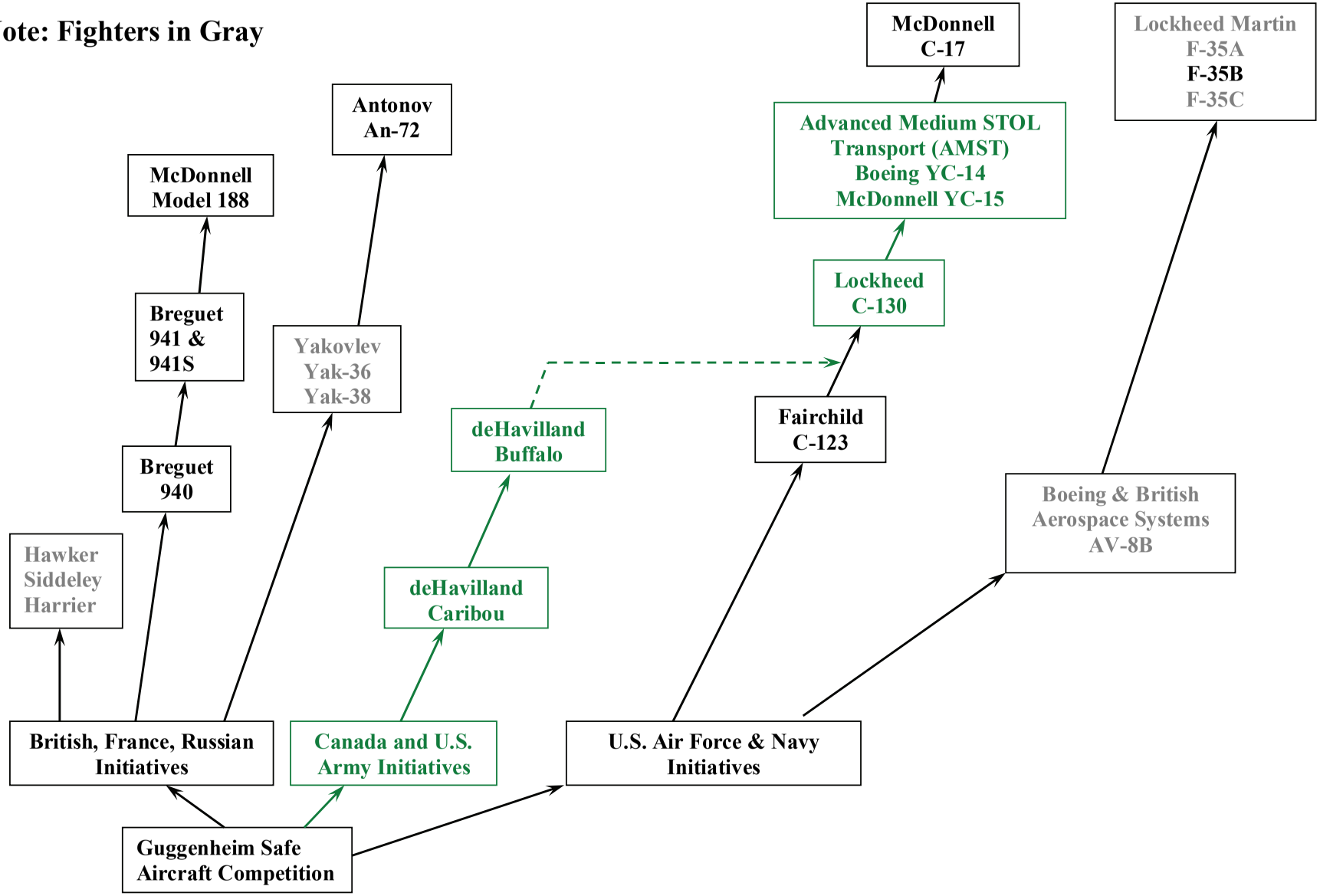

Boeing's Vice President of R&D, George Schairer, Presented This View on Aircraft Landing Field Lengths in Sept. 1969.

Ref: Schairer, G. S.: *A Summary and Overview of V/STOL Concepts*. V/STOL Technology and Planning Conference, Las Vegas, Nevada September 26, 1969. (Lecture Note: May 19, 1913-Oct. 28, 2004, Operation Paperclip, Seattle World's Fair late summer 1962)

Note: Assumes Multi-Engine Aircraft

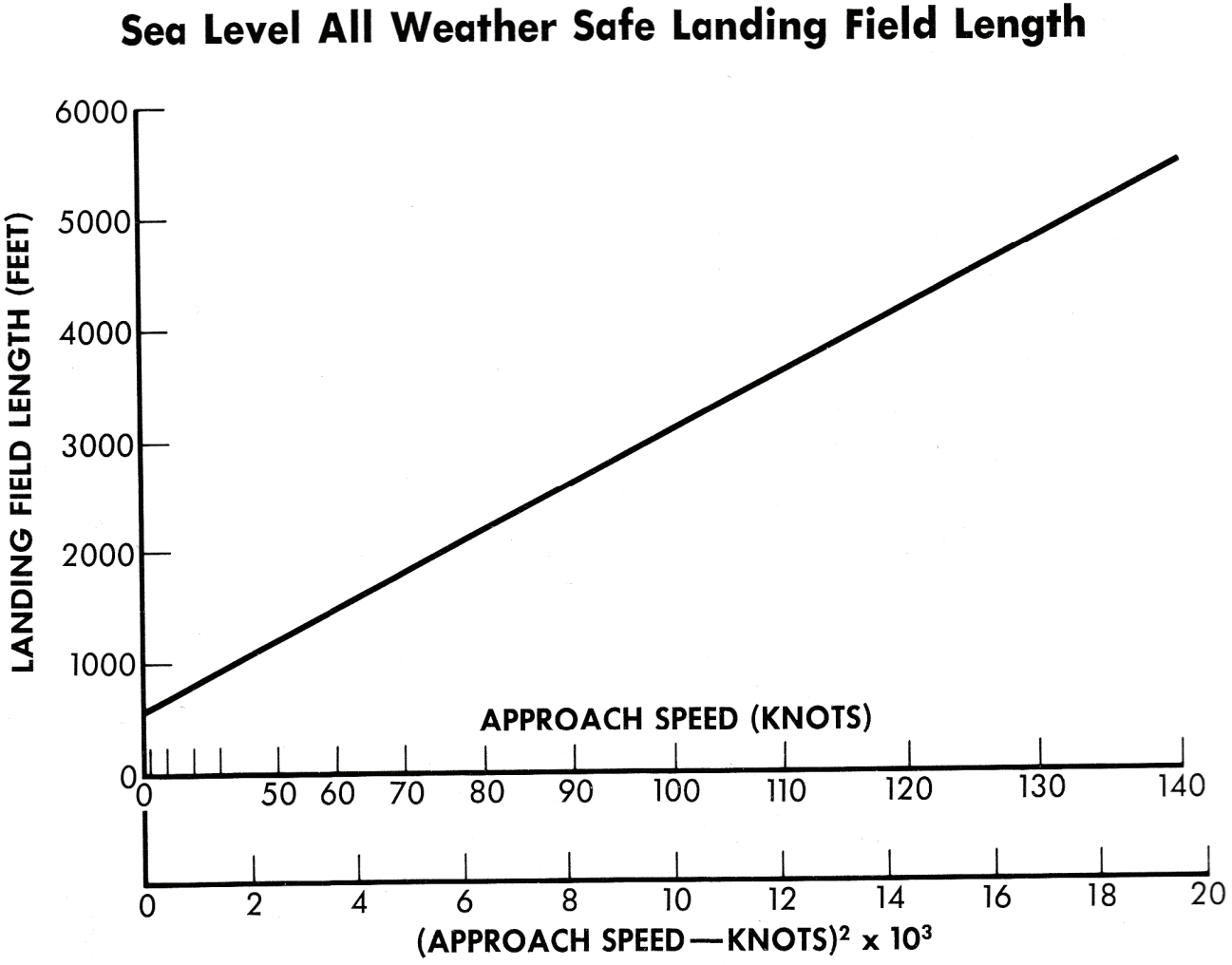

My Concept Design Chart for STOL Takeoff.

Ref: Harris, *Introduction to Autogyros, Helicopters and Other V/STOL Aircraft* (derivation in *Other V/STOL Aircraft*, Volume III)

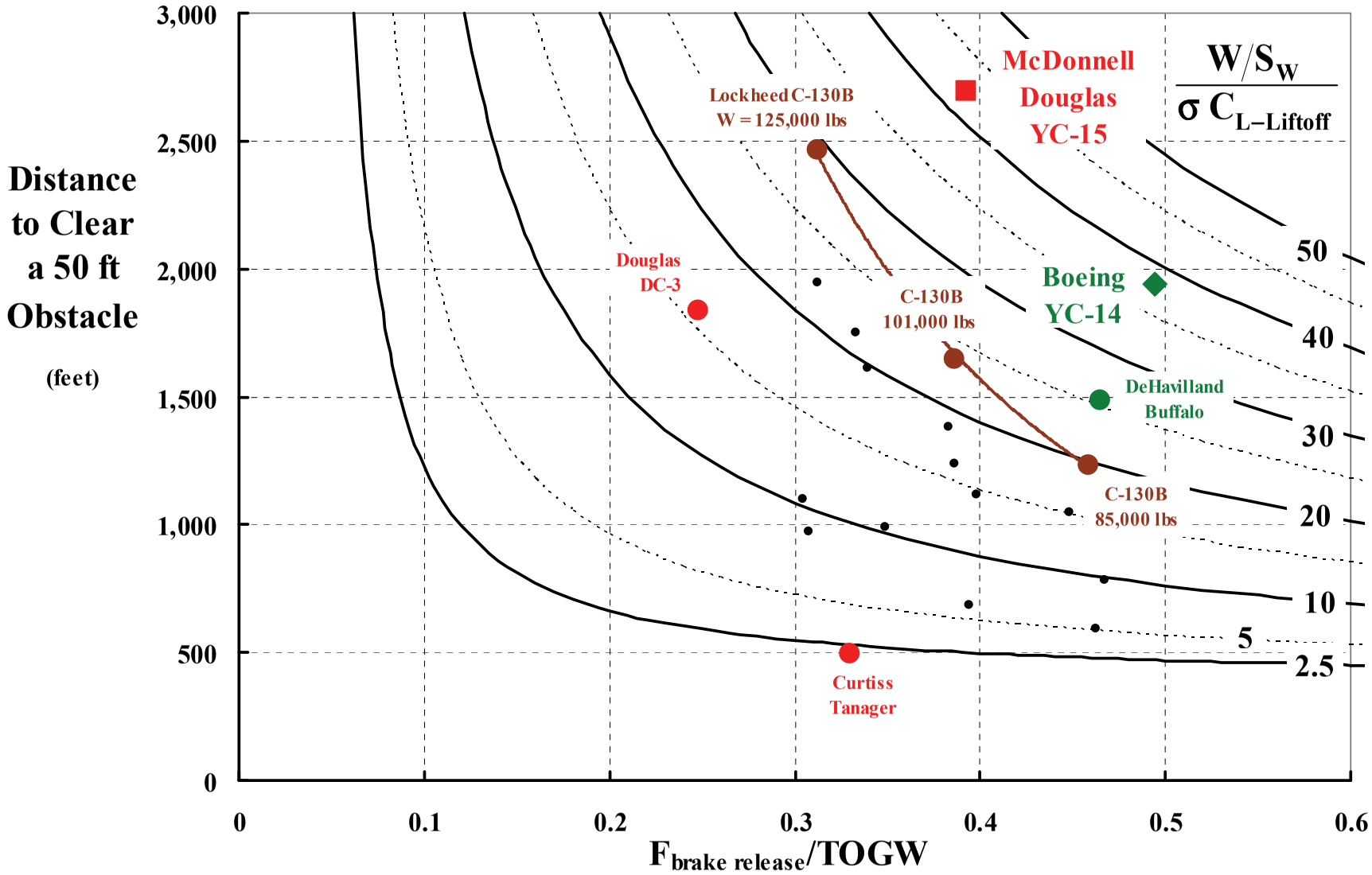

APPENDIX B

C81Gen/ARC2D Airfoil Tables for Cruise

C81Gen/ARC2D EXCEL Worksheet June 13, 2016

For SC(2) 00xx Airfoils on Harris' Proprotor

SECTION	**Number**	**1**	**2**	**3**	**4**	**5**	**6**	**7**	**8**
	r/R	0.1015	0.1065	0.1150	0.1275	0.1425	0.1600	0.1850	0.2150
	Airfoil	SC(2) 0012	SC(2) 0012	SC(2) 0012	SC(2) 0012	SC(2) 0012	SC(2) 0012	SC(2) 0012	SC(2) 0012
	RN	5.21E+06	5.19E+06	5.15E+06	5.10E+06	5.05E+06	5.01E+06	4.96E+06	4.92E+06
	RN/10^6	5.21	5.19	5.15	5.10	5.05	5.01	4.96	4.92
	Mach	**0.8108**	**0.8070**	**0.8012**	**0.7938**	**0.7865**	**0.7797**	**0.7723**	**0.7660**
	Alpha	CL	CL	CL	CL	CL	CL	CL	CL
	0.0	0.000499	0.000090	0.000031	-0.000004	-0.000003	-0.000004	-0.000004	-0.000004
	0.5	0.090766	0.096438	0.104823	0.107737	0.103982	0.098997	0.094685	0.091870
	1.0	0.163351	0.177032	0.194782	0.208088	0.209165	0.202781	0.193602	0.186582
	1.5	0.215198	0.238427	0.262094	0.287232	0.300132	0.303005	0.296396	0.287533
	2.0	0.254990	0.278144	0.310763	0.335706	0.365943	0.381043	0.388305	0.384388
	2.5	0.278430	0.300607	0.335860	0.362729	0.380000	0.430434	0.450597	0.460907
	3.0	0.296946	0.316639	0.353772	0.382074	0.382074	0.453426	0.485658	0.509907
	Alpha	CD	CD	CD	CD	CD	CD	CD	CD
	0.0	0.013537	0.011848	0.010217	0.009368	0.009130	0.009034	0.008955	0.008897
	0.5	0.014677	0.013021	0.011236	0.009901	0.009290	0.009090	0.009003	0.008940
	1.0	0.017768	0.016275	0.014419	0.012332	0.010646	0.009688	0.009228	0.009072
	1.5	0.022007	0.019806	0.018853	0.016632	0.014316	0.012399	0.010835	0.010022
	2.0	0.026627	0.023964	0.023272	0.021520	0.019755	0.017532	0.015217	0.013446
	2.5	0.031971	0.028774	0.028765	0.028765	0.026902	0.023781	0.021193	0.019342
	3.0	0.037822	0.034040	0.034831	0.034831	0.033697	0.030087	0.027914	0.026369
	Alpha	CM	CM	CM	CM	CM	CM	CM	CM
	0.0	-0.000123	-0.000018	-0.000004	0.000002	0.000001	0.000001	0.000001	0.000001
	0.5	-0.000642	-0.000645	-0.000521	0.000880	0.002117	0.002546	0.002533	0.002437
	1.0	0.000423	-0.000568	-0.001027	0.000173	0.002645	0.004765	0.005759	0.005730
	1.5	0.004759	-0.001068	0.000790	0.000361	0.002073	0.004560	0.007514	0.009081
	2.0	0.010662	0.000544	0.004759	0.004502	0.002863	0.004104	0.006463	0.009406
	2.5	0.016921	0.004759	0.010662	0.004759	0.004672	0.006377	0.007299	0.008625
	3.0	0.022732	0.010662	0.016921	0.010662	0.004391	0.011235	0.011030	0.010141

Number	**9**	**10**	**11**	**12**	**13**	**14**	**15**	**16**
r/R	0.2450	0.2800	0.3200	0.3600	0.4000	0.4400	0.4800	0.5250
Airfoil	SC(2) 0012	SC(2) 0010	SC(2) 0010	SC(2) 0010	SC(2) 0010	SC(2) 0008	SC(2) 0008	SC(2) 0008
RN	4.89E+06	4.87E+06	4.86E+06	5.11E+06	5.84E+06	6.53E+06	7.15E+06	7.76E+06
RN/10^6	4.89	4.87	4.86	5.11	5.84	6.53	7.15	7.76
Mach	**0.7617**	**0.7584**	**0.7562**	**0.7553**	**0.7553**	**0.7559**	**0.7571**	**0.7590**
Alpha	CL	CL	CL	CL	CL	CL	CL	CL
0.0	-0.000004	-0.000001	-0.000001	0.000000	0.000000	-0.000003	-0.000003	-0.000003
0.5	0.090245	0.087380	0.086780	0.086582	0.086700	0.085819	0.086163	0.086679
1.0	0.182548	0.176003	0.174682	0.174228	0.174472	0.172545	0.173267	0.174421
1.5	0.280765	0.267855	0.265580	0.264818	0.265084	0.261412	0.262564	0.264318
2.0	0.379598	0.366189	0.362496	0.361125	0.361502	0.354218	0.356332	0.359129
2.5	0.462343	0.467768	0.462384	0.459912	0.461158	0.453949	0.456811	0.461267
3.0	0.518624	0.558788	0.555615	0.554381	0.554993	0.556265	0.559921	0.565387
Alpha	CD	CD	CD	CD	CD	CD	CD	CD
0.0	0.008862	0.009126	0.009121	0.009056	0.008896	0.008140	0.008042	0.007957
0.5	0.008902	0.009155	0.009149	0.009084	0.008922	0.008165	0.008067	0.007982
1.0	0.009028	0.009247	0.009242	0.009176	0.009012	0.008255	0.008157	0.008070
1.5	0.009680	0.009601	0.009560	0.009479	0.009315	0.008642	0.008556	0.008495
2.0	0.012474	0.011234	0.011080	0.010959	0.010799	0.010118	0.010081	0.010089
2.5	0.017936	0.015303	0.014872	0.014549	0.014506	0.013392	0.013446	0.013611
3.0	0.024842	0.021947	0.021275	0.020953	0.020816	0.019117	0.019323	0.019724
Alpha	CM	CM	CM	CM	CM	CM	CM	CM
0.0	0.000001	0.000000	0.000000	0.000000	0.000000	0.000001	0.000001	0.000001
0.5	0.002369	0.001961	0.001939	0.001932	0.001933	0.001489	0.001494	0.001505
1.0	0.005522	0.004458	0.004392	0.004369	0.004374	0.003463	0.003489	0.003534
1.5	0.009589	0.008938	0.008710	0.008623	0.008653	0.007152	0.007274	0.007465
2.0	0.011074	0.014144	0.014090	0.014073	0.014110	0.012846	0.012974	0.013229
2.5	0.010367	0.015697	0.016492	0.016844	0.016772	0.017510	0.017463	0.017324
3.0	0.011196	0.013717	0.014899	0.015381	0.015399	0.018429	0.017936	0.017082

Number	**17**	**18**	**19**	**20**	**21**	**22**	**23**	**24**
r/R	0.5700	0.6100	0.6500	0.6900	0.7300	0.7700	0.8050	0.8350
Airfoil	SC(2) 0008	SC(2) 0008	SC(2) 0008	SC(2) 0008	SC(2) 0006	SC(2) 0006	SC(2) 0006	SC(2) 0006
RN	8.24E+06	8.59E+06	8.85E+06	9.03E+06	9.14E+06	9.16E+06	9.06E+06	8.84E+06
RN/10^6	8.24	8.59	8.85	9.03	9.14	9.16	9.06	8.84
Mach	**0.7613**	**0.7638**	**0.7665**	**0.7695**	**0.7727**	**0.7762**	**0.7794**	**0.7823**
Alpha	CL	CL	CL	CL	CL	CL	CL	CL
0.0	-0.000003	-0.000003	-0.000003	-0.000003	-0.000003	-0.000003	-0.000003	-0.000003
0.5	0.087282	0.087936	0.088656	0.089477	0.089892	0.089892	0.090704	0.091458
1.0	0.175771	0.177179	0.178708	0.180494	0.181142	0.181142	0.182858	0.184502
1.5	0.266584	0.269045	0.271836	0.275051	0.275991	0.275991	0.279277	0.282427
2.0	0.362951	0.367094	0.372119	0.377916	0.379163	0.379163	0.384994	0.390884
2.5	0.466764	0.472760	0.479816	0.487572	0.493565	0.493565	0.502934	0.511730
3.0	0.571799	0.578380	0.586233	0.593509	0.614082	0.614082	0.625236	0.635176
Alpha	CD	CD	CD	CD	CD	CD	CD	CD
0.0	0.007897	0.007857	0.007831	0.007816	0.007252	0.007252	0.007264	0.007290
0.5	0.007922	0.007883	0.007857	0.007842	0.007280	0.007280	0.007293	0.007320
1.0	0.008008	0.007969	0.007944	0.007931	0.007410	0.007410	0.007431	0.007465
1.5	0.008466	0.008461	0.008474	0.008512	0.008191	0.008191	0.008272	0.008365
2.0	0.010156	0.010262	0.010411	0.010598	0.010493	0.010493	0.010731	0.010981
2.5	0.013882	0.014222	0.014653	0.015191	0.015341	0.015341	0.015913	0.016495
3.0	0.020274	0.020929	0.021738	0.022672	0.023466	0.023466	0.024506	0.025534
Alpha	CM	CM	CM	CM	CM	CM	CM	CM
0.0	0.000001	0.000001	0.000001	0.000001	0.000001	0.000001	0.000001	0.000001
0.5	0.001520	0.001538	0.001558	0.001582	0.001077	0.001077	0.001098	0.001117
1.0	0.003593	0.003666	0.003757	0.003862	0.002962	0.002962	0.003088	0.003207
1.5	0.007682	0.007943	0.008233	0.008570	0.007295	0.007295	0.007654	0.007989
2.0	0.013454	0.013682	0.013823	0.013909	0.013081	0.013081	0.013284	0.013341
2.5	0.017033	0.016604	0.015890	0.014896	0.015697	0.015697	0.014684	0.013483
3.0	0.015915	0.014510	0.012610	0.010456	0.011068	0.011068	0.008224	0.005295

Number	**25**	**26**	**27**	**28**	**29**	**30**	**31**	**32**
r/R	0.8750	0.9150	0.9400	0.9575	0.9725	0.9850	0.9935	0.9985
Airfoil	SC(2) 0006	SC(2) 0006	SC(2) 0006	SC(2) 0006	SC(2) 0006	SC(2) 0006	SC(2) 0006	SC(2) 0006
RN	8.26E+06	7.17E+06	6.11E+06	5.13E+06	4.11E+06	3.10E+06	2.33E+06	1.85E+06
RN/10^6	8.26	7.17	6.11	5.13	4.11	3.10	2.33	1.85
Mach	**0.7863**	**0.7905**	**0.7932**	**0.7951**	**0.7968**	**0.7982**	**0.7992**	**0.7998**
Alpha	CL	CL	CL	CL	CL	CL	CL	CL
0.0	-0.000003	-0.000003	-0.000003	-0.000003	-0.000003	-0.000004	-0.000004	-0.000005
0.5	0.092519	0.093619	0.094296	0.094708	0.095036	0.095214	0.095242	0.095205
1.0	0.186810	0.189127	0.190641	0.191647	0.192478	0.192861	0.192984	0.192953
1.5	0.287023	0.292197	0.295625	0.298043	0.300095	0.301295	0.301479	0.301563
2.0	0.399502	0.409014	0.415458	0.420019	0.423908	0.426631	0.428418	0.429189
2.5	0.524517	0.538464	0.547079	0.552653	0.557092	0.560099	0.561030	0.561751
3.0	0.648289	0.660801	0.666732	0.669779	0.670544	0.670448	0.668539	0.667411
Alpha	CD	CD	CD	CD	CD	CD	CD	CD
0.0	0.007360	0.007507	0.007678	0.007871	0.008127	0.008470	0.008840	0.009156
0.5	0.007391	0.007539	0.007712	0.007907	0.008164	0.008510	0.008883	0.009202
1.0	0.007552	0.007725	0.007916	0.008123	0.008390	0.008746	0.009125	0.009449
1.5	0.008542	0.008815	0.009069	0.009327	0.009641	0.010031	0.010435	0.010771
2.0	0.011392	0.011959	0.012434	0.012855	0.013321	0.013831	0.014323	0.014706
2.5	0.017420	0.018598	0.019491	0.020211	0.020938	0.021624	0.022234	0.022718
3.0	0.027094	0.028917	0.030146	0.031056	0.031794	0.032610	0.033119	0.033598
Alpha	CM	CM	CM	CM	CM	CM	CM	CM
0.0	0.000001	0.000001	0.000001	0.000001	0.000001	0.000001	0.000001	0.000001
0.5	0.001148	0.001185	0.001214	0.001237	0.001262	0.001286	0.001305	0.001314
1.0	0.003395	0.003615	0.003770	0.003882	0.003985	0.004067	0.004128	0.004155
1.5	0.008452	0.008918	0.009197	0.009363	0.009490	0.009575	0.009602	0.009604
2.0	0.013224	0.012771	0.012231	0.011720	0.011179	0.010699	0.010286	0.010023
2.5	0.011275	0.008183	0.005827	0.004042	0.002379	0.001002	0.000081	-0.000580
3.0	0.000727	-0.004656	-0.008099	-0.010478	-0.012164	-0.013818	-0.014499	-0.015239

APPENDIX C

C81Gen/ARC2D Airfoil Tables and Graphs for Hover

Number	**1**	**2**	**3**	**4**	**5**
r/R	0.125	0.175	0.225	0.275	0.325
Airfoil	SC(2) 0012	SC(2) 0012	SC(2) 0012	SC(2) 0012	SC(2) 0012
RN	1.42E+06	1.94E+06	2.46E+06	2.98E+06	3.50E+06
RN/10^6	1.42	1.94	2.46	2.98	3.50

Mach	**0.0944**	**0.1288**	**0.1631**	**0.1975**	**0.2320**
Alpha	CL	CL	CL	CL	CL
0.0	-0.000008	-0.000004	0.000000	-0.000003	0.000002
2.0	0.206306	0.207734	0.209062	0.210545	0.212288
4.0	0.409681	0.412917	0.415797	0.418869	0.422435
6.0	0.607112	0.613046	0.617914	0.622833	0.628337
8.0	0.794680	0.805013	0.812629	0.819785	0.829542
10.0	0.966724	0.984435	0.996184	1.006152	1.016062
11.0	1.072589	1.079999	1.087779	1.096457	1.106032
12.0	1.152534	1.161409	1.171382	1.180580	1.190493

Alpha	CD	CD	CD	CD	CD
0.0	0.010639	0.010020	0.009580	0.009243	0.008972
2.0	0.010855	0.010216	0.009764	0.009418	0.009142
4.0	0.011554	0.010861	0.010380	0.010016	0.009728
6.0	0.012795	0.012008	0.011482	0.011093	0.010793
8.0	0.014695	0.013763	0.013171	0.012748	0.012429
10.0	0.017484	0.016330	0.015631	0.015167	0.014861
11.0	0.019002	0.017929	0.017283	0.016858	0.016593
12.0	0.021067	0.019793	0.019246	0.018794	0.018580

Alpha	CM	CM	CM	CM	CM
0.0	0.000001	0.000001	0.000000	0.000001	0.000000
2.0	0.003317	0.003359	0.003426	0.003504	0.003589
4.0	0.007016	0.007049	0.007159	0.007318	0.007499
6.0	0.011472	0.011379	0.011487	0.011720	0.012031
8.0	0.017117	0.016666	0.016694	0.016993	0.017304
10.0	0.024387	0.023223	0.023033	0.023379	0.024090
11.0	0.024099	0.024852	0.025573	0.026422	0.027520
12.0	0.027706	0.028343	0.029105	0.030164	0.031527

Number	**6**	**7**	**8**	**9**	**10**	**11**	**12**
r/R	0.375	0.425	0.475	0.525	0.575	0.63	0.69
Airfoil	SC(2) 0010	SC(2) 0010	SC(2) 0008	SC(2) 0008	SC(2) 0008	SC(2) 0008	SC(2) 0008
RN	4.41E+06	5.89E+06	7.37E+06	8.85E+06	1.03E+07	1.18E+07	1.32E+07
RN/10^6	4.41	5.89	7.37	8.85	10.32	11.78	13.25

Mach	**0.2667**	**0.3010**	**0.3351**	**0.3693**	**0.4034**	**0.4405**	**0.4810**
Alpha	CL	CL	CL	CL	CL	CL	CL
0	-0.000006	-0.000001	-0.000001	0.000002	-0.000001	-0.000002	-0.000002
1	0.108049	0.109391	0.112559	0.114269	0.116188	0.118564	0.121604
2	0.216085	0.218773	0.225054	0.228478	0.232329	0.237107	0.243181
3	0.323633	0.327684	0.337058	0.342229	0.348045	0.355275	0.364474
4	0.430609	0.436065	0.448469	0.455399	0.463189	0.472834	0.484971
5	0.536811	0.543710	0.559021	0.567625	0.577075	0.588347	0.595668
6	0.641964	0.650347	0.668147	0.677583	0.685097	0.681742	0.670517
7	0.745726	0.755570	0.773864	0.776413	0.761215	0.730971	0.696130
8	0.847640	0.858798	0.865746	0.833722	0.73639269	0.737157	0.70597953
9	0.946967	0.958742	0.911062				
10	1.042624	1.051791					
11	1.132238	1.121268					
12	1.207065	1.139081					

Alpha	CD	CD	CD	CD	CD	CD	CD
0	0.009635	0.009197	0.008444	0.008181	0.007962	0.007765	0.007594
1	0.009673	0.009233	0.008484	0.008220	0.008002	0.007804	0.007635
2	0.009795	0.009350	0.008611	0.008346	0.008128	0.007933	0.007767
3	0.010019	0.009566	0.008843	0.008578	0.008362	0.008171	0.008014
4	0.010352	0.009891	0.009194	0.008932	0.008723	0.008549	0.008431
5	0.010805	0.010336	0.009687	0.009440	0.009271	0.009187	0.009631
6	0.011392	0.010918	0.010370	0.010217	0.010390	0.011634	0.014058
7	0.012134	0.011658	0.011425	0.012061	0.014711	0.019970	0.029581
8	0.013059	0.012598	0.013867	0.018687	0.03324336	0.075384	0.03324336
9	0.014216	0.013830	0.021736				
10	0.015687	0.015635					
11	0.017831	0.019488					
12	0.021517	0.028396					

Alpha	CM	CM	CM	CM	CM	CM	CM
0	0.000001	0.000000	0	0.000000	0.000000	0.000000	0.000000
1	0.001645	0.001672	0.001233	0.001260	0.001298	0.001353	0.001431
2	0.003329	0.003387	0.002526	0.002591	0.002682	0.002814	0.003005
3	0.005075	0.005176	0.003933	0.004061	0.004237	0.004495	0.004879
4	0.006916	0.007074	0.005508	0.005738	0.006058	0.006543	0.007319
5	0.008885	0.009121	0.007315	0.007726	0.008334	0.009341	0.012158
6	0.011020	0.011361	0.009468	0.010282	0.011905	0.016129	0.022437
7	0.013364	0.013861	0.012280	0.014751	0.019973	0.026680	0.031229
8	0.015970	0.016697	0.017098	0.023695	0	-0.039310	-0.06000
9	0.018913	0.020028	0.025970				
10	0.022281	0.024248					
11	0.026056	0.030716					
12	0.034304	0.038964					

Number	**13**	**14**	**15**	**16**	**17**	**18**	**19**	**20**
r/R	0.745	0.79	0.83	0.865	0.895	0.925	0.955	0.985
Airfoil	SC(2) 0006	SC(2) 0006	SC(2) 0006	SC(2) 0006	SC(2) 0006	SC(2) 0006	SC(2) 0006	SC(2) 0006
RN	1.44E+07	1.51E+07	1.54E+07	1.50E+07	1.41E+07	1.28E+07	1.02E+07	6.48E+06
RN/10^6	14.41	15.09	15.39	15.01	14.14	12.77	10.22	6.48
Mach	**0.5180**	**0.5486**	**0.5754**	**0.5946**	**0.6086**	**0.6284**	**0.6511**	**0.6796**
Alpha	CL	CL	CL	CL	CL	CL	CL	CL
0	-0.000001	-0.000001	-0.000001	-0.000001	-0.000001	-0.000001	-0.000002	-0.000002
1	0.126226	0.129324	0.132396	0.134828	0.136706	0.139597	0.143192	0.148287
2	0.252414	0.258650	0.264873	0.269815	0.273679	0.279663	0.287344	0.297666
3	0.377944	0.386443	0.394353	0.400374	0.404533	0.410969	0.421592	0.440533
4	0.489307	0.494429	0.501346	0.508457	0.515388	0.529015	0.548675	0.579940
5	0.568797	0.569187	0.574544	0.582121	0.590491	0.611885	0.648528	0.698949
6	0.610424	0.610480	0.611963	0.613738	0.615459	0.619001	0.632025	0.666370
7	0.651555	0.639253	0.643456	0.639404	0.637727	0.635596	0.634610	0.635557
8	0.666754	0.658928	0.654466	0.652264	0.651131	0.650341	0.650310	0.649883
9	0.673211	0.668696	0.666469					0.670775
10	0.682928							0.694822

Alpha	CD	CD	CD	CD	CD	CD	CD	CD
0	0.007065	0.006978	0.006923	0.006922	0.006961	0.007026	0.007217	0.007650
1	0.007113	0.007027	0.006975	0.006976	0.007016	0.007086	0.007282	0.007727
2	0.007274	0.007197	0.007154	0.007164	0.007213	0.007296	0.007509	0.008059
3	0.007624	0.007655	0.007761	0.007944	0.008226	0.008842	0.009919	0.011734
4	0.009408	0.010262	0.011477	0.012631	0.013631	0.015276	0.017537	0.021130
5	0.016984	0.019096	0.020867	0.022448	0.023706	0.025808	0.029412	0.035371
6	0.035719	0.039287	0.042155	0.044211	0.045645	0.047063	0.048737	0.051592
7	0.063173	0.066190	0.070277	0.071883	0.073062	0.074652	0.076308	0.078416
8	0.088837	0.093501	0.093501	0.094847	0.095791	0.097130	0.098645	0.100238
9	0.109196	0.113519	0.113519					0.120703
10	0.128207							0.140774

Alpha	CM	CM	CM	CM	CM	CM	CM	CM
0	0.000000	0.000000	0.000000	0.000000	0.000000	0.000000	0.000000	0.000000
1	0.000969	0.001032	0.001101	0.001161	0.001215	0.001299	0.001423	0.001628
2	0.002162	0.002356	0.002574	0.002773	0.002950	0.003252	0.003700	0.004690
3	0.003942	0.004650	0.005596	0.006514	0.007394	0.008812	0.010403	0.012793
4	0.008988	0.011379	0.013527	0.015078	0.016208	0.017771	0.019986	0.023611
5	0.017499	0.020486	0.023144	0.024943	0.026300	0.028426	0.030747	0.033601
6	0.021036	0.019896	0.018217	0.016571	0.015318	0.014493	0.014388	0.018303
7	-0.006765	-0.010720	-0.017181	-0.019070	-0.020427	-0.022266	-0.023674	-0.024942
8	-0.040503	-0.042450	-0.043667	-0.044308	-0.044668	-0.045123	-0.045433	-0.044823
9	-0.057723	-0.058518	-0.058805					-0.058304
10	-0.068332							-0.068501

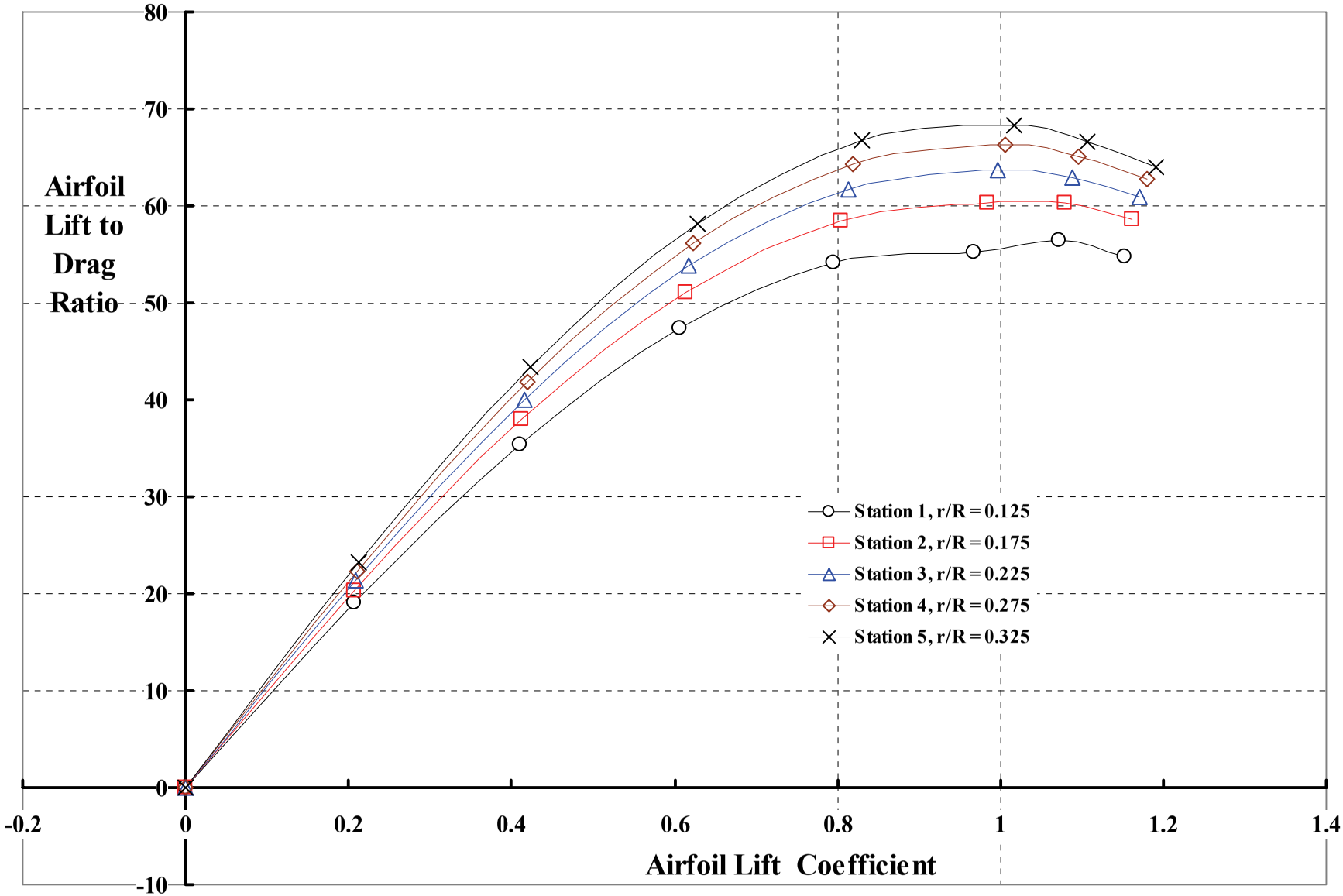

Figure C-1. SC(2)–0012

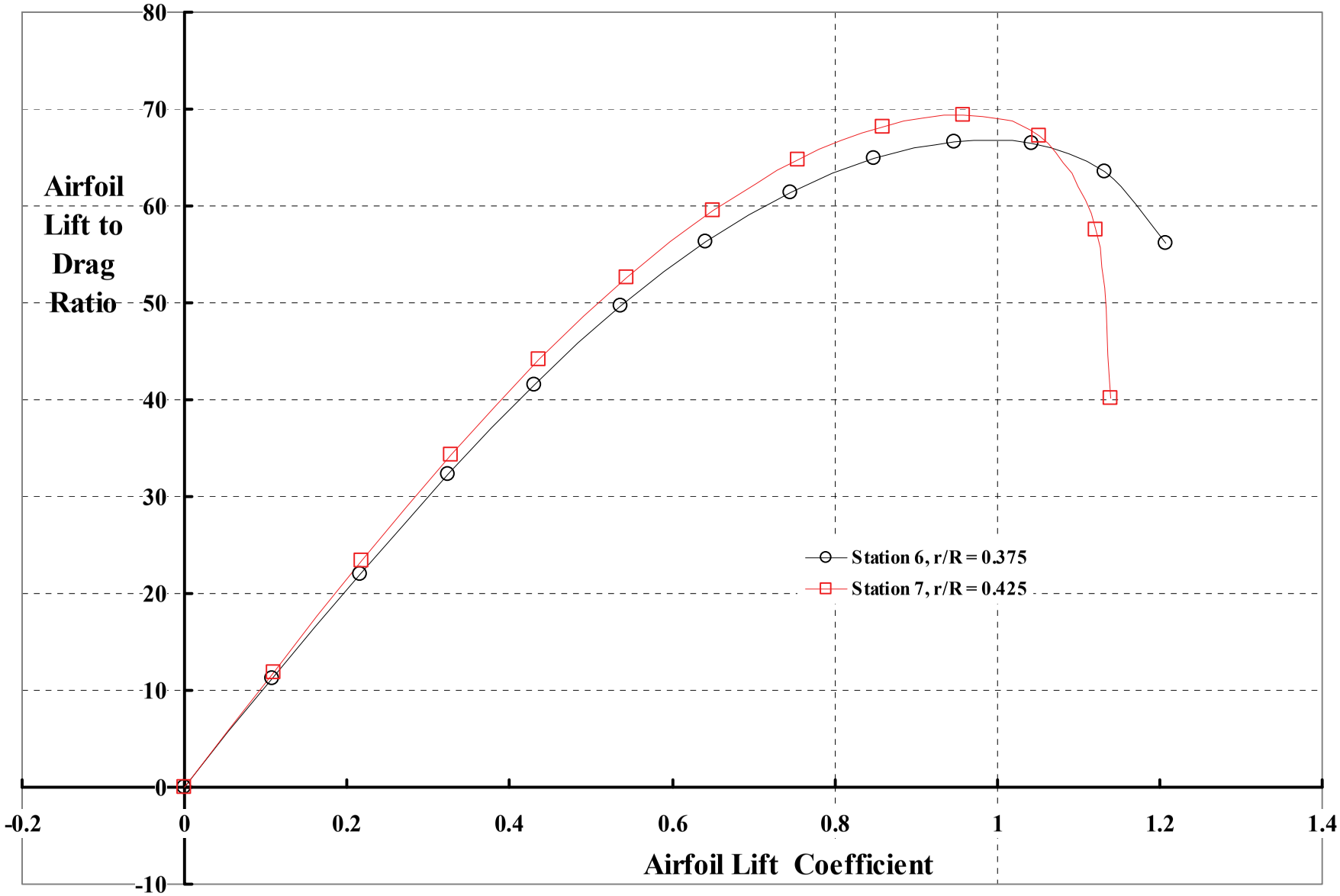

Figure C-2. SC(2)–0010

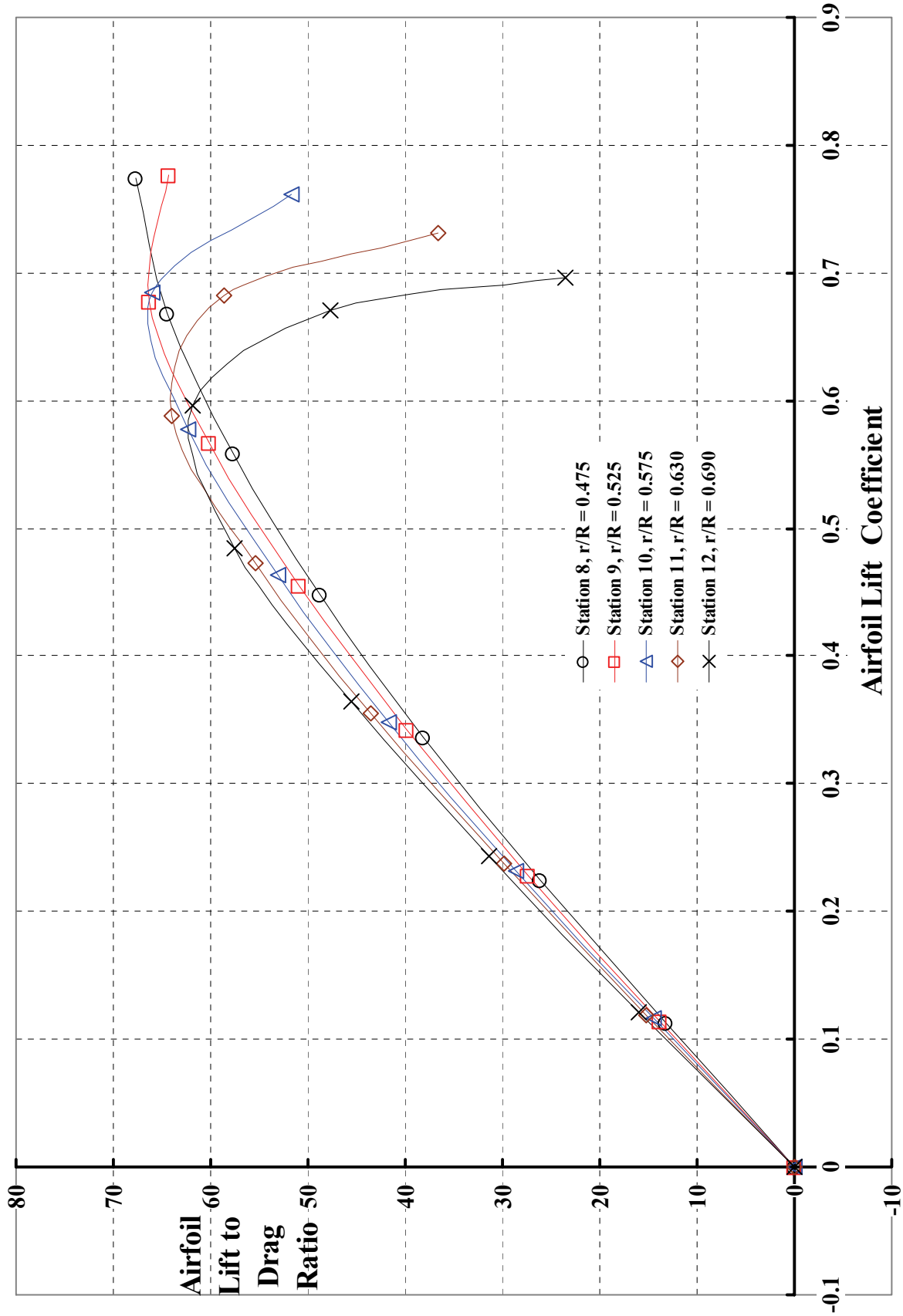

Figure C-3. SC(2)–0008

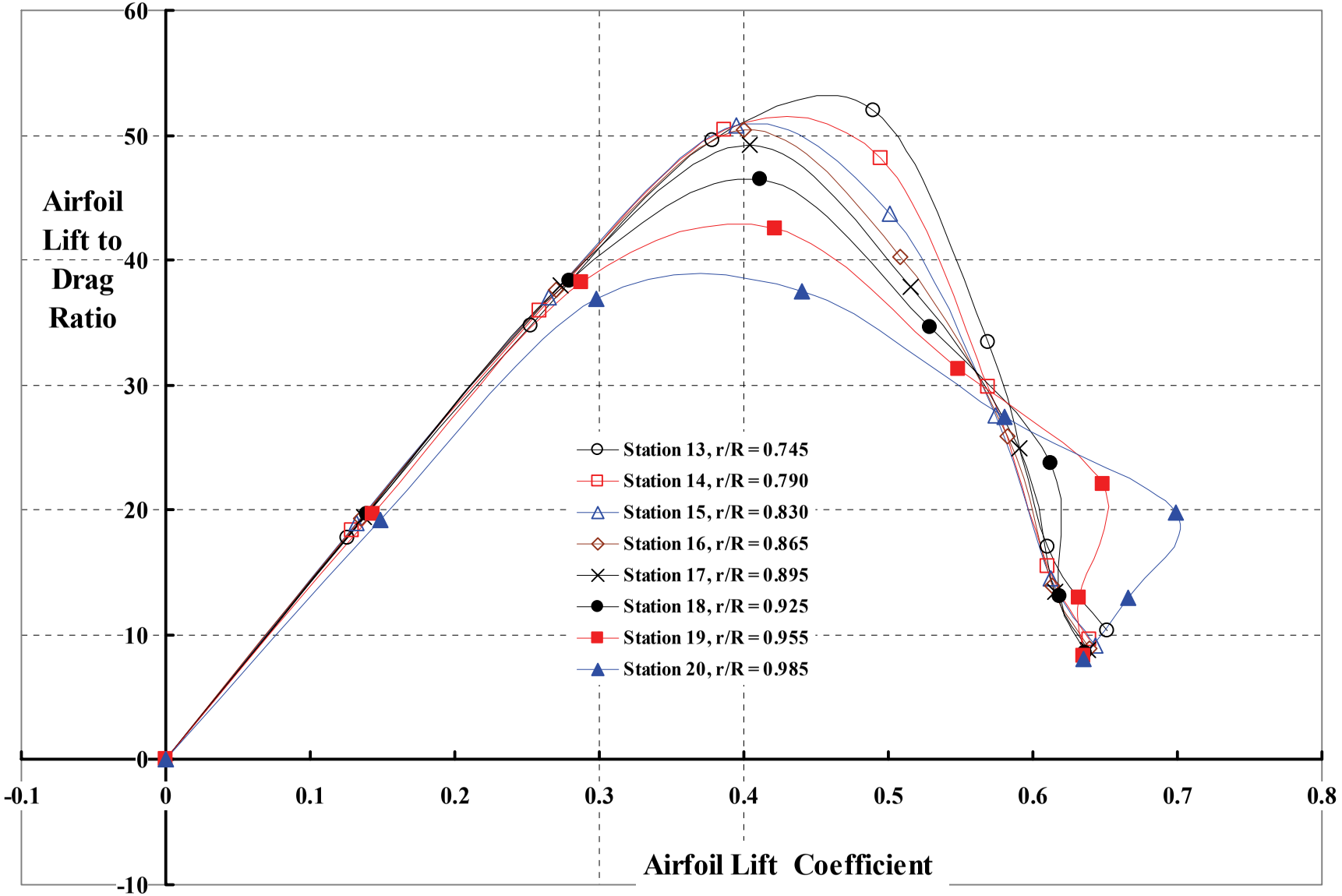

Figure C-4. SC(2)–0006

APPENDIX D

C81Gen/ARC2D Evaluation Using NACA 0012 Airfoil Data

Memorandum of Record

To: Bill Warmbrodt

Cc: Roger Strawn

From: Frank Harris

Subject: C81Gen Evaluation Using NACA 0012 Airfoil Data

Date: April 3, 2016

Attachments: 1. Master NACA 0012 Data File, March 28, 2016

2. Detailed Data Analysis Files (2-1 through 2-11), March 2016

3. Summary of Summaries, March 29, 2016

Introduction

In early February of this year, Roger designated me as a beta tester of C81Gen (Ref. 1 and 2). I was happy to do this evaluation because it would give me a way to "quickly" create C81 airfoil decks for CAMRAD II. And I wanted to have some confidence in the tool since my intention is to use super critical airfoil lift, drag, and pitching moment data in the conceptual design of a 425-knot, 35,000-foot, Large Civil Tiltrotor (LCTR 120 passenger). Super critical airfoils have evolved from Dick Whitcomb's original work at NASA Langley begun in the late 1960s (Ref. 3), and C81 airfoil decks are not currently available for this class of airfoils.

My immediate objective is a proprotor design having a propulsive efficiency of at least 0.8 at the high speed and altitude cruise condition. Proprotor designing requires airfoil data up to at least Mach numbers on the order of 0.82 with relatively low Reynolds numbers in the range of 6 million in cruise and lower for hover. Wing designing requires data more in the Mach number range of 0.75 and Reynolds number on the order of 45 million for LCTRs. Basically, this is a transonic aerodynamic design problem, which is bread and butter for companies like Boeing and Airbus, but most certainly not for the rotorcraft industry.

As you know, C81Gen is a working engineer's CFD tool that has a graphical user interface (GUI) on the front end coupled to the Ames Research Center 2D CFD solver known as ARC2D. My purpose in writing this memorandum is to record my evaluation of C81Gen first from a user's point of view and second from an evaluation of the ARC2D solver using the NACA 0012 airfoil as a test versus theory example.

C81Gen User Interface Evaluation

With Gloria Yamauchi's help, I had very little trouble installing the tool on my Dell XPS computer. My computer uses the Intel I7-2600 processor having 4 cores and 8 logical threads. The CPU runs at 3.40 GHz. The hard drive is solid state. I found that C81 Gen has very little graphic requirements.

In terms of user friendly, I found C81Gen quite acceptable from the input point of view. The manuals are, however, inadequate with respect how to use the add/delete buttons because one box is where you type your data point to be run. But then in the other box, the entry is written twice. I found my self entering a Mach number, hitting enter by force of habit, but then needing to click on the add button which produces a double entry and this required hitting the delete button on the extra entry. Secondly, I wanted to run cases in the custom mode by holding constant Mach number and varying Reynolds number, but couldn't find a way to do it.

From an output point of view, the "create a C81 table mode" lacks sufficient significant figures for engineering work. For example, drag coefficient is outputted as 0.007, but it is, in fact, 0.007xxxx when you look at the CASESUM data files or the AFSSUM data files. Most of my cases were run in the Custom mode to obtain theory versus test results, and this required me to access about 1,000 data points (i.e., a point is one Mach number, one Reynolds number, one angle of attack). Most frequently for the NACA 0012 study, I ran 8 data points at a clip and the run time was about 45 minutes with a course grid and 2 hours with a fine grid. I found that not having Reynolds number listed with the output data of Mach number and angle of attack was a major shortcoming. Thankfully, Gloria found a friend (Larry ??) who wrote a script file that gathered data from the AFSSUM files and put the output data into an Microsoft EXCEL spreadsheet (my application of choice) with a touch of a button.

C81Gen did not tell me where the transition point from laminar to turbulent flow occurred. As I understand it, this transition point is an input. But what it's value was for the cases I ran is unknown to me. However, I was told by Mark that the calculations were made assuming a fully turbulent boundary layer. Later, I began to suspect that this was the case because comparisons between theory and test at a Reynolds number of 3 million were poor compared to the comparisons at 6 million.

Also, Mark Potsdam and I found a situation where we couldn't duplicate cases because our airfoil contours differed by something the GUI did (or we did) and the GUI did not tell us. You will have to ask Mark about this situation. I don't understand why the ARC2D input doesn't require a chord length and some grid geometry selection. And I don't understand why a temperature is required when I have stated the Reynolds number and the Mach number. For years a single C81 airfoil deck as been misused by applying it without regard to Reynolds number. Perhaps C81Gen can at least state it was created for a specific configuration. This might at least improve rotor performance calculations for models and full scale designs in static conditions and most certainly improve proprotor calculations in axial flight. It does seem to me that the output data should include more information about the user input because guys like me may be the user.

Finally, this is the first time a CFD code has been given to me so I could play around with some engineering questions. I've had the time of my life during this month being able to ask a practical engineering question and getting an answer in 2 to 12 hours in MY office with MY computer. *And I didn't have to bother anybody*. Now, I want a very fast, 16 core machine ASAP because my questions are getting serious.

Impression of ARC2D Theory versus NACA 0012 Test Data

General Discussion

To gain some feeling of how CFD is doing versus recently available test data, I first reviewed Jim McCroskey's landmark paper on tests conducted with the NACA 0012 airfoil (Ref. 4) and also, Marilyn Smith's (et al.) paper (Ref. 5). My conclusion was that test results covering a wide range in both Mach and Reynolds numbers are absolutely required before any assessment of theory versus test can be reached. Even then, important issues associated with how results vary with wind tunnels and with different CFD codes reduce confidence. Nevertheless, I chose to use Ladson's test reports (Refs. 6, 7, and 8) as the data base for NACA 0012 wind tunnel results. Ladson's report, NASA TM 100526, provides tabulated data for the following test conditions:

TABLE 1

RN / M	3 mil	6 mil	9 mil	15 mil	30 mil	45 mil
0.30	●	●	●	●		
0.40	●	●	●	●		
0.50	●	●	●	●	●	
0.60	●	●	●	●	●	
0.65	●	●	●	●	●	
0.70	●	●	●	●	●	
0.74		●	●	●	●	
0.76		●	●	●	●	●
0.78		●	●	●	●	●
0.80		●	●	●	●	●
0.82		●	●	●	●	Limited

The tabulated data in Ladson's report were entered onto a master EXCEL spread sheet (Attachment 1). To save me from hand entering nearly 1,200 6-digit numbers for about 200 angles of attack (and going blind), I called Preston Martin and asked if he would track down the original test data in digitized format somewhere at NASA Langley. He had no luck. So I began the hand entering. It quickly became clear that my eyes were going to be severely strained because the PDF of Ladson's tables was too small and scanning the tables didn't work. Fortunately, Michelle Dominguez in your group came to my rescue and I thank her very, very much for entering the bulk of the numbers.

As you might guess, the Ladson test data never had wall corrections applied although the drag measurements (made with a wake rake) were corrected for blockage. This means that the pressure integrations for normal force (C_n) and chord force (C_c) are associated with an uncorrected angle of attack (α_{uncor}). Despite this less than desirable situation, I calculated lift coefficient for my comparative and correlation purposes as

$$C_\ell = C_n \cos\alpha_{uncor} - C_d \sin\alpha_{uncor}$$

Maybe the staff at the Langley 0.3 meter gryogenic wind tunnel will—in the future—repair this situation if and when they find the original test results.

Let me add that CFD advocates frequently state that the codes are "pretty good in the linear range," so one could assume that when the test data is corrected one would expect that the ARC2D angle of attack will be obtained. Either way, the angle of attack is in the small angle range so I feel that my calculation of lift coefficient is quite adequate for this NACA 0012 airfoil study because most of my comparisons and correlations are plotted versus lift coefficient, not angle of attack. I didn't bother with any pressure drag (C_d) data analysis, which I did calculate as

$$C_d = C_n \sin\alpha_{uncor} + C_c \cos\alpha_{uncor}$$

However, I consider this approximation to be inadequate for my study.

It seems to me that CFD solvers should include the wind tunnel test section geometry so that this fundamental issue of wall effects is minimized. Furthermore, presuming CFD solvers do calculate normal and chord force coefficients from the airfoil pressure distribution, then I think this data should be available in the output.

With respect to the ARC2D results, which you will also find on the master EXCEL spread sheet (Attachment 1), I ran the code for a coarse grid and Mark Potsdam ran the code for a fine grid. I don't know what the C81Gen ARC2D input numbers mean, but they are as follows:

TABLE 2

C81Gen ARC2D Input Item	Coarse Grid	Fine Grid
Type of Grid	C	C
Standard Settings		
Total streamwise points	301	751
Total normal points	101	251
Total wake points	51	126
Advanced Settings		
Domain radius (in chords)	50.0	50.0
y+ at airfoil	1.0	0.4
Leading edge cluster spacing	0.001	0.0004
Trailing edge cluster spacing	0.001	0.0004
Mach number used for y+ calculation	1.0	1.0

There is one other C81Gen input in the Flow Condition set that is a box to be checked or unchecked. This box is labeled Constant Reynolds. Both Mark and I made our calculations with the box checked. I thought that the use of this box is not well explained in the user manual.

Finally, both the input conditions and calculated results for both the coarse and fine grid cases tabulated in Attachment 1 (titled Master NACA 0012 Data File March 28, 2016) are on the same EXCEL spread sheet along with the test data from Ladson's NASA TM 100526. This one sheet formed my data base for this NACA 0012 airfoil study.

Detailed Data Analysis

I examined the overall comparisons between C81Gen/ARC2D and NASA TM 100526 with a four graph set compiled for the Reynolds numbers at each Mach number. This work is provided as Attachment 2, which actually contains 11 large EXCEL files, one for each Mach number. Each Mach number file is about 6 meg in size so I will forward each of the 11 files as separated attachments to an E-mail.

To illustrate these comparison graphs, you only need to look at the following Figures 1 thru 4, which show a rather good comparison that Mark and I got for a Mach number of 0.70 and a Reynolds number of 9 million using the tabulated data from the Master NACA 0012 Data File March 28, 2016 (Attachment 1). Let me discuss each one of the graphs in turn starting with Figure 1:

With Figure 1 you have a comparison of lift coefficient versus angle of attack. I curve fit each curve with an EXCEL trendline and displayed its equation for later study in my data summary, which I will discuss shortly. You will see the same basic format of color and symbols in all the graphs. Since the test data had no wind tunnel wall corrections applied as I mentioned earlier, one could "correct" the test lift curve slope up to the ARC2D results with just a little arithmetic. Then data versus angle of attack might be of interest.

Figure 2 shows the typical drag coefficient versus lift coefficient (i.e., a classical drag polar) comparison that working engineers need. In this case, an unusually good comparison is presented.

I created Figure 3 showing drag coefficient versus the square of lift coefficient as a way to measure the drag polar in the linear range with an EXCEL trendline and its equation. The theory value of CDo at CL equal to zero was forced on the coarse and find grid cases. This approach gave me confidence in the trendline for the test data.

To me an airfoil's value of maximum lift-to-drag ratio is a key parameter. Therefore, you have Figure 4. Here you will see small data symbols perched at the peak of each curve. These data points (and the associated lift coefficient) correspond to my selection of max L/D to be used in the correlation portion of this memorandum.

You might note in passing from Table 1 that there are 47 combinations of Mach and Reynolds numbers. Given that for each combination, there are four graphs like Figures 1 thru 4. This makes a total of 188 detailed graphical comparisons.

Summary of Correlation and Comparison

To gather up the data from the 188 graphs, I created a third EXCEL file that I titled Summary of Summaries, March 29, 2016, which is Attachment 3 to this memorandum. The first tab on this sheet gathers up and tabulates data from each of the 188 graphs. A typical example of the format used in this summary of summaries data sheet is shown Table 3 of this memo. The summary data is also tabulated at constant Reynolds number on the same data sheet, since certain

trends are clearer with that variable. Keep in mind that the sets of data results are from the trendline equations shown on graphs such as Figures 1 and 3 and the selected points for maximum L/D from Figure 4.

I used data from the first tabbed worksheet to construct two correlation graphs and two comparison graphs that interested me. You have these graphs transposed to this memo as Figures 5 thru 8.

Closing Remarks

The C81Gen I was offered is currently designed to create airfoil decks for any analysis that needs them. I found that the current version is adequate for this purpose; though not enough of the input data is reproduced in the output. Also, the aerodynamic coefficients returned had only 3 or 4 significant digits, which is quite insufficient. For example, being told that CDo equals 0.007, when at least 0.007xx is available is very important particularly when the ratio of lift to drag is at issue. A 1-percent gain in maximum L/D can be worth its weight in gold, a point emphasized in Reference 9.

However, I used the tool to compare ARC2D theory versus test and in this regard I found a number of improvements that could be incorporated should this GUI be extended to broader use. I offered my suggestions in the previous pages. My impression of the ARC2D theory with respect to the many comparisons and the few correlations I have compiled is no where near as favorable as the impression the GUI made on me. For one thing, I do not share a view that the NACA 0012 test data obtained by Ladson using the Langley 0.3-meter, cryogenic wind tunnel is "garbage"—as one engineer expressed it—because wall corrections were not applied. Lack of wall corrections being applied hardly accounts for the difference between test and theory that my study uncovered.

For example, the apparently well known CFD deficiency in accurately predicting airfoil lift, drag and moment coefficients beyond the angle of attack for well attached flow (as illustrated by Figures 1 and 2) means that prediction of aircraft behavior near and above the flight envelope is still a high risk problem. Of no less importance, the correlation of maximum lift to drag as shown on Figure 5 is very disturbing to me. This correlation shows that neither the influence of Reynolds number nor Mach number *is not well predicted* in my NACA 0012 study. Discounting the correlation at a Reynolds number of 3 million because the model was tested free of any force transition point and the ARC2D calculation was made assuming completely turbulent flow (I think) does not change my opinion. Furthermore, scaling model wind tunnel results to full scale with ARC2D theory must still be considered a necessary step during conceptual and preliminary design—but I would take the CFD scaled results with a grain of salt.

In conclusion, I believe (1) the GUI should be extended beyond just providing a C81 airfoil deck, (2) several other airfoil tests should be compared to CFD over the wide range in Mach and Reynolds number as reported in this memo, and (3) CFD advocates should not yet let up in improving their theories because the theory is not—today—good enough based on my study.

TABLE 3

Mach Number	Reynolds Number	ARC2D Coarse Grid dCL/dα	ARC2D Coarse Grid for CL at α = 0	ARC2D Coarse Grid CDo	ARC2D Coarse Grid CL for Max. CL/CD	ARC2D Coarse Grid Max. CL/CD
0.30	3,000,000	0.11328	-0.00115	0.009642	0.9810	64.12
0.30	6,000,000	0.11451	-0.00108	0.008796	0.9760	70.65
0.30	9,000,000	0.11513	-0.00105	0.008353	0.9800	74.18
0.30	15,000,000	0.11586	-0.00101	0.007846	0.9850	79.30
0.40	3,000,000	0.11790	-0.00129	0.009375	0.9500	64.05
0.40	6,000,000	0.11928	-0.00119	0.008541	0.9430	70.60
0.40	9,000,000	0.12088	-0.00043	0.008105	0.9500	74.34
0.40	15,000,000	0.12080	-0.00086	0.007608	0.9500	79.18
0.50	3,000,000	0.12635	-0.00068	0.009180	0.7376	61.66
0.50	6,000,000	0.12790	-0.00061	0.008350	0.7459	68.20
0.50	9,000,000	0.12906	0.00038	0.007979	0.7536	72.11
0.50	15,000,000	0.12913	0.00158	0.007429	0.7560	77.20
0.50	30,000,000	0.13024	0.00149	0.006850	0.7560	83.70
0.60	3,000,000	0.13780	0.00220	0.009072	0.6059	53.57
0.60	6,000,000	0.13968	0.00218	0.008240	0.5980	59.15
0.60	9,000,000	0.14242	-0.00020	0.007809	0.6000	62.60
0.60	15,000,000	0.14177	0.00212	0.007323	0.5916	67.01
0.60	30,000,000	0.14306	0.00213	0.006754	0.5906	72.80
0.65	3,000,000	0.14784	0.00126	0.009070	0.5155	45.79
0.65	6,000,000	0.14994	0.00132	0.008233	0.5000	50.38
0.65	9,000,000	0.15102	0.00135	0.007801	0.4954	53.31
0.65	15,000,000	0.15225	0.00136	0.007320	0.4899	56.87
0.65	30,000,000	0.15375	0.00138	0.006775	0.4881	61.90
0.70	3,000,000	0.16146	0.00135	0.009131	0.4000	34.78
0.70	6,000,000	0.16553	0.00009	0.008283	0.4000	37.86
0.70	9,000,000	0.16524	0.00143	0.007848	0.3908	39.60
0.70	15,000,000	0.16833	0.00012	0.007360	0.3828	42.00
0.70	30,000,000	0.17014	0.00015	0.006790	0.3750	45.12
0.74	6,000,000	0.17643	0.00424	0.008406	0.3056	24.90
0.74	9,000,000	0.17818	0.00413	0.007965	0.3026	25.98
0.74	15,000,000	0.18000	0.00416	0.007473	0.2997	27.15
0.74	30,000,000	0.18198	0.00431	0.006901	0.3010	28.61
0.76	6,000,000	0.18583	0.00438	0.008625	0.3007	18.95
0.76	9,000,000	0.18822	0.00406	0.008189	0.3008	19.53
0.76	15,000,000	0.19071	0.00385	0.007703	0.2829	20.16
0.76	30,000,000	0.19301	0.00393	0.007139	0.2750	21.06
0.76	45,000,000	0.19416	0.00395	0.006848	0.2640	21.55
0.78	6,000,000	0.19661	0.00365	0.010425	0.2812	13.97
0.78	9,000,000	0.20018	0.00314	0.010027	0.2853	14.31
0.78	15,000,000	0.20367	0.00285	0.009587	0.2750	14.71
0.78	30,000,000	0.20679	0.00289	0.009078	0.2663	15.20
0.78	45,000,000	0.19802	0.00797	0.008814	0.2750	15.41
0.80	6,000,000	0.20464	0.00204	0.015926	0.2750	9.93
0.80	9,000,000	0.20958	0.00176	0.015600	0.2734	10.21
0.80	15,000,000	0.21552	0.00158	0.015244	0.2750	10.49
0.80	30,000,000	0.22005	0.00180	0.014827	0.2883	10.79
0.80	45,000,000	0.22235	0.00189	0.014604	0.2960	11.04
0.82	6,000,000	0.18118	0.00058	0.026545	0.2170	5.88
0.82	9,000,000	0.19225	0.00088	0.026317	0.2313	6.20
0.82	15,000,000	0.20317	0.00067	0.026214	0.2349	6.33
0.82	30,000,000	0.21364	-0.00018	0.025765	0.2444	6.89
0.82	45,000,000	0.22134	-0.00024	0.025592	0.2473	6.82

References

1. Sukra Heliteck, Inc.: *C81 Generator How–To Guide*, Jan. 28, 2016.

2. Sukra Heliteck, Inc.: *C81 Generator User Manual*, Jan. 28, 2016.

3.Harris, Charles D.: *NASA Supercritical Airfoils—A Matrix of Family-Related Airfoils*, NASA TP 2969, Mar. 1990.

4. McCroskey, W.J.: *A Critical Assessment of Wind Tunnel Results for the NACA 0012 Airfoil*, NASA TM 100019, Oct. 1987.

5. Smith, M.J., et al.: *Evaluation of Computational Fluid Dynamics to Determine Two–Dimensional Airfoil Characteristics for Rotorcraft Applications*. AHS Journal, vol. 51, no. 1, Jan. 2006.

6. Ladson, C.L.; Hill, A.S.; and Johnson, W.G.: *Pressure Distributions from High Reynolds Number Transonic Tests of an NACA 0012 Airfoil in the Langley 0.3-Meter Transonic Cryogenic Tunnel*. NASA TM 100526, Dec. 1987.

7. Ladson, C.L. and Hill, A.S.: *High Reynolds Number Transonic Tests of an NACA 0012 Airfoil in the Langley 0.3–Meter Transonic Cryogenic Tunnel*, NASA TM 100527, Dec. 1987.

8. Ladson, C.L.: *Effects of Independent Variation of Mach and Reynolds Numbers on the Low–Speed Aerodynamic Characteristics of the NACA 0012 Airfoil Section*, NASA TM 4074, Oct. 1988.

9. Spalart, P.R. and Venkatakrishman, V.: *On the Role and Challenges of CFD in the Aerospace Industry*, Royal Aeronautical Society Aeronautical Journal, vol. 120, no. 1223, Jan. 2016.

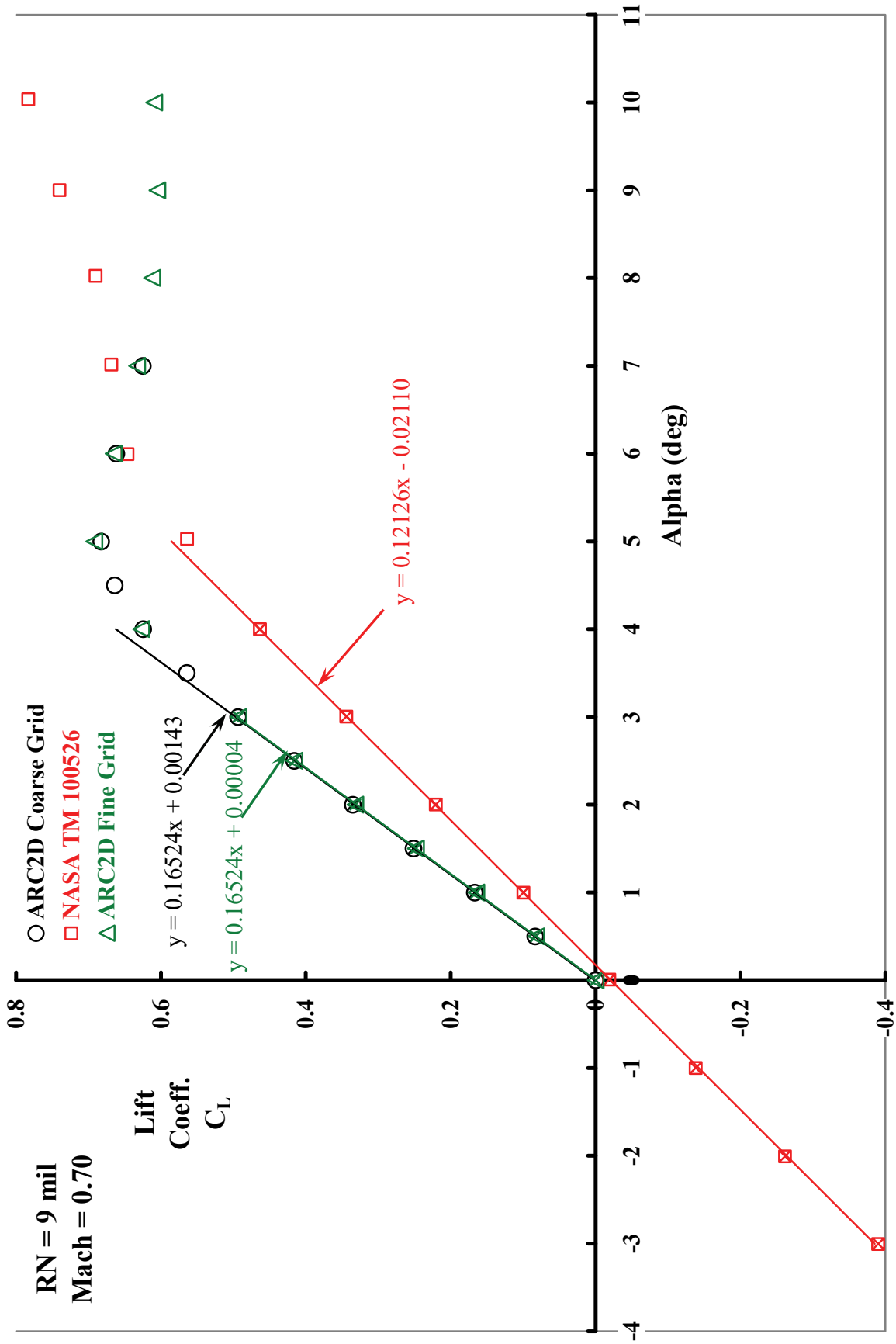
RN = 9 mil
Mach = 0.70
Lift
Coeff.
C_L
Alpha (deg)
○ ARC2D Coarse Grid
□ NASA TM 100526
△ ARC2D Fine Grid
y = 0.16524x + 0.00143
y = 0.16524x + 0.00004
y = 0.12126x - 0.02110
0.8
0.6
0.4
0.2
0
-0.2
-0.4
-4
-3
-2
-1
0
1
2
3
4
5
6
7
8
9
10
11

Figure 1

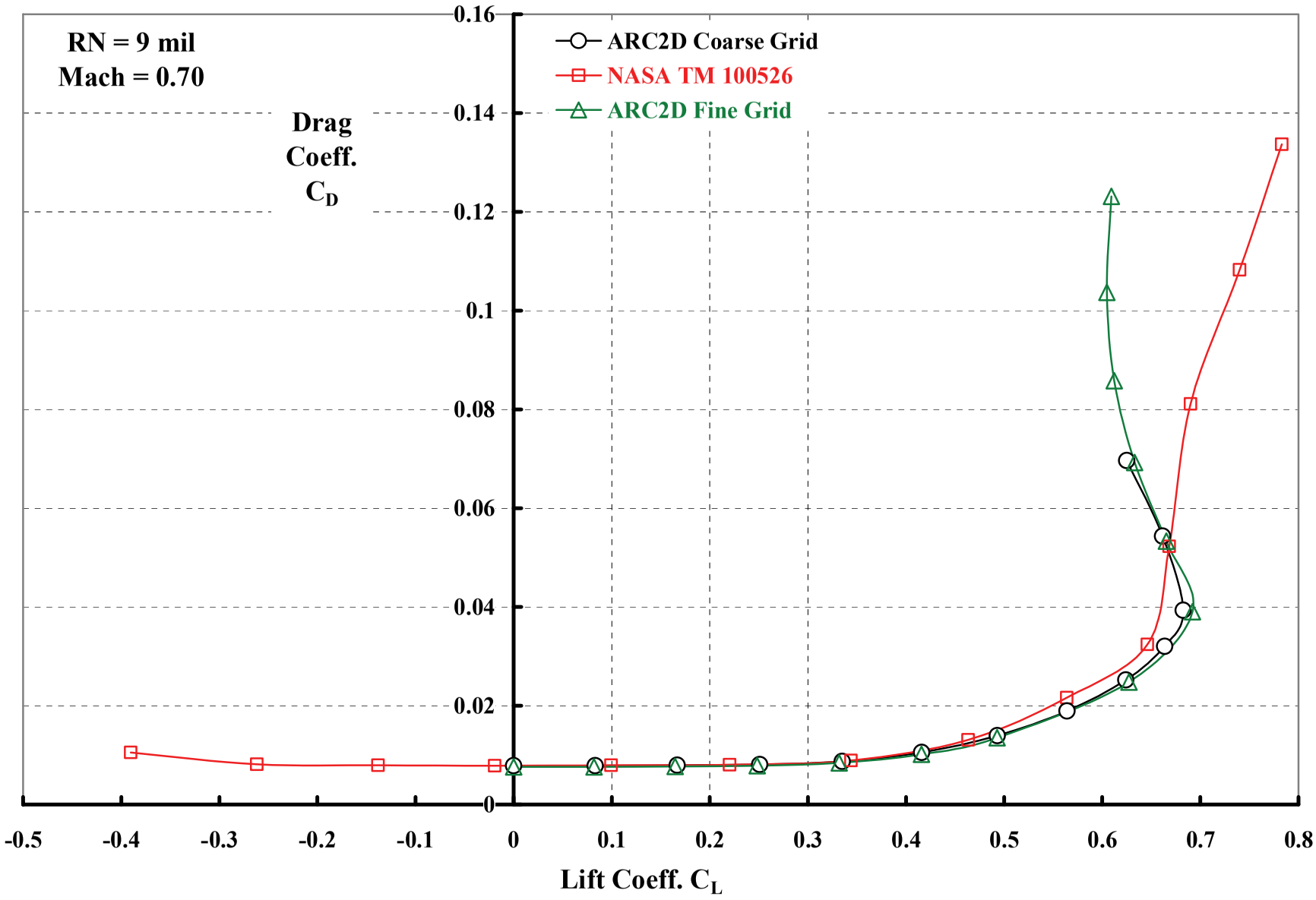
RN = 9 mil
Mach = 0.70
Drag Coeff. C_D
ARC2D Coarse Grid
NASA TM 100526
ARC2D Fine Grid
0.16
0.14
0.12
0.1
0.08
0.06
0.04
0.02
0
-0.5
-0.4
-0.3
-0.2
-0.1
0
0.1
0.2
0.3
0.4
0.5
0.6
0.7
0.8
Lift Coeff. C_L

Figure 2

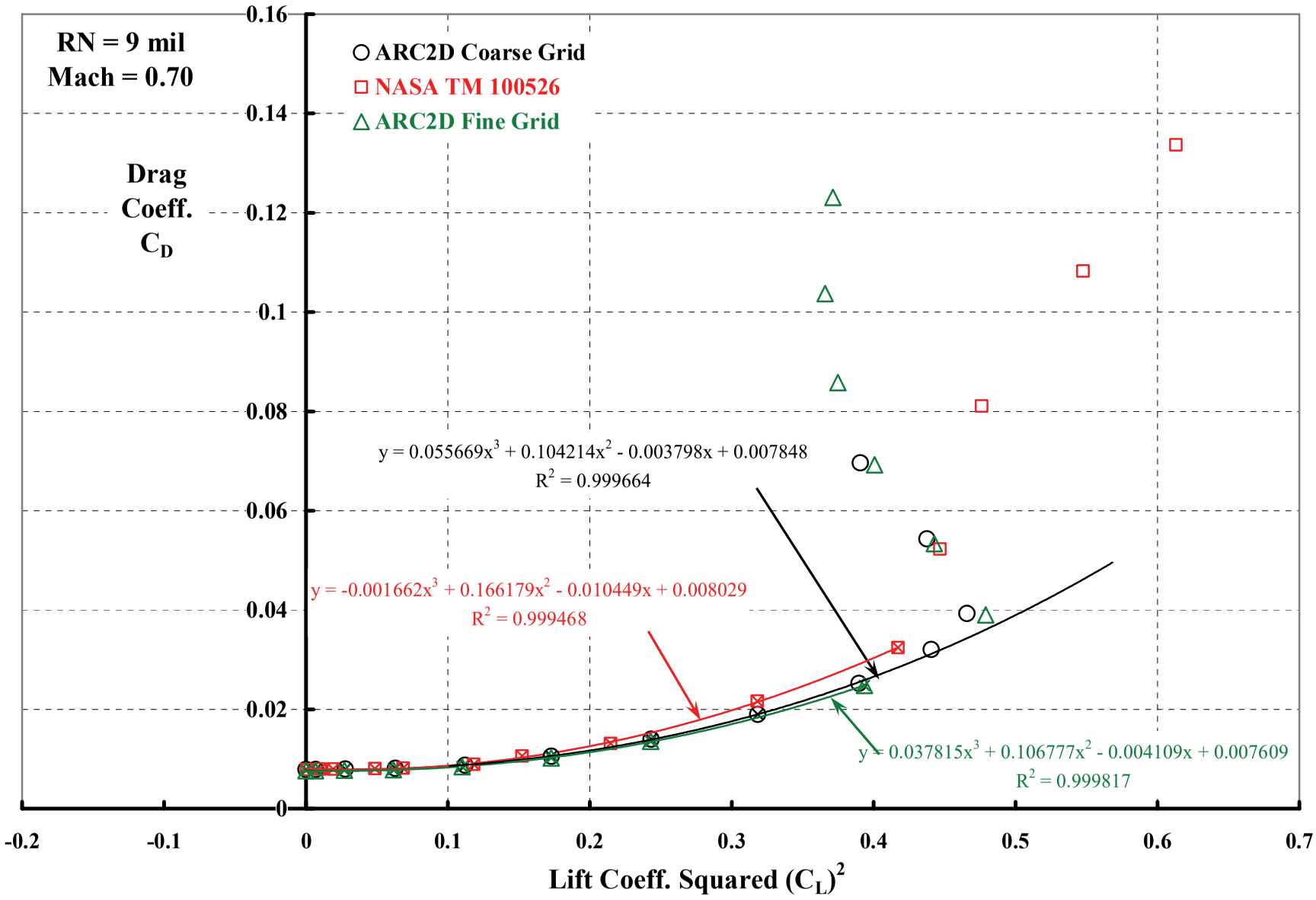
RN = 9 mil
Mach = 0.70
Drag Coeff. C_D
ARC2D Coarse Grid
NASA TM 100526
ARC2D Fine Grid
$y = 0.055669x^3 + 0.104214x^2 - 0.003798x + 0.007848$
$R^2 = 0.999664$
$y = -0.001662x^3 + 0.166179x^2 - 0.010449x + 0.008029$
$R^2 = 0.999468$
$y = 0.037815x^3 + 0.106777x^2 - 0.004109x + 0.007609$
$R^2 = 0.999817$
0.16
0.14
0.12
0.1
0.08
0.06
0.04
0.02
0
-0.2
-0.1
0
0.1
0.2
0.3
0.4
0.5
0.6
0.7
Lift Coeff. Squared $(C_L)^2$

Figure 3

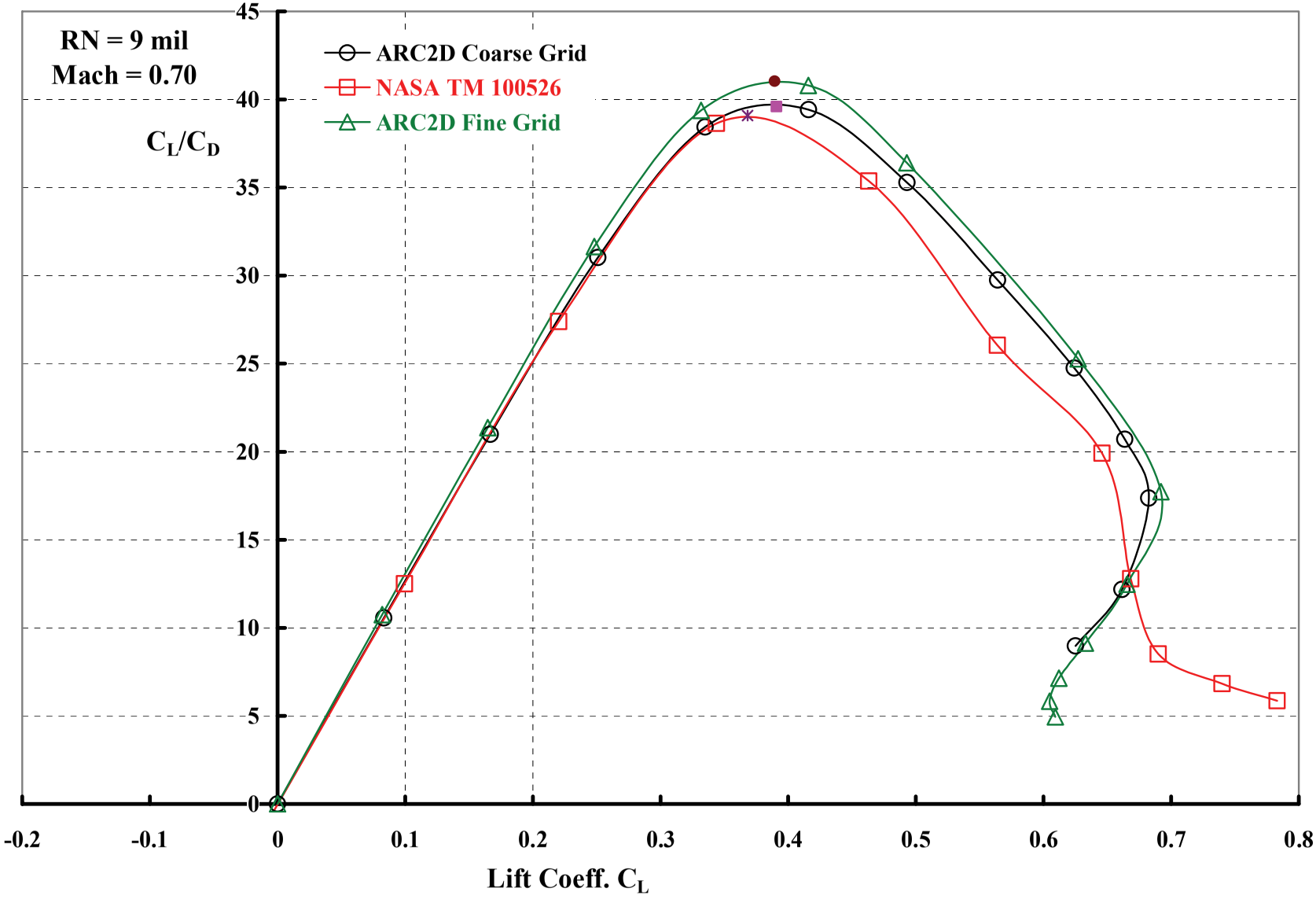
RN = 9 mil
Mach = 0.70
C_L/C_D
ARC2D Coarse Grid
NASA TM 100526
ARC2D Fine Grid
45
40
35
30
25
20
15
10
5
0
-0.2
-0.1
0
0.1
0.2
0.3
0.4
0.5
0.6
0.7
0.8
Lift Coeff. C_L

Figure 4

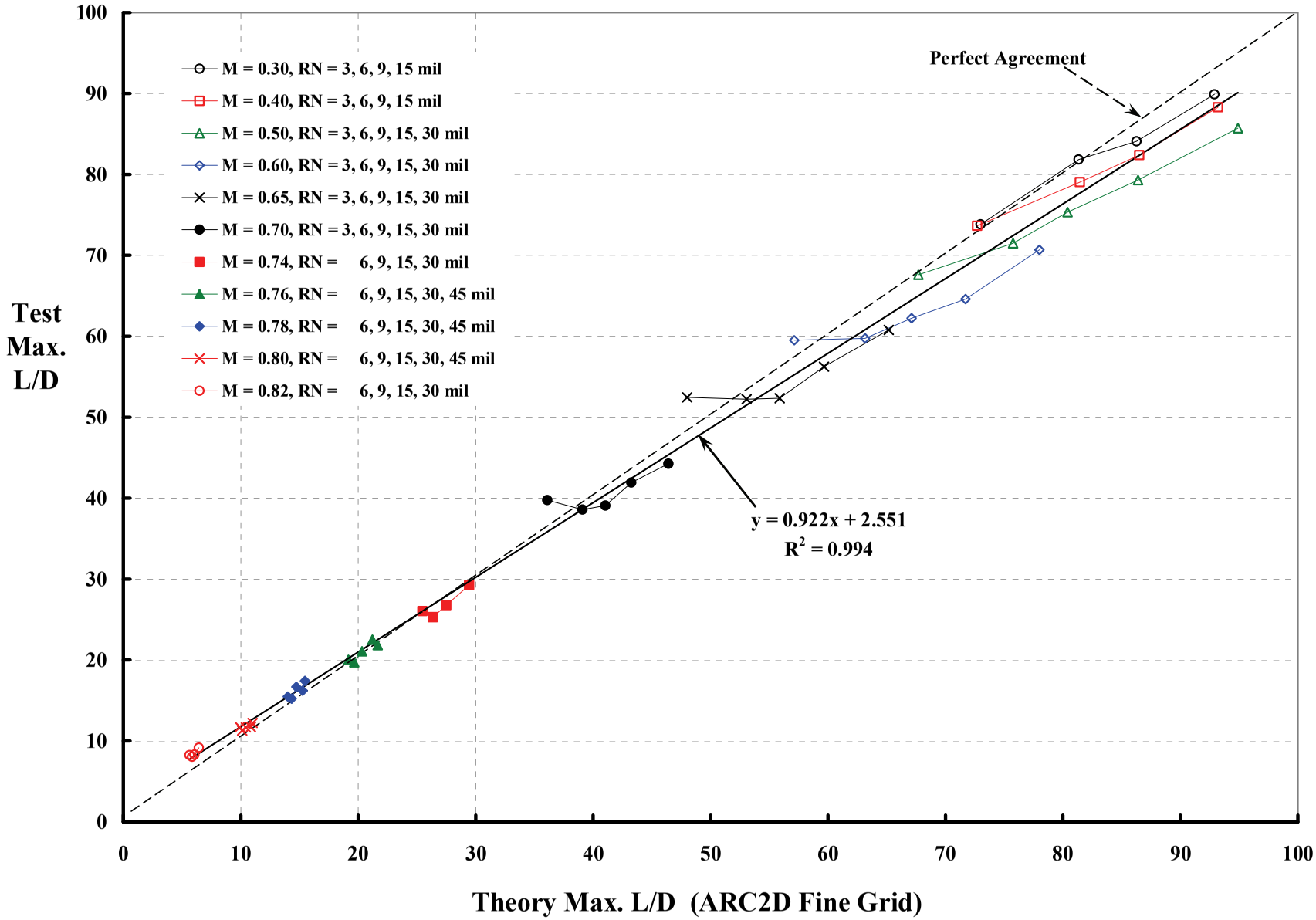
M = 0.30, RN = 3, 6, 9, 15 mil
M = 0.40, RN = 3, 6, 9, 15 mil
M = 0.50, RN = 3, 6, 9, 15, 30 mil
M = 0.60, RN = 3, 6, 9, 15, 30 mil
M = 0.65, RN = 3, 6, 9, 15, 30 mil
M = 0.70, RN = 3, 6, 9, 15, 30 mil
M = 0.74, RN = 6, 9, 15, 30 mil
M = 0.76, RN = 6, 9, 15, 30, 45 mil
M = 0.78, RN = 6, 9, 15, 30, 45 mil
M = 0.80, RN = 6, 9, 15, 30, 45 mil
M = 0.82, RN = 6, 9, 15, 30 mil
Perfect Agreement
y = 0.922x + 2.551
R2 = 0.994
Test Max. L/D
Theory Max. L/D (ARC2D Fine Grid)
0
10
20
30
40
50
60
70
80
90
100

Figure 5

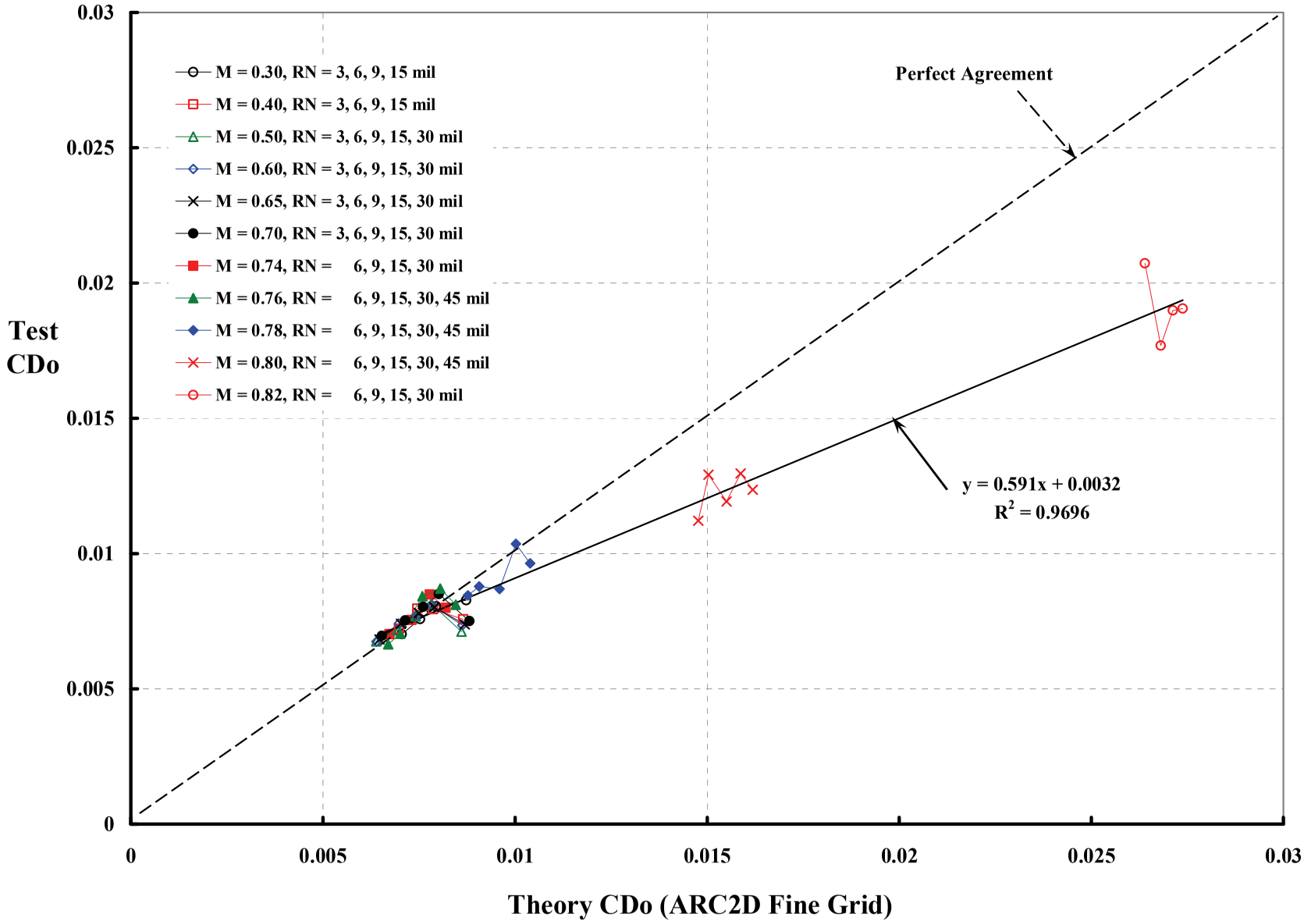
M = 0.30, RN = 3, 6, 9, 15 mil
M = 0.40, RN = 3, 6, 9, 15 mil
M = 0.50, RN = 3, 6, 9, 15, 30 mil
M = 0.60, RN = 3, 6, 9, 15, 30 mil
M = 0.65, RN = 3, 6, 9, 15, 30 mil
M = 0.70, RN = 3, 6, 9, 15, 30 mil
M = 0.74, RN = 6, 9, 15, 30 mil
M = 0.76, RN = 6, 9, 15, 30, 45 mil
M = 0.78, RN = 6, 9, 15, 30, 45 mil
M = 0.80, RN = 6, 9, 15, 30, 45 mil
M = 0.82, RN = 6, 9, 15, 30 mil
Perfect Agreement
y = 0.591x + 0.0032
R2 = 0.9696
Test CDo
Theory CDo (ARC2D Fine Grid)
0
0.005
0.01
0.015
0.02
0.025
0.03

Figure 6

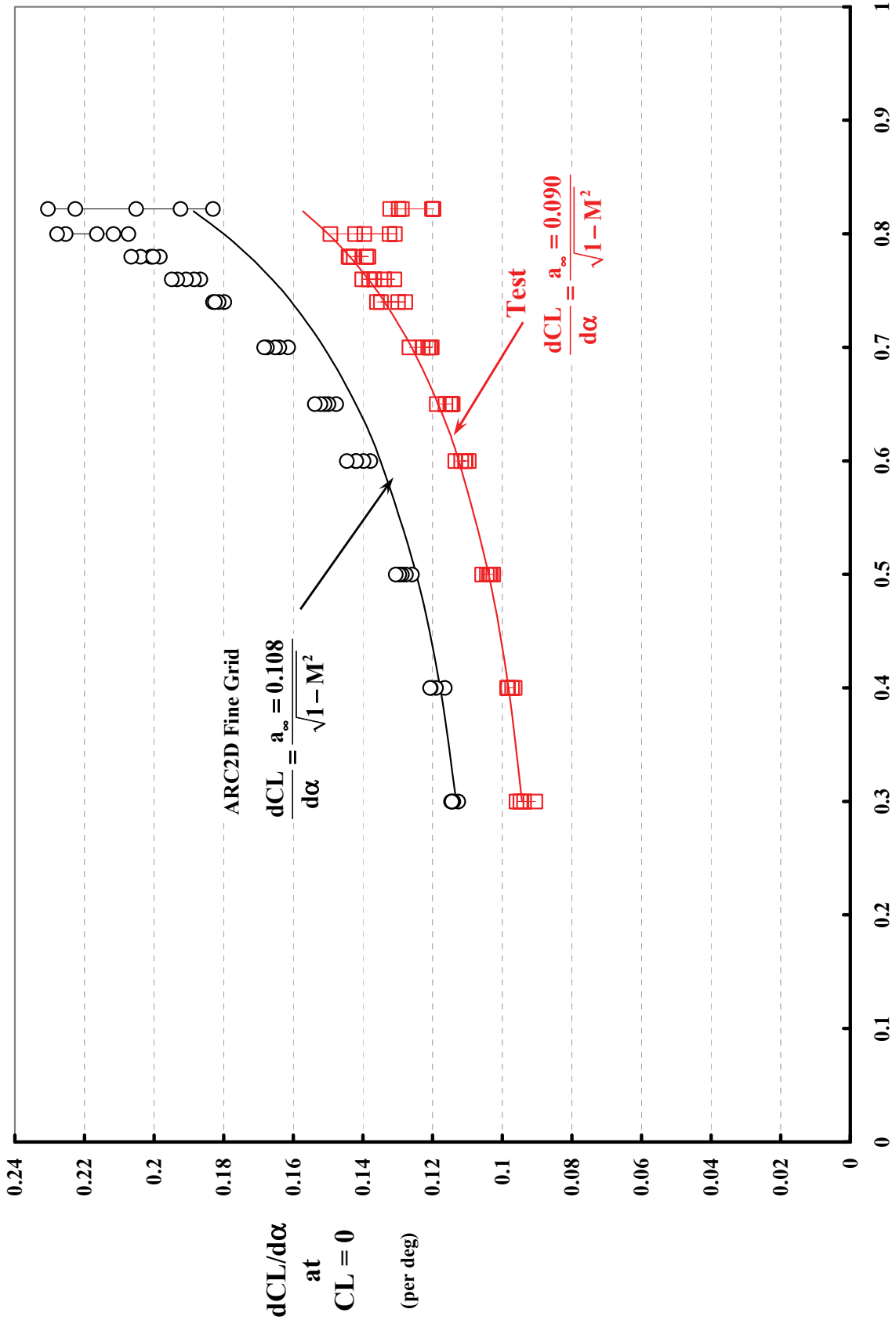
dCL/dα at CL = 0 (per deg)
0.24
0.22
0.2
0.18
0.16
0.14
0.12
0.1
0.08
0.06
0.04
0.02
0
0
0.1
0.2
0.3
0.4
0.5
0.6
0.7
0.8
0.9
1
Mach Number
ARC2D Fine Grid
dCL/dα = a∞ = 0.108 / √(1 − M²)
Test
dCL/dα = a∞ = 0.090 / √(1 − M²)

Figure 7

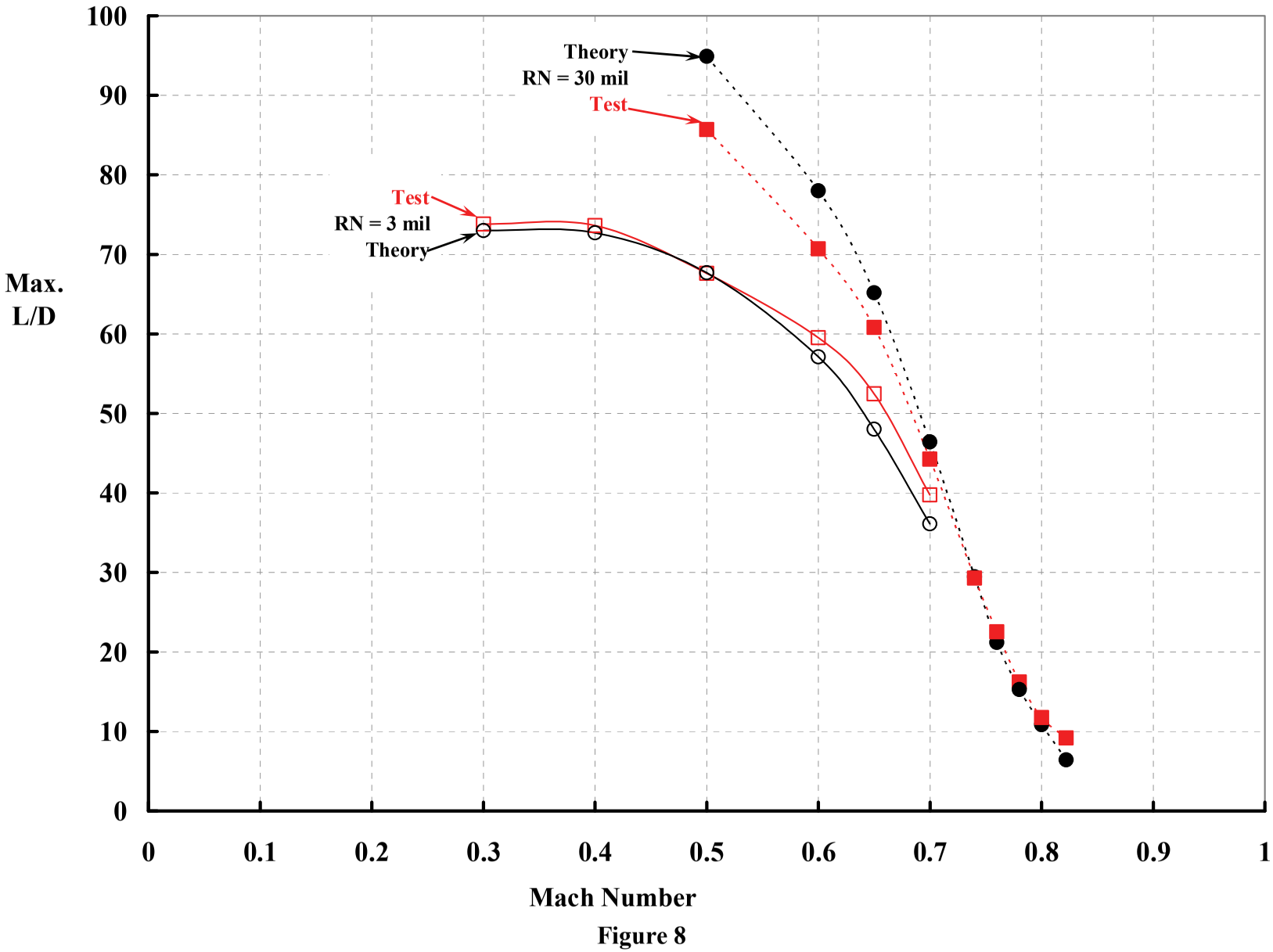
Theory
RN = 30 mil
Test
Test
RN = 3 mil
Theory
Max.
L/D
100
90
80
70
60
50
40
30
20
10
0
0
0.1
0.2
0.3
0.4
0.5
0.6
0.7
0.8
0.9
1
Mach Number

Figure 8